Aapo Ristaniemi

Linearization of piping supports in dynamic analyses

School of Engineering

Thesis submitted for examination for the degree of Master of Science in Technology.

Espoo 4.9.2015

Thesis supervisor:

Assistant Professor Arttu Polojärvi

Thesis advisor:

M.Sc. Juha Kuutti

Aalto University
School of Engineering

AALTO UNIVERSITY
SCHOOL OF ENGINEERING

ABSTRACT OF THE
MASTER'S THESIS

Author: Aapo Ristaniemi

Title: Linearization of piping supports in dynamic analyses

Date: 4.9.2015 Language: English Number of pages: 10+84

Department of Applied Mechanics

Professorship: Solid Mechanics Code: K-3006

Supervisor: Assistant Professor Arttu Polojärvi

Advisor: M.Sc. Juha Kuutti

Nuclear power plant piping systems exhibit dynamic behaviour, and piping supports keep the displacements of the pipes within acceptable limits. This study investigates linear modelling methods for nonlinear piping supports in dynamic analyses and presents a procedure to linearize nonlinear supports. The procedure and methods are found in literature and they were furher developed here. The study is limited to supports with gap and friction. The goal is to represent the nonlinear system as accurately as possible by an equivalent linear system. Using the linear system, computational effort can be saved in the dynamic analyses.

The nonlinear supports are replaced by linear springs or spring-damper systems to obtain a linear system. The equivalent spring and damping constants are found by iterative procedure, based on selected linearization method. Several methods are presented. Once the equivalent properties have been found, the equivalent linear system is obtained. Linearization procedure was investigated using single and multiple degree-of-freedom examples. Linearization was then applied to a real-world piping system with four gap supports.

For the real-world system, an equivalent linear system was determined and comparison with original nonlinear model was made for the load case investigated. The compared parameters were maximum displacements, support forces and bending moments in the pipe at the support locations. For the system studied, maximum displacements were of the same order of magnitude, though large differences occured at single locations. Maximum support forces were generally smaller in the linear system. Pipe bending moments differed significantly, and were both higher and smaller in the linear system. Linearization methods of piping supports need to be further developed, so that other types of supports can be linearized and that the equivalent linear system corresponds better to the original nonlinear system.

Keywords: Piping support, gap support, friction support, linearization, dynamic analysis

AALTO-YLIOPISTO
INSINÖÖRITIETEIDEN KORKEAKOULU

DIPLOMITYÖN
TIIVISTELMÄ

Tekijä: Aapo Ristaniemi

Työn nimi: Putkistotukien lineaarinen mallintaminen dynaamisissa analyyseissä

Päivämäärä: 4.9.2015 Kieli: Englanti Sivumäärä: 10+84

Sovelletun mekaniikan laitos

Professuuri: Lujuusoppi Koodi: K-3006

Valvoja: Apulaisprofessori Arttu Polojärvi

Ohjaaja: DI Juha Kuutti

Ydinvoimalaitosten putkistot käyttäytyvät dynaamisesti, ja putkistotuet estävät siirtymiä kasvamasta liian suuriksi. Tässä työssä tutkitaan epälineaaristen putkistotukien lineaarisia mallinnusmenetelmiä dynaamisissa analyyseissä ja esitetään menettelytapa epälineaaristen tukien linearisoimiseksi. Menettelytapa ja mallinnusmenetelmät löytyvät kirjallisuudesta ja tässä työssä niitä kehitettiin edelleen. Työ rajoittuu välys- ja kitkatukiin. Tavoitteena on kuvata epälineaarinen systeemi mahdollisimman tarkasti ekvivalentilla lineaarisella systeemillä. Lineaarisen systeemin käytöllä voidaan säästää aikaa dynaamisissa analyyseissä.

Epälineaariset tuet korvataan lineaarisilla jousilla tai jousi-vaimennin systeemeillä lineaarisen systeemin saamiseksi. Ekvivalentti jousivakio ja vaimennuskerroin määritetään iteraatiomenettelyllä perustuen valittuun linearisointimenetelmään. Useita menetelmiä esitetään. Kun ekvivalentit arvot on löydetty, ekvivalentti lineaarinen systeemi on saatu. Linearisointimenettelyä tutkittiin yhden vapausasteen ja monen vapausasteen esimerkkisysteemeillä. Menettelyä sovellettiin todelliseen putkistoon, jossa oli neljä välystukea.

Todelliselle putkistolle muodostettiin ekvivalentti lineaarinen systeemi, jota verrattiin alkuperäiseen epälineaariseen malliin tutkitulla kuormitustapauksella. Tukien kohdalla verrattiin maksimisiirtymiä, tukien voimia ja putken taivutusmomenttia. Tutkitulle systeemille maksimisiirtymät olivat samaa suuruusluokkaa, mutta suuria eroja esiintyy yksittäisissä paikoissa. Tukien maksimivoimat ovat yleensä pienempiä lineaarisessa systeemissä. Putken taivutusmomentit eroavat merkittävästi ja ovat sekä suurempia että pienempiä lineaarisessa systeemissä.

Putkistotukien linearisointimenetelmiä on tarpeen jatkokehittää siten, että myös muunlaisia tukia voidaan linearisoida ja että ekvivalentti lineaarinen systeemi vastaisi paremmin alkuperäistä epälineaarista systeemiä.

Avainsanat: Putkistotuki, välystuki, kitkatuki, linearisointi, dynaaminen analyysi

Preface

This Master's thesis was carried out in VTT Technical Research Centre of Finland as a part of the FOUND project. FOUND is a part of SAFIR2018 research programme, and the project focuses on ensuring structural integrity of nuclear power plant components. The work was funded by the State Nuclear Waste Management Fund (VYR), Teollisuuden Voima Oyj (TVO), Beräkningsgrupp (BG) consisting of Swedish plant operators and the Technical Research Centre of Finland (VTT).

I would like to thank my advisor M.Sc. Juha Kuutti for his time, guidance and thoughts that were helpful and valuable during the work. The guidance was especially important when difficulties were encountered. I would like to express my gratitude to the supervisor Assistant Professor Arttu Polojärvi for the active tutelage and for showing keen interest in the subject. His ideas helped me throughout the writing of this thesis.

Espoo, 4.9.2015

Aapo Ristaniemi

Contents

Symbols

$\mathbf{C}$	damping matrix of a system
c_1	damping coefficient of support
c_{eq}	equivalent damping coefficient
d	gap size
d_1	gap size in the positive direction
d_2	gap size in the negative direction
$e(x, \dot{x}, t)$	error term
E_c	energy dissipated by the equivalent damper
E_{linear}	maximum potential energy of the linear system
$E_{nonlinear}$	maximum potential energy of the nonlinear system
E_μ	energy dissipated by the friction force
f	function of recurrence relation
F	support force
F'	force of the support at displacement x_i
F_{amp}	force amplitude
F_c	force of the equivalent damper
$f_m(t)$	force per unit mass
F_{max}	maximum force of the support
F_{min}	minimum force of the support
F_n	surface normal force
$F(t)$	applied loading
$\mathbf{F}(t)$	force vector

F_μ	friction force
g	function to determine iteration variables $\mathbf{x_{i+1}}$ based on $\mathbf{p_{eq}}$; gravitational acceleration 9,81 $\frac{\mathrm{m}}{\mathrm{s}^2}$
$\mathbf{g}(x, \dot{x}, \ddot{x}, t)$	nonlinear force vector
h	function to determine equivalent properties $\mathbf{p_{eq}}$ based on $\mathbf{x_i}$
i	iteration number
$\mathbf{K}$	stiffness matrix of a system
k_{eq}	equivalent stiffness
k_p	system stiffness, pipe stiffness
k_1	support stiffness on positive side
k_2	support stiffness on negative side
L	length of a beam element; length of a bar element
m	mass of a system; mass of an element
$\mathbf{M}$	mass matrix of a system
$\vec{n}_1$	unit vector pointing to the positive direction of a gap
$\vec{n}_2$	unit vector pointing to the positive direction of a gap
$\mathbf{p_{eq}}$	vector containing equivalent properties, $\mathbf{p_{eq}} = \begin{Bmatrix} k_{eq} \\ c_{eq} \end{Bmatrix}$
q	system nonlinearity in force per unit mass
r_1	inner radius of a beam; inner radius of a bar
r_2	outer radius of a beam; outer radius of a bar
s	coordinate travelling through the force-displacement curve
t	time
v	velocity of a system

v_i	initial value of maximum velocity for the iteration step
v_{i+1}	resulting maximum velocity of iteration i
$\hat{v}_{i+1}$	starting point of the next iteration, calculated using v_i and v_{i+1}
x	displacement of a system
$\mathbf{x}$	vector containing displacement and velocity, $\mathbf{x} = \begin{Bmatrix} x \\ v \end{Bmatrix}$; displacement vector of a system
x_i	initial value of maximum displacement for the iteration step
$\mathbf{x_i}$	vector containing iteration variables, $\mathbf{x_i} = \begin{Bmatrix} x_i \\ v_i \end{Bmatrix}$
$x_i^{(err)}$	relative error of x_i to the solution
x_{i+1}	resulting maximum displacement of iteration i
$\mathbf{x_{i+1}}$	vector containing iteration variables, $\mathbf{x_{i+1}} = \begin{Bmatrix} x_{i+1} \\ v_{i+1} \end{Bmatrix}$
$\hat{x}_{i+1}$	starting point of the next iteration, calculated using x_i and x_{i+1}
$\hat{\mathbf{x}}_{\mathbf{i+1}}$	vector containing iteration variables, $\hat{\mathbf{x}}_{\mathbf{i+1}} = \begin{Bmatrix} \hat{x}_{i+1} \\ \hat{v}_{i+1} \end{Bmatrix}$
x_{max}	maximum displacement of a system
x_{min}	minimum displacement of a system
x_∞	solution of an iterative procedure
α	relaxation factor
ϵ	convergence criterion
η	parameter, coefficient of nonlinearity
θ	parameter used in Caughey's method, $\theta = \arcsin \frac{d}{x_i}$
μ	coefficient of friction

ξ damping ratio, $\xi = \frac{c_{eq}}{2m\omega_n} = \frac{c_{eq}}{2\sqrt{m(k_p+k_{eq})}}$

ρ density

ω angular velocity of an excitation force; angular velocity of a system

ω_n natural angular velocity of a system

1 Introduction and background

1.1 Introduction

Nuclear power plants contain a great amount of piping systems that are needed for the plant operation. During the operation, piping systems have dynamic behaviour, or vibration, due to different sources of excitation in the system. Piping systems are supported with various types of piping supports that keep the displacements within acceptable limits. Dynamic structural analyses are performed to ensure the structural integrity of the piping system.

As Escoe stated [1] "The prime function of piping is to transport fluids from one location to another". In nuclear power plant piping systems, the transported fluid commonly consists of water or steam at various pressures and temperatures [2]. For the operation of a nuclear power plant, these piping systems form a key component in ensuring the functionality and electricity production of the plant. High demands are set for the safety of the piping systems and their supporting structures, as their failure could result in a serious accident. Therefore, ensuring the structural integrity of the piping systems and their supporting structures is vital for safe and reliable operation of the plant. Structural analyses to assess safety have to be performed rigorously in order to ensure that the high demands can be met.

Most nuclear power plant piping systems have dynamic behaviour i.e. they vibrate at least to some extent during operation. Common sources of piping vibration excitation include mechanical, pulsation and flow induced excitations and pressure surges. Mechanical induced vibration can result from imbalanced forces and moments in machinery, whereas pulsation-induced vibration can arise due to pressure pulsations caused by compressors and pumps. Flow-excited vibration can originate due to turbulence or flow past obstructions. Pressure surges are instantaneous loadings that can occur as a result of discrete events. [3]

One purpose of dynamic piping analyses is to determine the response of the piping system subjected to an excitation. The response can be displacement, velocity or acceleration. The response is further used to assess, for example, strains and stresses of the pipe. Another important purpose of dynamic analyses is to find the eigenfrequencies of the system. They are used, for example, in the design of piping to avoid resonance with excitations. Dynamic analyses of piping systems are usually performed using the finite element method [4]. The equation of motion for a linear piping system is

$$\mathbf{M}\ddot{\mathbf{x}} + \mathbf{C}\dot{\mathbf{x}} + \mathbf{K}\mathbf{x} = \mathbf{F}(t) \tag{1}$$

where $\mathbf{M}$, $\mathbf{C}$ and $\mathbf{K}$ represent the mass, damping and stiffness matrices, $\mathbf{F}(t)$ the excitation force vector and $\mathbf{x}$ the displacement vector of the system with the dot denoting derivation with respect to time.

Typical solution methods include the response spectrum method and time history analysis. The response spectrum method is based on modal superposition that is applicable only to the analysis of linear systems, and is commonly used, for example, in seismic analyses. In time history analyses a dynamic problem is solved one short time step at a time. The equation of motion is directly integrated time step by

time step to obtain the response. Time history analyses require knowledge of the time history of excitation, e.g. $\mathbf{F}(t)$, and is applicable to various dynamic problems, including analysis of nonlinear systems.

The equation of motion for a nonlinear piping system is

$$\mathbf{M}\ddot{\mathbf{x}} + \mathbf{C}(x, \dot{x}, \ddot{x}, t)\dot{\mathbf{x}} + \mathbf{K}(x, \dot{x}, \ddot{x}, t)\mathbf{x} = \mathbf{F}(x, \dot{x}, \ddot{x}, t) \tag{2}$$

This can be expressed in a form of

$$\mathbf{M}\ddot{\mathbf{x}} + \mathbf{C}\dot{\mathbf{x}} + \mathbf{K}\mathbf{x} + \mathbf{g}(x, \dot{x}, \ddot{x}, t) = \mathbf{F}(t) \tag{3}$$

where $\mathbf{g}(x, \dot{x}, \ddot{x}, t)$ denotes the nonlinear force vector and contains all the system nonlinearities. These nonlinearities arise, for instance, from piping supports whose support forces are not linear functions of system displacement or velocity. Time history analysis is usually used to solve these problems. However, analysis of nonlinear systems using time history analysis requires generally more computing effort than response spectrum analyses of linear systems.

1.2 Scope of this work

The purpose of this study is to investigate linear modelling methods for nonlinear piping supports in dynamic analyses. The aim is also to investigate the accuracy of dynamic piping analyses performed with the linearized supports. Among the various types of supports found in a nuclear power plant, the scope of this study is limited on the supports involving gap and friction.

In this study, a procedure and methods are presented to model nonlinear piping supports linearly using an equivalent linear system. The procedure and methods are found in literature and they are further developed here. The equivalent linear system can then be used in subsequent analyses of the system, thereby obviating the need to perform nonlinear time history analysis.

1.3 Structure of the thesis

First, background information is given on piping vibrations in general and an introduction is given to different piping supports typically found in a nuclear power plant. The modeling of nonlinearities in piping supports is briefly reviewed. Then, a procedure and methods are presented to linearize the nonlinear piping supports with gap or friction in dynamic analyses. The procedure and methods are found in literature and they are further developed here. They are investigated using two single degree-of-freedom and two multiple degree-of-freedom examples.

The linearization is then applied to a multiple degree-of-freedom real-world piping system involving several supports. The piping system and supports are presented and linearization is performed using a postulated example load case. Finally, the results are evaluated and discussion, conclusion and recommendations are given.

2 Nonlinear supports

2.1 Piping supports

Piping supports are needed to counteract forces and moments from operational loadings such as weight, thermal deformation and vibration and special events such as earthquake or pressure surge [1]. Supports are designed to keep the piping displacements within acceptable limits in all predetermined conditions. Various kinds of supports are used and their design depends on their function. The most common types of supports are weight supports, rigid restraints, snubbers and sway braces [5]. Information on piping supports can be found in reference [5]. This study is limited on supports that induce friction forces or have gaps. Friction is usually present in certain weight supports and gaps are usually induced by certain rigid restraints, which are presented in the following.

Weight supports, such as in Figure 1, provide supporting forces to compensate for gravity loading and other loads that act in gravity direction. They support mainly the dead weight of the pipe and its contents. Typical weight supports include rod hangers, spring hangers and sliding supports [5]. Sliding supports induce friction forces when the pipe is moving or kept in place by the friction force. Cross-section figures of a rod hanger and a sliding support are presented in Figure 1.

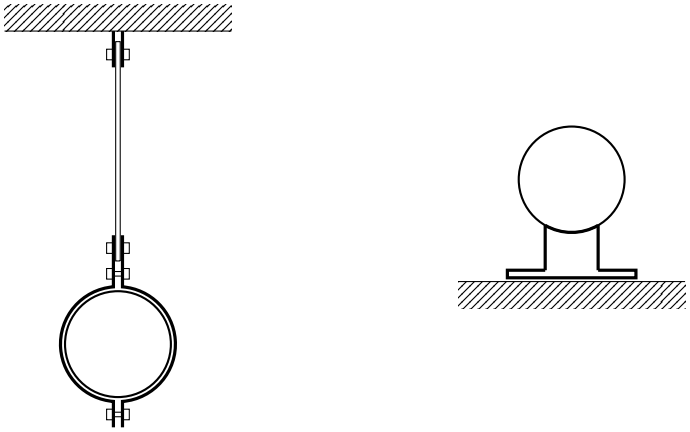

Figure 1: Schematic figures of a) a rod hanger and b) a sliding support. Reproduced from reference [5].

Rigid restraints, such as in Figure 2, limit some or all degrees of freedom of the pipe to practically zero at the point of the restraint. Rigid restraints can be constructed using struts or with direct contact with a steel structure. Struts can be attached from one end to piping using clamps or by welding and from the other end to the building structures. Direct contact with steel structure means that the pipe is supported with very rigid steel structures. The pipe can be on the steel structure, boxed by it or welded to it. If all three translational and three rotational degrees of freedom are restrained, the support is called an anchor. [5] It is to be

noted, however, that no restraints are infinitely rigid and a finite stiffness can be determined in translation and rotation [1]. Schematic figures of a strut assembly and a steel structure boxing the pipe are shown in Figure 2. This study focuses on supports with gaps similar to Figure 2 b) and supports with friction similar to Figure 1 b).

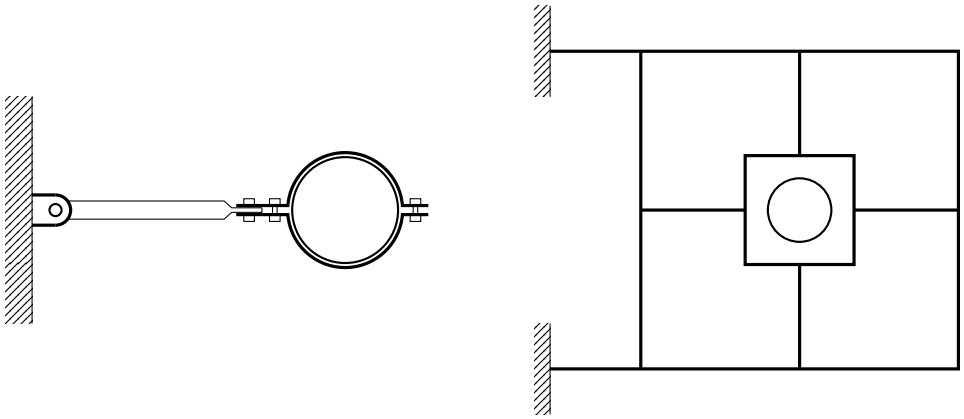

a) b)

Figure 2: Schematic figures of a) a strut and b) a support of steel structure boxing the pipe. Reproduced from reference [5].

2.2 Nonlinearities in piping supports

In many cases, piping support force-displacement behaviour is nonlinear. This means that the force acting on the pipe from the support is not a linear function of pipe displacement or velocity at the location of support. Support nonlinearities arise from the following [6, 7, 8, 9, 10]:

- Gaps
- Friction
- Nonlinear material behaviour
- Geometry

A gap is left between the pipe and the support to allow free thermal displacements of the pipe [11]. Gaps induce contact between the pipe and the support if pipe displacement is sufficiently large. Friction is involved when the pipe is in contact with the support and the pipe is moving or kept in place by the friction force. Material behaviour can be nonlinear for example due to plasticity. Geometric nonlinearity arises when changes in geometry have an influence on the load-deformation behaviour of the structure [10]. In this study, supports with gaps similar to Figure 2 b) and supports with friction similar to Figure 1 b) are investigated. The nonlinearities arising from gap and friction are linearized.

2.3 Nonlinear modeling methods

The aim of this study is to linearize the nonlinear behaviour of piping supports arising from gap and friction. Some information about usual nonlinear methods to account for these support nonlinearities is presented briefly. Methods to linearize these effects are presented thoroughly in Section 3.

2.3.1 Gap modeling

A gap and a contact resulting from gap closure can be modeled in various ways. Popular methods include Lagrange multiplier method and penalty method. A thorough discussion of these methods is given in [12]. Gap can be incorporated in nonlinear material behaviour, nonlinear spring behaviour or nonlinear force-displacement behaviour of the support as, for example, in [6, 13, 14]. A gap and a contact could also be modeled as boundary pseudo forces [15]. After gap closure the support produces supporting force proportinal to the displacement as is shown in Figure 3, which illustrates a typical nonlinear force-displacement behaviour of a gap support.

In finite element analyses, a support with a gap can be modeled for example with a gap element (sometimes called contact element) and a spring element, as in [13, 16]. It is to be noted that for example in the ANSYS finite element code the gap element applies the Lagrange multiplier method, penalty method or some other method according to the user's choice [17].

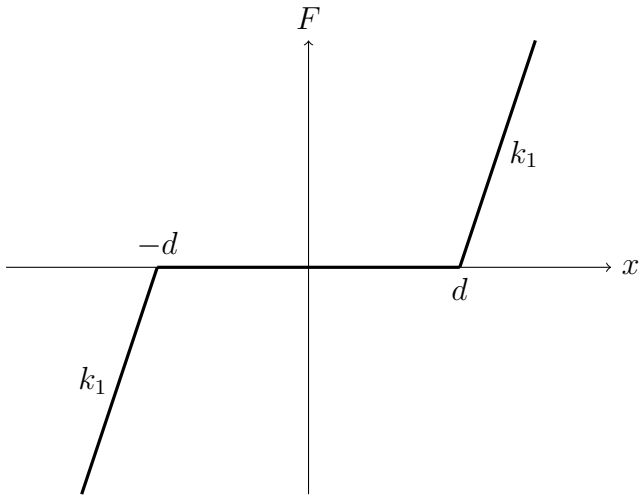

Figure 3: Typical nonlinear force-displacement behaviour of a gap support. Reaction force of support is denoted with F, displacement of system with x, gap size with d and support stiffness with k_1.

2.3.2 Friction modeling

A general discussion on friction modeling is given in [12] and a discussion of support friction in piping analyses is given in [7]. A classic model of friction is the Coulomb law [12]. An example of nonlinear force-displacement behaviour of friction

support under periodic excitation is presented in Figure 4. The force-displacement relationship depends on the friction model chosen and here the classical Coulomb law is used. A constant normal force is assumed. Friction forces occur for example in sliding supports.

In piping analyses, friction force can be modeled as an elastic-perfectly plastic spring, with the maximum friction force kept constant or varying with normal force of the contact which varies with time [18]. Friction can act in two directions on a plane in which case two orthogonal springs can be used [7]. In some cases friction is completely neglected, which could lead to conservative results since friction absorbs energy [19]. However, local loads are then smaller than with friction taken into account. It is to be noted that, for example, in the ANSYS finite element code the friction is incorporated in gap element which applies for example the Coulomb friction law [17].

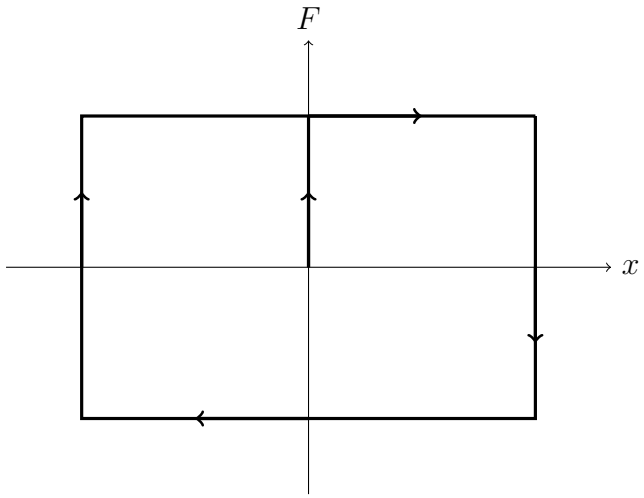

Figure 4: Nonlinear force-displacement behaviour of friction support under periodic excitation with constant normal force. The support force is denoted with F and the displacement of the system with x.

3 Methods for linearization

The goal of linearization is to represent the current nonlinear system as accurately as possible with an equivalent linear system in dynamic analysis. The task is to linearize the nonlinear force-displacement behaviour of the support. In practice, the original nonlinear system is replaced by an equivalent spring or spring-damper system and the spring and damping constants are defined by methods described in this section. An illustration of a single degree-of-freedom gap support and corresponding linearized support along with support force-displacement relationships is shown in Figure 5. The linearized gap support is constructed by replacing the gap support with an equivalent spring.

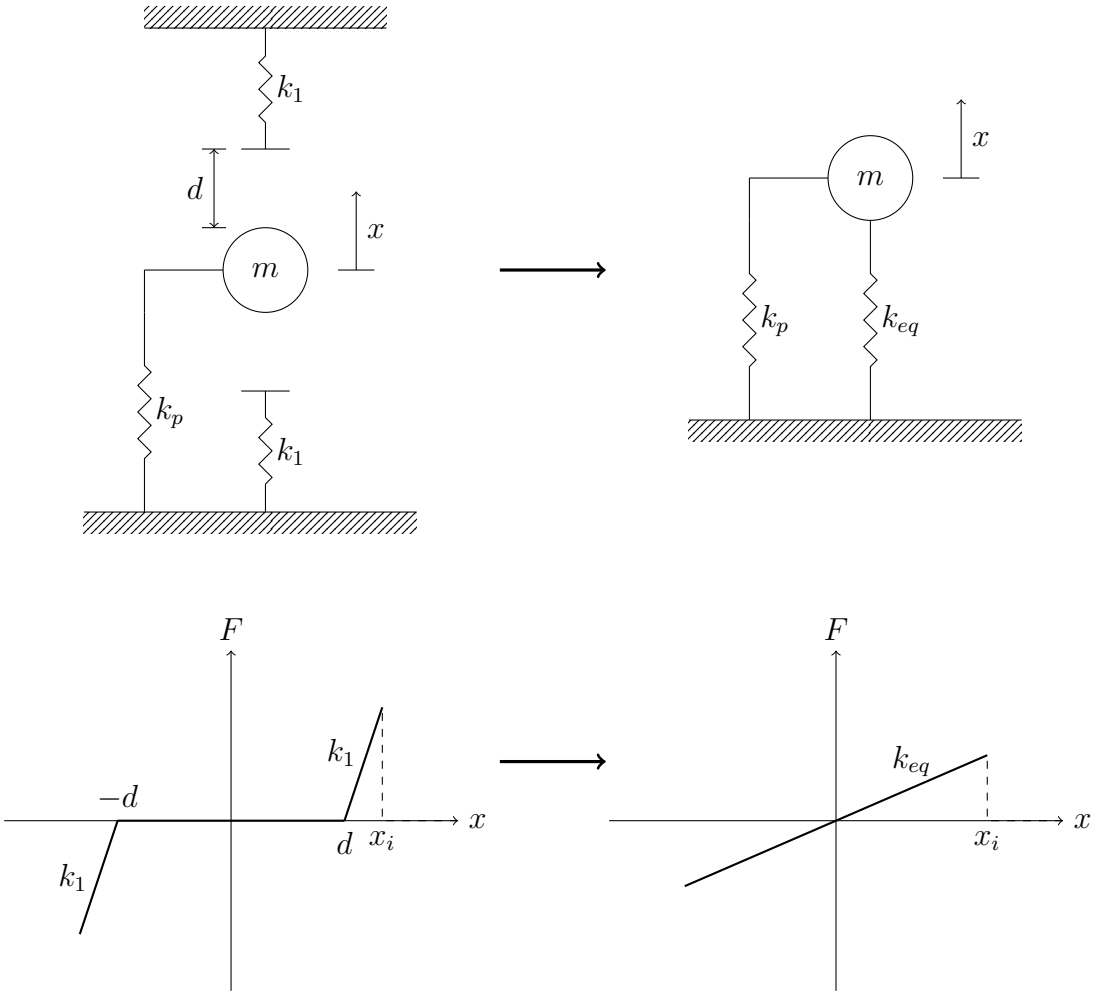

Figure 5: Nonlinear system and equivalent linear system for a single degree-of-freedom gap support. Corresponding force-displacement relationships of the supports are also shown. In the figure d is the gap size, m the mass of the system, k_p the system stiffness, k_1 the nonlinear support stiffness, k_{eq} the equivalent stiffness, F the support force, x the displacement of the system and x_i the maximum displacement of the system.

Several authors [9, 15, 20, 21] suggest that in order to define and analyse an equivalent linear system without solving the original nonlinear problem an iterative procedure is needed. Also original nonlinear support properties are needed. The equivalent linear system depends on the loading and consequently the linearization has to be performed separately to each load case.

Flow chart of the linearization procedure is shown in Figure 6. Linearization methods are presented in Section 3.2 and they are based on minimization of mean squared error between nonlinear and linear system force-displacement relationships, secant stiffness and equivalent energy approach.

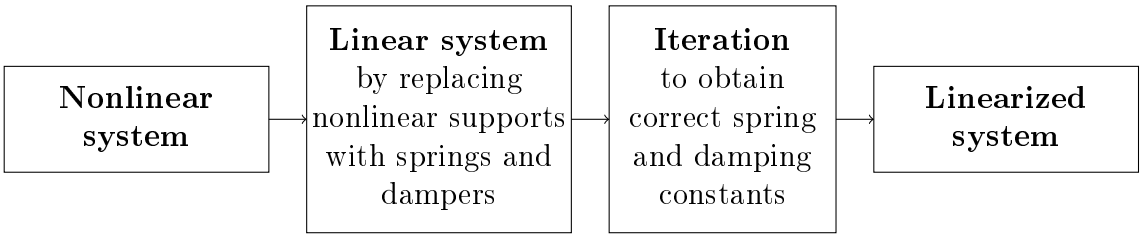

Figure 6: Flow chart of linearization procedure. The linearization has to be performed separately to each load case.

3.1 Iterative procedure

As seen in the flow chart of Figure 6 the iteration plays an essential role in the linearization process. The iterative procedure described here is identical to the procedures described in references [9, 15, 20, 21].

Following the flow chart of Figure 6, the nonlinear supports are replaced with springs and dampers to obtain a linear system. For the iteration, a flow chart is presented in Figure 7. An initial guess is made to determine the spring and damping constants. Iteration is then performed to obtain the correct equivalent spring and damping constants. Once correct equivalent properties have been found, the system is linearized and an equivalent linear system is obtained for the studied load case.

The properties of the equivalent linear system are determined based on the maximum displacement and velocity obtained from dynamic analysis. The analysis is done over the full time period using the linear system. In other words, the maximum displacement and velocity are functions of linearized system properties, which in turn are functions of the maximum displacement and velocity. Hence, an iterative procedure is needed to find such maximum displacement and velocity, that give equivalent stiffness k_{eq} and damping c_{eq}, that give the same maximum displacement and velocity in the analysis.

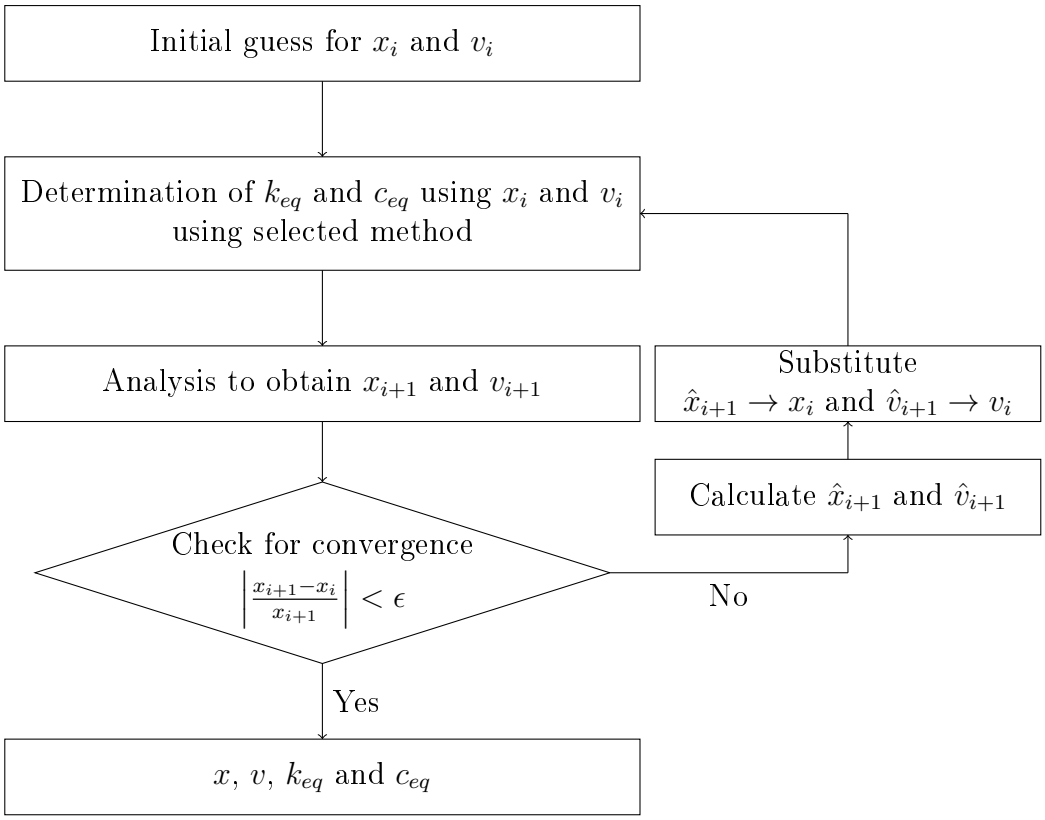

Figure 7: Flow of iterative procedure for one support. In the figure x_i and v_i are the initial values of maximum displacement and velocity for the iteration step, k_{eq} and c_{eq} are the equivalent stiffness and damping, x_{i+1} and v_{i+1} are the resulting maximum displacement and velocity of iteration, $\hat{x}_{i+1}$ and $\hat{v}_{i+1}$ are the initial values for the next iteration step and ϵ is the convergence criterion.

The iteration procedure can be expressed in the form of a flow chart as is presented in Figure 7. A mathematical expression of the iteration procedure is shown later. First an initial guess of the linear system response is made i.e. a guess of maximum displacement x_i and velocity v_i is made. Using x_i and v_i the equivalent system properties k_{eq} and c_{eq} are determined using the selected linearization method. Different methods are presented in Sections 3.2.1 and 3.2.2. Then, using k_{eq} and c_{eq} the linear system response is calculated i.e. analysis is performed to obtain x_{i+1} and v_{i+1}. The convergence of the iteration is checked using relative difference of the starting point x_i and the resulting maximum displacement x_{i+1}. If the relative difference is within some chosen tolerance ϵ, the solution is considered converged and the linearized system and its response is obtained. If the relative difference is larger than ϵ, starting points for the next iteration $\hat{x}_{i+1}$ and $\hat{v}_{i+1}$ are calculated. They are then substituted $\hat{x}_{i+1} \rightarrow x_i$ and $\hat{v}_{i+1} \rightarrow v_i$ and x_i and v_i are used as starting points for the next iteration.

Mathematically iterative procedures are usually expressed in the form

$x_{i+1} = f(x_i)$. Let us denote the iteration variables with vectors

$$\mathbf{x_i} = \begin{Bmatrix} x_i \\ v_i \end{Bmatrix}, \tag{4}$$

and

$$\mathbf{x_{i+1}} = \begin{Bmatrix} x_{i+1} \\ v_{i+1} \end{Bmatrix} \tag{5}$$

and equivalent properties with

$$\mathbf{p_{eq}} = \begin{Bmatrix} k_{eq} \\ c_{eq} \end{Bmatrix} \tag{6}$$

The equivalent properties are a function of displacement and velocity

$$\mathbf{p_{eq}} = h(\mathbf{x_i}) \tag{7}$$

and the new displacement and velocity are a function of equivalent properties

$$\mathbf{x_{i+1}} = g(\mathbf{p_{eq}}) \tag{8}$$

Combining Equations (7) and (8) gives

$$\mathbf{x_{i+1}} = g(h(\mathbf{x_i})) \tag{9}$$

which can be rewritten as

$$\mathbf{x_{i+1}} = f(\mathbf{x_i}) \tag{10}$$

The function h in Equation (7) represents the way that an equivalent stiffness and damping are calculated based on the displacement x_i and velocity v_i. Different methods are presented in Sections 3.2.1 and 3.2.2.

Function g in Equation (8) represents the calculation of the displacement and velocity or analysis with the linear system properties. When analysing complex systems this is done for example using the finite element method. Function g might be difficult to define analytically. Equation (10) is a recurrence relation or iterative formula which defines a sequence of values of $\mathbf{x}$. Function g and Equation (10) are derived for a single degree-of-freedom gap support system in Section 3.3.1 and friction support system in Section 3.3.2.

It is desirable that the sequence of values $\mathbf{x}$, i.e. displacement x and velocity v, converges to some finite value as number of iterations i increases. However, it is not evident that an iteration defined by Equation (10) will converge. In a simple iteration the result of the previous iteration is used as the starting point for the next iteration i.e. substituting $\mathbf{x_{i+1}} \rightarrow \mathbf{x_i}$. To improve convergence, the starting point for the next iteration is calculated based on both $\mathbf{x_i}$ and $\mathbf{x_{i+1}}$. In this study the under-relaxation method is used, and the starting point for the next iteration $\hat{\mathbf{x}}_{\mathbf{i+1}}$ is calculated as [22]

$$\hat{\mathbf{x}}_{\mathbf{i+1}} = \mathbf{x_i} + (\mathbf{x_{i+1}} - \mathbf{x_i})\alpha \tag{11}$$

The relaxation factor α can be kept constant or varied between iterations. For under-relaxation method the value of α is in the interval $0 < \alpha < 1$. Practically this means that the starting point for next iteration is somewhere between $\mathbf{x_i}$ and $\mathbf{x_{i+1}}$, in a position determined by α. The $\mathbf{x_{i+1}}$ "drags" the starting point for next iteration away from $\mathbf{x_i}$ towards $\mathbf{x_{i+1}}$ by the amount of α times the difference.

3.2 Linearization of piping supports

3.2.1 Gap supports

For a gap support, damping is neglected for simplicity in this study. This can be justified by the fact that real-world gap supports investigated in Section 4 exhibit very small damping characteristics. As will be shown later, equivalent stiffness depends only on displacement x, whereas equivalent damping could depend on the velocity v as well. Neglecting damping means that the velocity v and equivalent damping c_{eq} can be dropped out of the iteration. Thus in the iterative procedure the only iteration variable is the displacement x and the only equivalent property concerned is the stiffness k_{eq}. The determination of equivalent stiffness is based on maximum displacement and methods are presented in this section. The different methods introduced here are Caughey's method, secant stiffness, min-max stiffness and equivalent energy approach. This section follows references [6, 9, 15, 20, 21, 23, 24, 25, 26, 27, 28, 29, 30, 31, 32, 33, 34, 35].

Equivalent stiffness by Caughey's method

Caughey's method has been used in piping analyses in references [6, 20, 23, 24] and in structural analyses in [9]. Illustration of equivalent stiffness by the method is presented in Figure 8. Caughey's method for calculating the equivalent stiffness is based on minimization of mean squared error between the nonlinear and equivalent linear support force-displacement response, as follows. The derivation is given in reference [25] and the main idea is presented in the following. The equation of motion for a nonlinear single degree-of-freedom system is

$$\ddot{x} + \frac{c_1}{m}\dot{x} + \frac{k_1}{m}x + \eta q(x, \dot{x}, t) = f_m(t) \tag{12}$$

where c_1 is support damping, m is mass, k_1 is stiffness, q is nonlinearity of the system expressed in force per unit mass and $f_m(t)$ is force per unit mass. Parameters c_1 and η are assumed to be small so that the system is lightly damped and weakly nonlinear. Equation (12) can be expressed using equivalent linear properties and error term as

$$\ddot{x} + \frac{c_{eq}}{m}\dot{x} + \frac{k_{eq}}{m}x + e(x, \dot{x}, t) = f_m(t) \tag{13}$$

where c_{eq} and k_{eq} are equivalent linear damping and stiffness and $e(x, \dot{x}, t)$ is the error term. To obtain a linear system the equivalent linear properties c_{eq} and k_{eq} should be chosen so that the error term is minimized. Combining Equations (12) and (13) and solving for error term yields

$$e(x, \dot{x}, t) = \left(\frac{c_1}{m} - \frac{c_{eq}}{m}\right)\dot{x} + \left(\frac{k_1}{m} - \frac{k_{eq}}{m}\right)x + \eta q(x, \dot{x}, t) \tag{14}$$

In reference [25] this error term is minimized by minimizing its mean squared value. As a result, for a gap support of Figure 3 the equivalent stiffness according to

Caughey's method is [20]

$$k_{eq} = \frac{k_1}{\pi}(\pi - 2\theta - \sin 2\theta) \tag{15}$$

where

$$\theta = \arcsin \frac{d}{x_i} \tag{16}$$

and k_1 is the support stiffness, d the gap size and x_i the maximum displacement. From Equation (16) we have $\sin\theta = \frac{d}{x_i}$ and it is immediately seen that $0 \leq \frac{d}{x_i} \leq 1$ must hold since the codomain of sine function is $[-1, 1]$ and d and x_i are positive. This means that the displacement x_i must be greater or equal to gap size d to be able to calculate the equivalent stiffness. If $x_i < d$ then the equivalent stiffness according to Caughey's method cannot be calculated. Illustration of stiffness by Caughey's method is presented in Figure 8.

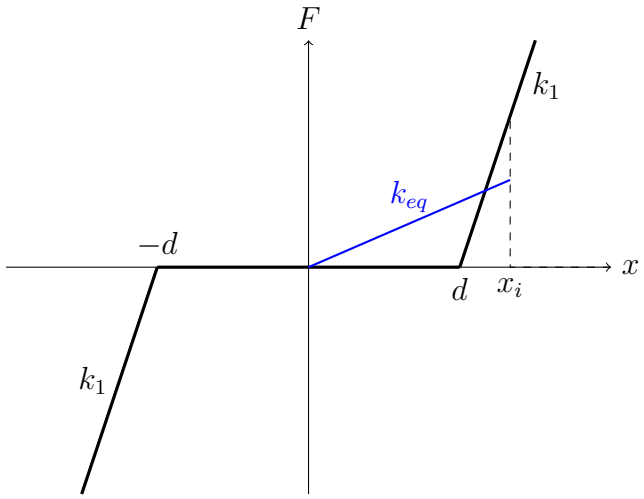

Figure 8: The illustration of stiffness by Caughey's method. In the figure x is the system displacement, F is the support force, x_i is the initial value of maximum displacement for the iteration step, d is the gap size, k_1 is the support stiffness and k_{eq} is the equivalent stiffness.

In this study damping is neglected for gap supports. However, if damping is desired to be taken into account, the equivalent damping for a gap support according to Caughey's method is [20]

$$c_{eq} = \frac{c_1}{\pi}(\pi - 2\theta - \sin 2\theta) \tag{17}$$

where θ is calculated using Equation (16) and c_1 is the nonlinear support damping.

Equivalent stiffness by secant stiffness

Secant stiffness is used for example in seismic analyses of buildings and in analyses of hysteretic systems in references [9, 26, 27, 28, 29, 30, 31, 32]. Secant stiffness

has been used in piping analysis in reference [20]. Sometimes the secant stiffness method is referred to as Jacobsen's method [20].

The secant stiffness is obtained by drawing a straight line from the origin to the nonlinear force-displacement curve at displacement x_i as illustrated by Figure 9.

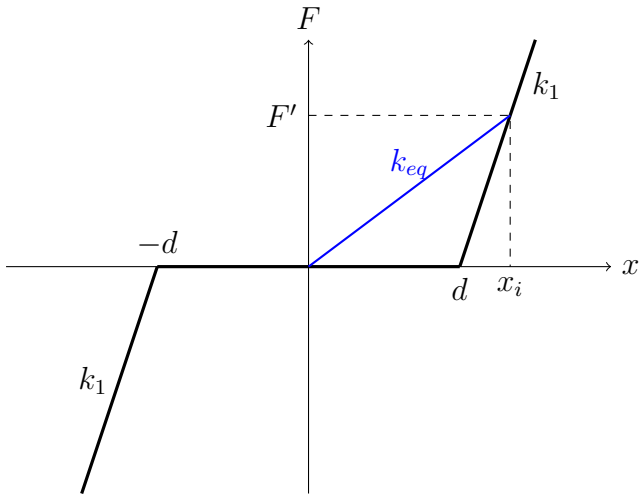

Figure 9: The illustration of secant stiffness method. In the figure x is the system displacement, F is the support force, x_i is the initial value of maximum displacement for the iteration step, d is the gap size, k_1 is the support stiffness and k_{eq} is the equivalent stiffness.

Using the notations of Figure 9, the equivalent stiffness based on secant stiffness is calculated as

$$k_{eq} = \frac{F'}{x_i} = \frac{k_1(x_i - d)}{x_i} = k_1\left(1 - \frac{d}{x_i}\right) \tag{18}$$

Equivalent stiffness by min-max stiffness

One method to calculate the equivalent stiffness is to consider the minimum and maximum displacements of the system obtained from dynamic analysis and calculating the stiffness using the corresponding minimum and maximum points of nonlinear force-displacement relationship [33]. This is illustrated in Figure 10. This method can be described as min-max stiffness and is more accurate than secant stiffness method if the gaps are unequal on both sides of the pipe. If the gaps on both sides of the pipe are equal, the min-max stiffness is reduced to secant stiffness.

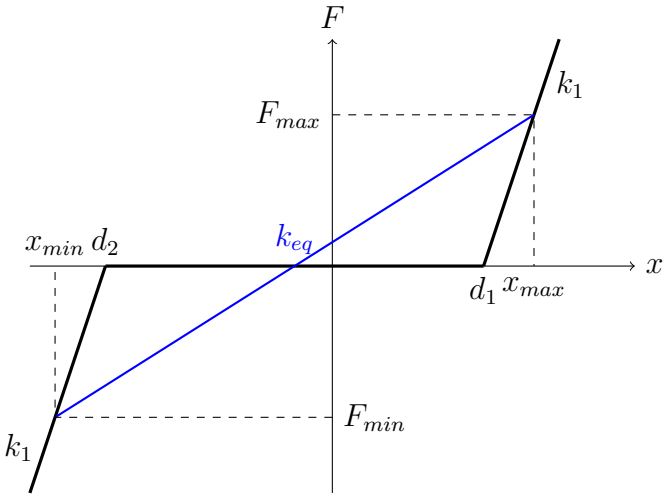

Figure 10: The illustration of min-max stiffness with unequal gaps. In the figure x is the system displacement, F is the support force, F_{min} is the minimum support force, F_{max} is the maximum support force, x_{min} is the minimum displacement of the system, x_{max} is the maximum displacement of the system, d_1 and d_2 are the gap sizes on the positive and negative sides, k_1 is the support stiffness and k_{eq} is the equivalent stiffness.

The equivalent stiffness based on min-max stiffness is calculated as

$$k_{eq} = \frac{F_{max} - F_{min}}{x_{max} - x_{min}} = \frac{k_1(x_{max} - d_1) - k_1(x_{min} - d_2)}{x_{max} - x_{min}} \tag{19}$$

Equivalent stiffness by equivalent energy approach

Following the ideas of references [15], [21] and [34] the equivalent energy approach can be used to determine the equivalent stiffness. The idea is that the maximum potential energy stored by the original nonlinear support equals the maximum potential energy stored by the equivalent linear spring. Iwan [35] comments that the maximum displacement obtained this way might not represent accurately the displacement of the original nonlinear system. An illustration of the equivalent stiffness by equivalent energy approach is shown in Figure 11.

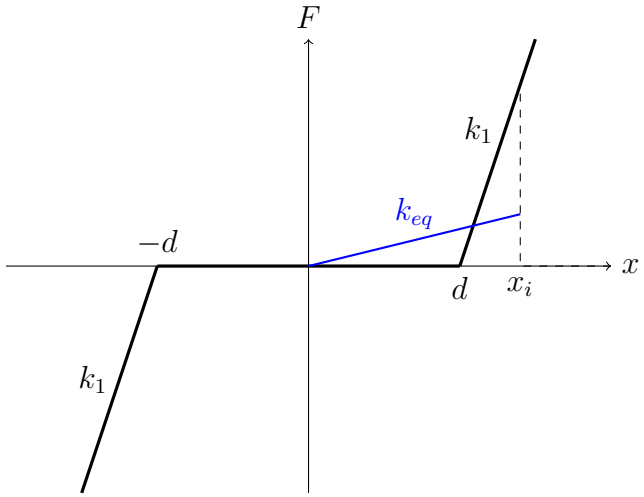

Figure 11: The illustration of stiffness by equivalent energy approach. In the figure x is the system displacement, F is the support force, x_i is the initial value of maximum displacement for the iteration step, d is the gap size, k_1 is the support stiffness and k_{eq} is the equivalent stiffness.

The equivalent stiffness based on equivalent energy approach is derived using the notations of Figure 11. The maximum potential energies of the nonlinear and linear supports are

$$E_{nonlinear} = \frac{1}{2}k_1(x_i - d)^2 \tag{20}$$

$$E_{linear} = \frac{1}{2}k_{eq}x_i^2 \tag{21}$$

Equating these gives

$$\frac{1}{2}k_1(x_i - d)^2 = \frac{1}{2}k_{eq}x_i^2 \tag{22}$$

from which k_{eq} can be calculated as

$$k_{eq} = \frac{k_1(x_i - d)^2}{x_i^2} \tag{23}$$

and when further simplified

$$k_{eq} = k_1\left(1 - \frac{d}{x_i}\right)^2 \tag{24}$$

Graphically the equivalent stiffness obtained with this method could be interpreted as the stiffness which gives the same area under the curve as the nonlinear system for a given displacement x_i. A summary of the methods for calculating the equivalent stiffness for a gap support is presented in Table 1.

Table 1: Summary of the methods to determine the equivalent stiffness k_{eq} for a gap support. For each method, the calculation formula is shown and a short description of the principle is given. The notations are as follows: k_1 is the nonlinear support stiffness, d the gap size, x_i and x_{max} maximum displacement of the system, x_{min} minimum displacment of the system and d_1 and d_2 gap sizes on the positive and negative sides.

Method	$\mathbf{k_{eq}}$	**Principle**
Caughey's method	$\frac{k_1}{\pi}(\pi - 2\theta - \sin 2\theta)$ where $\theta = \arcsin \frac{d}{x_i}$	Minimization of mean squared error
Secant stiffness	$k_1 \left(1 - \frac{d}{x_i}\right)$	Maximum displacement and corresponding nonlinear force
Min-max stiffness	$\frac{k_1(x_{max}-d_1)-k_1(x_{min}-d_2)}{x_{max}-x_{min}}$	Minimum and maximum displacements and corresponding nonlinear forces
Equivalent energy approach	$k_1 \left(1 - \frac{d}{x_i}\right)^2$	Equal maximum potential energies stored

As seen in Table 1, different methods give different values for the equivalent stiffness k_{eq}. A comparison of the values of k_{eq} is presented in Figure 12 for the methods. Min-max stiffness is drawn with secant stiffness since it gives a value equal to secant stiffness when gaps are equal on both sides. Results are presented as a function of the ratio of maximum displacement to the gap size, $\frac{x_i}{d}$.

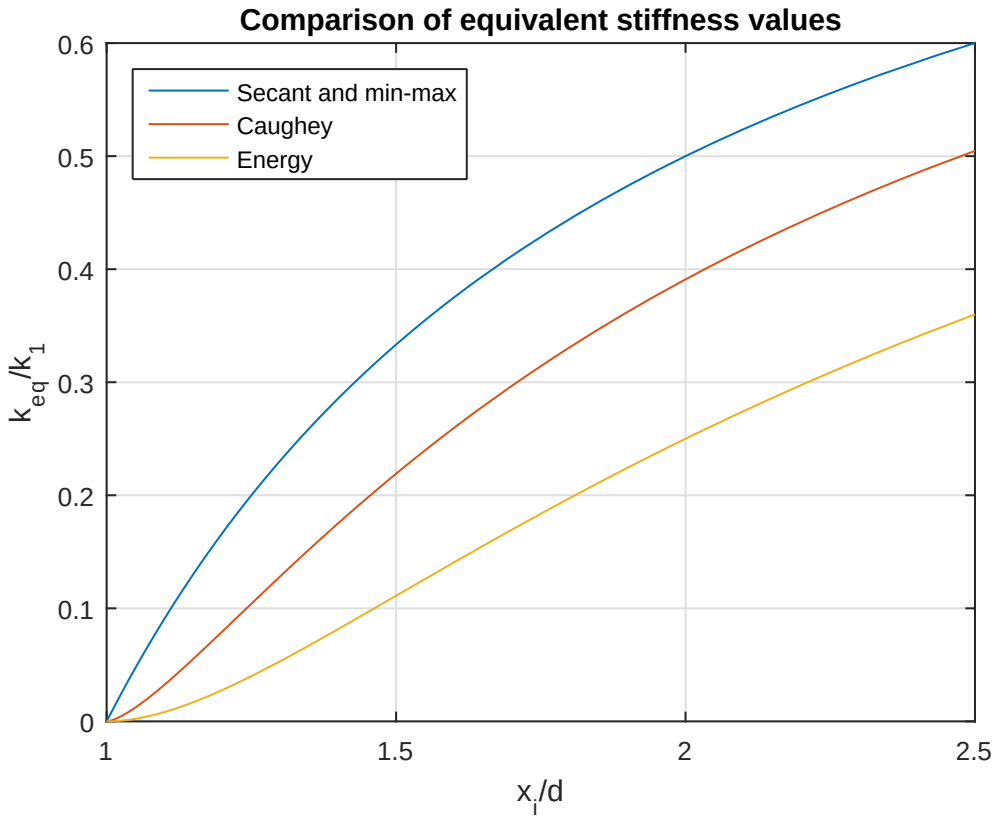

Figure 12: Comparison of methods to calculate the equivalent stiffness for a gap support. In the figure x_i is the initial value of maximum displacement for the iteration step, d is the gap size, k_1 is the support stiffness and k_{eq} is the equivalent stiffness.

The stiffnesses in Figure 12 are non-dimensionalized by dividing by stiffness of nonlinear support after gap closure, k_1. As seen in Figure 12, for a given ratio of $\frac{x_i}{d}$, secant stiffness and min-max stiffness give the highest value of the equivalent stiffness whereas equivalent energy approach gives the lowest equivalent stiffness and Caughey's method gives a stiffness in between.

If the displacement x_i is smaller than the gap d, the stiffness according to Caughey's method cannot be calculated. Moreover, with the other methods such a displacement would yield unrealistic stiffnesses. In this study, if the resulting displacement x_{i+1} is smaller than the gap, $x_{i+1} < d$, the displacement x_{i+1} is assigned the value of the gap. This is to make sure the starting point for the iteration x_i becomes such that the equivalent stiffness can be calculated. In the case where the starting point has the value of the gap, $x_i = d$, the equivalent stiffness becomes zero.

3.2.2 Friction supports

Iterative procedure for friction supports is as presented in Figure 7. The iteration variables are displacement x and velocity v and the equivalent properties related are stiffness k_{eq} and damping c_{eq}. Two methods, equivalent energy dissipation method

and Jacobsen's method, are presented to calculate the equivalent stiffness and damping for a friction support. This section follows references [20, 36, 37, 38].

Equivalent damping by equivalent energy dissipation

Friction force is often modelled in dynamic analyses by an equivalent damper. In the equivalent energy dissipation method the underlying idea is that the energy dissipated during one cycle at steady state vibration is equal in the linear and nonlinear cases. [36, 37, 38] Equivalent stiffness in this method is zero, $k_{eq} = 0$. The derivation of equivalent damping coefficient below follows references [36, 37, 38].

The nonlinear force-displacement behaviour of friction support under periodic excitation is presented in Figure 13. This force-displacement relationship depends on the friction model and here the classical Coulomb law is used, along with the assumption of constant normal force.

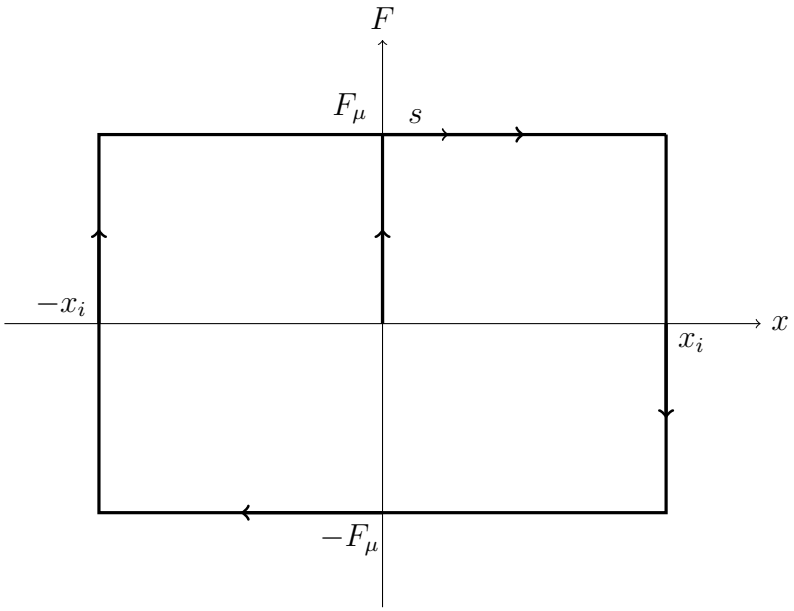

Figure 13: Nonlinear force-displacement behaviour of friction support under periodic excitation. In the figure x is the system displacement, F is the support force, x_i is the maximum displacement of the system, F_μ is the maximum friction force and s is the coordinate travelling through the force-displacement curve.

Assuming that the vibration of the system is sinusoidal with a constant amplitude x_i and angular velocity ω, and denoting the friction force with F_μ the energy dissipated by the friction force in Figure 13 during one cycle is

$$E_\mu = \oint_s F_\mu ds = 4F_\mu x_i = 4\mu F_n x_i \tag{25}$$

where μ is the coefficient of friction, F_n is the surface normal force and s is the coordinate travelling through the force-displacement curve. Both μ and F_n remain

constant. The energy dissipated by the equivalent damper during one cycle is

$$E_c = 2 \int_{-x_i}^{x_i} F_c dx \tag{26}$$

The force by the equivalent damper is given by $F_c = c_{eq}\dot{x}(t)$ where $\dot{x}(t)$ is the time derivative of displacement. Assuming a sinusoidal vibration with a constant amplitude x_i and angular velocity ω the displacement is $x(t) = x_i \sin(\omega t)$ and the time derivative is $\dot{x}(t) = x_i\omega\cos(\omega t)$. The force becomes $F_c = c_{eq}x_i\omega\cos(\omega t)$. The integration variable is changed $dx = \frac{dx}{dt}dt = \dot{x}dt$ and the limits are changed accordingly. Equation (26) becomes

$$E_c = \int_0^{\frac{2\pi}{\omega}} c_{eq}\dot{x}(t)^2 dt = \int_0^{\frac{2\pi}{\omega}} c_{eq}x_i^2\omega^2\cos^2(\omega t)dt = c_{eq}x_i^2\omega^2\frac{\pi}{\omega} = c_{eq}x_i^2\omega\pi \tag{27}$$

Equating the energies dissipated in Equations (25) and (27) gives

$$4\mu F_n x_i = c_{eq}x_i^2\omega\pi \tag{28}$$

which yields the expression for equivalent damping coefficient

$$c_{eq} = \frac{4\mu F_n}{x_i\omega\pi} \tag{29}$$

If the angular velocity of the vibration is not known, one can replace $x_i\omega = v_i$ which follows from the sinusoidal displacement assumption. The equivalent damping coefficient is then

$$c_{eq} = \frac{4\mu F_n}{v_i\pi} \tag{30}$$

where v_i is the maximum velocity of the system. The force-displacement behaviour of nonlinear and linearized friction support under periodic excitation is presented in Figure 14 for the equivalent energy dissipation method.

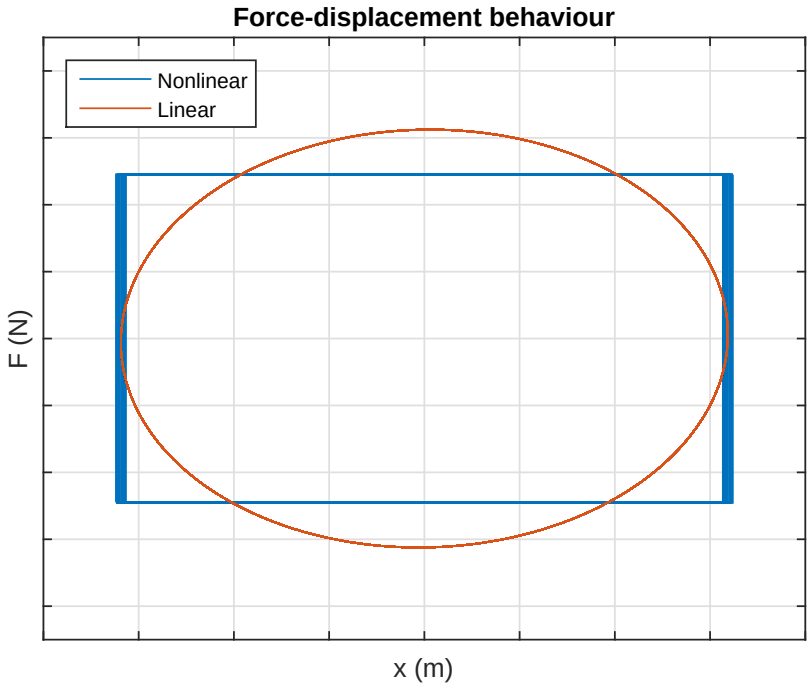

Figure 14: The force-displacement behaviour of nonlinear and linearized friction support under periodic excitation using the equivalent energy dissipation method. In the figure x is the system displacement and F is the support force.

Equivalent stiffness and damping by Jacobsen's method

In Jacobsen's method the equivalent stiffness and damping are determined independently. The stiffness is the same as slope of the line connecting the origin to the point of maximum displacement and maximum friction force [20]. The equation for equivalent stiffness is [20]

$$k_{eq} = \frac{\mu F_n}{x_i} \tag{31}$$

where x_i is the maximum displacement. This is similar to the secant stiffness introduced for a gap support. The equivalent damping is determined in the same way as in the equivalent energy dissipation method and is calculated using the Equation 30. The force-displacement behaviour of nonlinear and linearized friction support under periodic excitation is presented in Figure 15. Comparing Jacobsen's method with the equivalent energy dissipation, it is noticed that Jacobsen's method introduces an equivalent stiffness in addition to damping. Both methods thus dissipate equal amount of energy with the nonlinear system, but Jacobsen's method has also elastic energy.

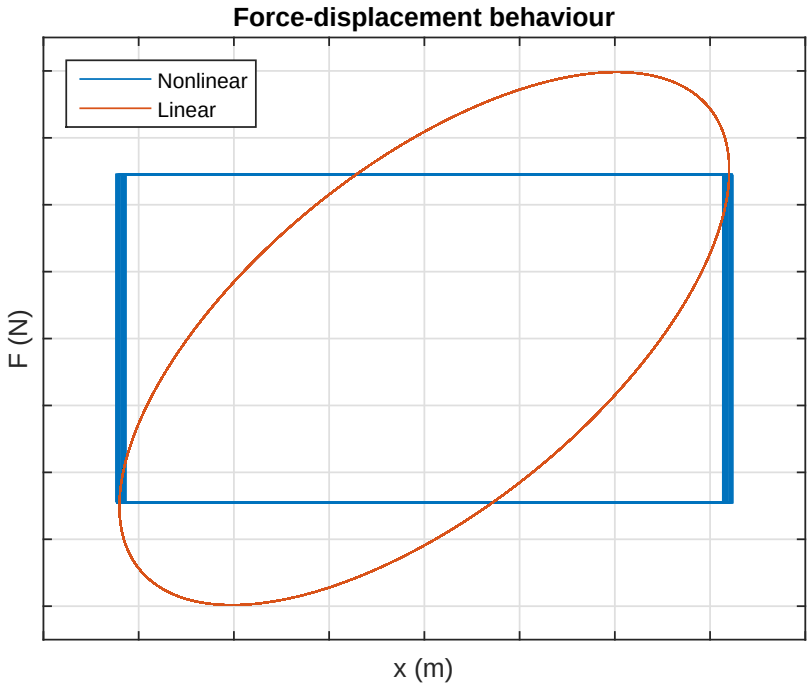

Figure 15: The force-displacement behaviour of nonlinear and linearized friction support under periodic excitation using the Jacobsen's method. In the figure x is the system displacement and F is the support force.

The formulas for equivalent stiffness and damping for a friction support are summarized in Table 2.

Table 2: Summary of the formulas to determine k_{eq} and c_{eq} for a friction support. In the table μ is the coefficient of friction, F_n is the surface normal force and x_i and v_i are the initial values of maximum displacement and velocity for the iteration step.

Method	$\mathbf{k_{eq}}$	$\mathbf{c_{eq}}$
Equivalent energy dissipation	0	$\frac{4\mu F_n}{v_i \pi}$
Jacobsen	$\frac{\mu F_n}{x_i}$	$\frac{4\mu F_n}{v_i \pi}$

3.3 Single degree-of-freedom systems

The linearization procedure for piping supports is investigated using two single degree-of-freedom examples: a gap support and a friction support. Using these examples the procedure can be demonstrated and examined. Deep understanding is aquired of the iteration and different methods to calculate the equivalent properties.

Convergence of the iteration is briefly studied. After this, the method is applied to the general multiple degree-of-freedom case in Section 3.4.

3.3.1 Gap support

Iteration procedure

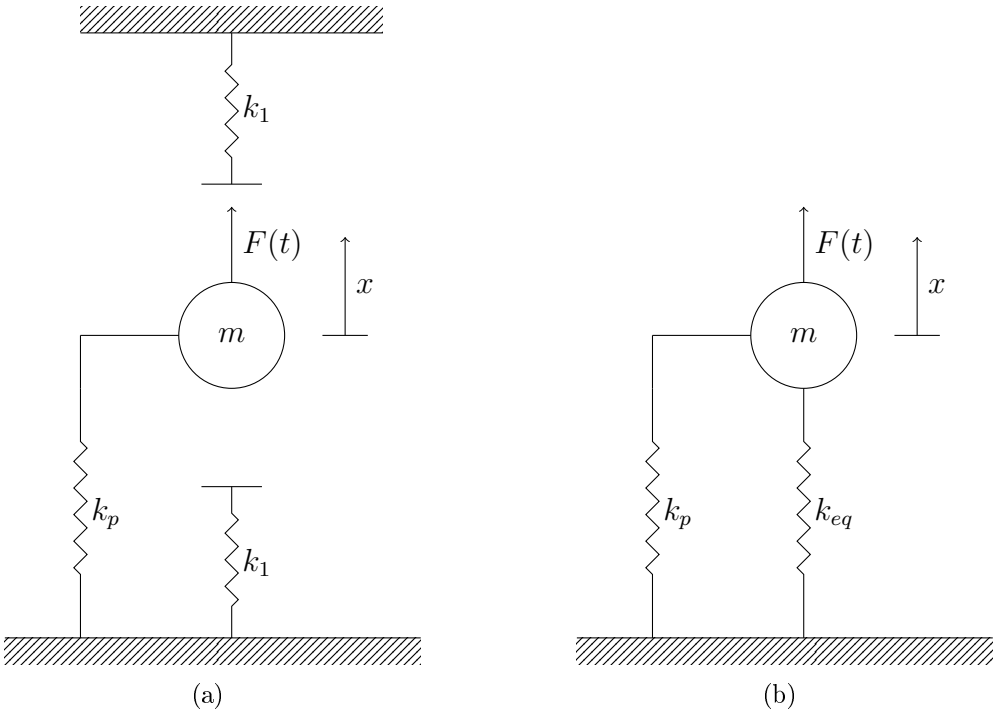

Figure 16: Single degree-of-freedom systems of a) a gap support and b) its linearized form. In the figure m is the mass of the system, k_p the system stiffness, k_1 the nonlinear support stiffness, k_{eq} the equivalent stiffness, $F(t)$ the applied loading and x the displacement of the system.

A single-degree-of-freedom gap support system is presented in Figure 16(a) and its linearized form in Figure 16(b). The system has a linear stiffness k_p, the mass of the system is m, the applied loading is $F(t)$ and the gap support stiffness is k_1. In principle, the supports can have mass that affects the system when the gap closes. Support mass is, however, neglected in this study. In the linearized system the gap support is replaced by an equivalent spring with stiffness k_{eq} as is shown in Figure 16(b).

The equation of motion of the system of Figure 16(b) is

$$-k_{eq}x - k_p x + F(t) = m\ddot{x} \tag{32}$$

where k_{eq} is the equivalent support stiffness, k_p is the system stiffness, $F(t)$ is the loading and m is the mass of the system. A harmonic excitation $F(t) = F_{amp}\sin(\omega t)$

is assumed. The maximum value of displacement is derived from the equation of motion and the derivation is given in Appendix A. The maximum value of displacement becomes

$$x_{max} = \left| \frac{F_{amp}/m}{\frac{k_{eq}+k_p}{m} - \omega^2} \left(1 + \frac{\omega}{\sqrt{\frac{k_{eq}+k_p}{m}}} \right) \right| \tag{33}$$

Right side of Equation (33) represents the function g of Equation (8). Equivalent stiffness k_{eq} could be calculated using any of the methods of Section 3.2.1 and in this example Caughey's method is used to calculate the equivalent stiffness.

Substituting the expression of Caughey's stiffness of Equation (15) and θ of Equation (16) to Equation (33) the following expression for maximum displacement is obtained

$$x_{max} = \left| \frac{F_{amp}/m}{\frac{\frac{k_1}{\pi}(\pi - 2\arcsin\frac{d}{x_i} - \sin(2\arcsin\frac{d}{x_i})) + k_p}{m} - \omega^2} \left(1 + \frac{\omega}{\sqrt{\frac{\frac{k_1}{\pi}(\pi - 2\arcsin\frac{d}{x_i} - \sin(2\arcsin\frac{d}{x_i})) + k_p}{m}}} \right) \right| \tag{34}$$

The equivalent stiffness is calculated based on maximum displacement x_i based on initial guess or previous iteration. The calculated x_{max} is a new maximum displacement and we may substitute $x_{max} \rightarrow x_{i+1}$. Using this notation Equation (34) can be rewritten

$$x_{i+1} = \left| \frac{F_{amp}/m}{\frac{\frac{k_1}{\pi}(\pi - 2\arcsin\frac{d}{x_i} - \sin(2\arcsin\frac{d}{x_i})) + k_p}{m} - \omega^2} \left(1 + \frac{\omega}{\sqrt{\frac{\frac{k_1}{\pi}(\pi - 2\arcsin\frac{d}{x_i} - \sin(2\arcsin\frac{d}{x_i})) + k_p}{m}}} \right) \right| \tag{35}$$

Equation (35) represents the recurrence relation or iterative formula of Equation (10) to calculate displacement of an equivalent linear system for a single degree-of-freedom gap support system under sinusoidal loading using Caughey's method to calculate equivalent stiffness. The iterative formula is then used with the under-relaxation method

$$\hat{x}_{i+1} = x_i + (x_{i+1} - x_i)\alpha \tag{36}$$

to calculate the initial value for the next iteration step. Equation (35) could be directly inserted into Equation (36) to get a simple iteration procedure, however, for clarity these are kept apart. Equation (35) is to be evaluated, and Equation (36) is a specific method to find the solution by refining the iteration. Using the under-relaxation was found necessary to achieve convergence of the iteration.

Numerical example

A numerical example is presented to illustrate the procedure. Equation (35) is used with Equation (36) to perform the iteration. The parameter values used in the example are shown in Table 3. If the resulting displacement is less than the gap,

$x_{i+1} < d$, the displacement x_{i+1} is given the value of the gap. This is to make sure that the equivalent stiffness can be calculated, see Section 3.2.1 for details. An initial guess of $x_0 = 0{,}2\,\mathrm{m}$ is made. Table 4 shows the progress of the iteration. Figures 17 and 18 show the progress in two graphs.

Table 3: Parameter values used in the single degree-of-freedom gap support example.

Parameter	**Symbol**	**Unit**	**Value**
Force amplitude	F_{amp}	N	10 000
Excitation angular velocity	ω	$\frac{1}{\mathrm{s}}$	40π
Mass of the system	m	kg	10
Nonlinear support stiffness	k_1	$\frac{\mathrm{N}}{\mathrm{m}}$	1 000 000
System stiffness	k_p	$\frac{\mathrm{N}}{\mathrm{m}}$	1000
Gap size	d	m	0,1
Convergence criterion	ϵ	–	0,001
Relaxation parameter	α	–	0,2

Table 4: Example of the iterative procedure for a single degree-of-freedom gap support. In the table x_i is the initial value of maximum displacement for the iteration step, x_{i+1} is the resulting maximum displacement, $\hat{x}_{i+1}$ is the initial value for the next iteration step and k_{eq} is the equivalent stiffness.

x_i[m]	$k_{eq}\left[10^5 \frac{\mathrm{N}}{\mathrm{m}}\right]$	x_{i+1}[m]	$\left\lvert\frac{x_{i+1}-x_i}{x_{i+1}}\right\rvert$	converged	$\hat{x}_{i+1}$[m]
$x_0 = 0{,}2$	3,9100	0,0698	1,864	no	0,18
$x_1 = 0{,}18$	3,3094	0,0971	0,8538	no	0,1640
$x_2 = 0{,}1640$	2,7487	0,1489	0,1012	no	0,1610
$x_3 = 0{,}1610$	2,6341	0,1665	0,0330	no	0,1621
$x_4 = 0{,}1621$	2,6761	0,1596	0,0156	no	0,1616
$x_5 = 0{,}1616$	2,6571	0,1626	0,0064	no	0,1618
$x_6 = 0{,}1618$	2,6652	0,1613	0,0028	no	0,1617
$x_7 = 0{,}1617$	2,6617	0,1619	0,0012	no	0,1617
$x_8 = 0{,}1617$	2,6632	0,1617	0,0005	yes	-

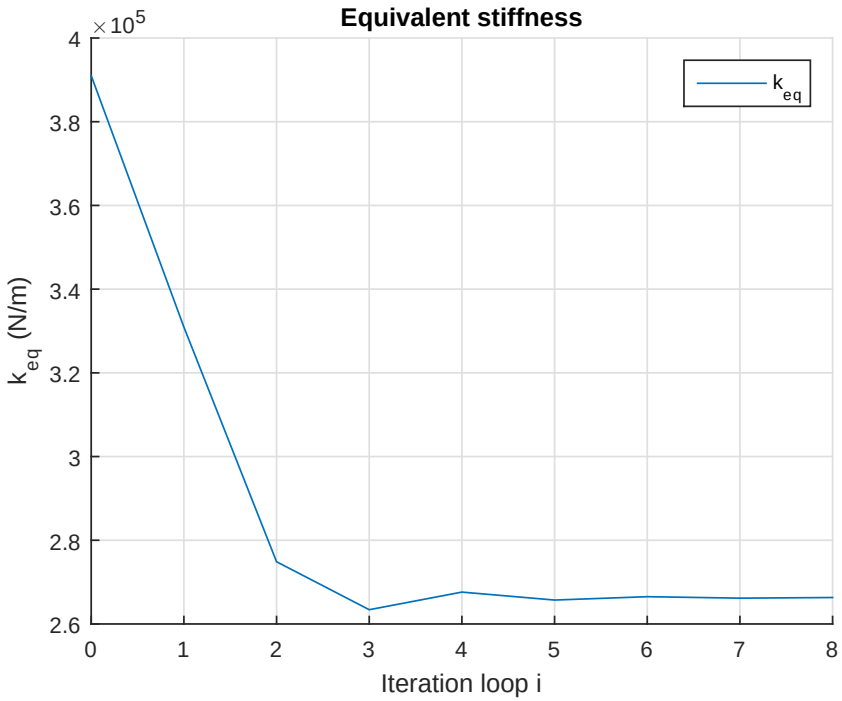

Figure 17: Progress of the equivalent stiffness k_{eq} during the iteration. Iteration loop number is denoted with i.

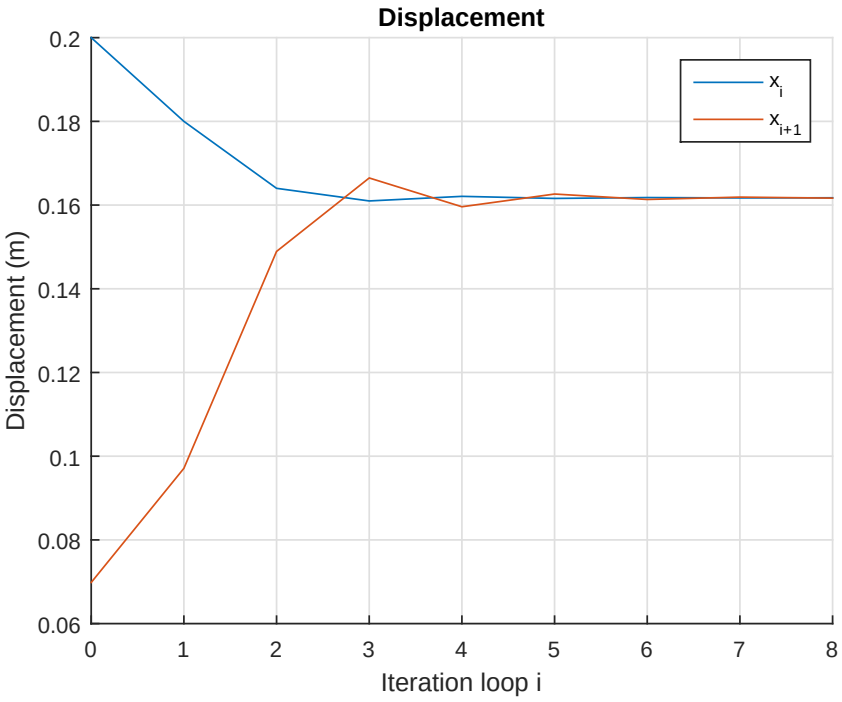

Figure 18: Progress of the displacements during iteration. In the figure x_i is the initial value of maximum displacement for the iteration step, x_{i+1} is the resulting maximum displacement and i is the iteration loop number.

Table 4 shows that for this problem, the resulting displacement is 0,1617 m and the equivalent stiffness for the gap support is $k_{eq} = 2{,}6632 \cdot 10^5 \frac{\mathrm{N}}{\mathrm{m}}$. These are the values of the equivalent linear system for this load case. Different methods to determine equivalent stiffness give different results. For comparison, these are presented in Table 5. Gaps are equal on both sides and consequently min-max stiffness is reduced to secant stiffness.

Table 5: Iterative procedure results for a single degree-of-freedom gap support using different methods to determine the equivalent stiffness k_{eq}. In the table x is the maximum displacement of the system.

Method	$k_{eq}\left[10^5 \frac{\mathrm{N}}{\mathrm{m}}\right]$	x [m]	Number of iterations
Caughey	2,6632	0,1617	8
Secant & Min-max	2,8233	0,1393	10
Energy	2,4734	0,1988	4

Different methods give different results due to their different principles. Iteration using equivalent energy approach converges faster than the other methods because of the initial guess (0,2 m) close to the solution.

3.3.2 Friction support

Iteration procedure

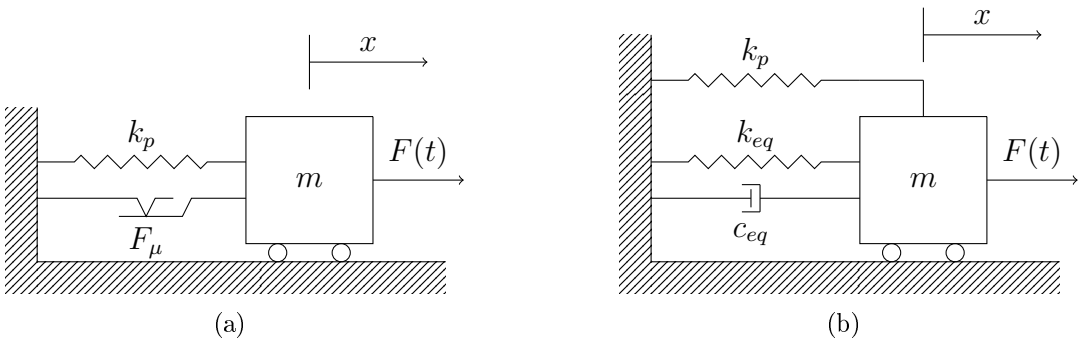

Figure 19: Single degree-of-freedom systems of a) a nonlinear friction support and b) a linearized friction support. In the figure m is the mass of the system, k_p is the system stiffness, F_μ is the frition force, $F(t)$ is the applied loading, x is the displacement of the system and k_{eq} and c_{eq} are the equivalent stiffness and damping.

A single degree-of-freedom friction support system is presented in Figure 19(a) and its linearized form in Figure 19(b). The system has a stiffness k_p, the mass of the system is m, the applied loading is $F(t)$ and the maximum friction force is $F_\mu = \mu F_n$.

In the linearized system the friction force is replaced by an equivalent spring-damper system.

The system of Figure 19(b) was studied and analytical expressions of maximum displacement and velocity were derived in the steady-state vibration. Steady state of the vibration is reached after some time when transient effects have decayed and the system oscillates with the same frequency as the excitation. In this way the linearization procedure can be further examined and demonstrated for the friction support.

The equation of motion for the system of Figure 19(b) is

$$-k_p x - k_{eq} x - c_{eq}\dot{x} + F(t) = m\ddot{x} \tag{37}$$

A harmonic excitation $F(t) = F_{amp}\sin(\omega t)$ is assumed. The maximum values of displacement x_{max} and velocity v_{max} are derived in Appendix B. These are respectively

$$x_{max} = \frac{\omega_n^2 F_{amp}}{(k_p + k_{eq})\sqrt{(\omega^2 - \omega_n^2)^2 + (2\xi\omega\omega_n)^2}} \tag{38}$$

and

$$v_{max} = \frac{\omega_n^2 F_{amp}}{(k_p + k_{eq})\left[(\omega^2 - \omega_n^2)^2 + (2\xi\omega\omega_n)^2\right]}\sqrt{(2\xi\omega^2\omega_n)^2 + ((\omega^2 - \omega_n^2)\omega)^2} \tag{39}$$

where $\omega_n = \sqrt{\frac{k_p+k_{eq}}{m}}$ and $\xi = \frac{c_{eq}}{2\sqrt{m(k_p+k_{eq})}}$. Equivalent stiffness and damping can be calculated using eiher the equivalent energy disspation method, where

$$\begin{cases} k_{eq} = 0 \\ c_{eq} = \frac{4\mu F_n}{v_i \pi} \end{cases} \tag{40}$$

or Jacobsen's method, where

$$\begin{cases} k_{eq} = \frac{\mu F_n}{x_i} \\ c_{eq} = \frac{4\mu F_n}{v_i \pi} \end{cases} \tag{41}$$

Investigating Equations (38) for x_{max} and (39) for v_{max} and using either Equation 40 or 41 to calculate the equivalent properties, we can construct an iterative procedure of the form

$$\begin{cases} x_{i+1} = f_1(x_i, v_i) \\ v_{i+1} = f_2(x_i, v_i) \end{cases} \tag{42}$$

namely

$$\begin{cases} x_{i+1} = \frac{\omega_n^2 F_{amp}}{(k_p+k_{eq})\sqrt{(\omega^2-\omega_n^2)^2+(2\xi\omega\omega_n)^2}} \\ v_{i+1} = \frac{\omega_n^2 F_{amp}}{(k_p+k_{eq})[(\omega^2-\omega_n^2)^2+(2\xi\omega\omega_n)^2]}\sqrt{(2\xi\omega^2\omega_n)^2 + ((\omega^2 - \omega_n^2)\omega)^2} \end{cases} \tag{43}$$

The iteration procedure here is done as a simple iteration, which means that the results of last step are used directly as initial values for the next iteration step. In

under-relaxation method of Equation (11) this means that $\alpha = 1$. The use of simple iteration was found sufficient to achieve convergence of the iteration. The initial values for the iteration step x_i and v_i are inserted into Equation (40) or (41) and so obtained k_{eq} and c_{eq} further to formulas of ω_n and ξ. ω_n and ξ are further inserted into Equation (43) to calculate x_{i+1} and v_{i+1}.

Numerical example

A numerical example is presented using both the equivalent energy dissipation method and Jacobsen's method. The parameter values used in the example are shown in Table 6. Initial guesses for displacement and velocity, respectively, are $x_0 = 0{,}2\,\mathrm{m}$ and $v_0 = 5\,\frac{\mathrm{m}}{\mathrm{s}}$. Tables 7 and 8 show the progress of the iterations and comparison of the results for the two methods is presented in Table 9.

Table 6: Parameter values used in the single degree-of-freedom friction support example.

Parameter	Symbol	Unit	Value
Coefficient of friction	μ	–	0,5
Mass of the system	m	kg	10
Force amplitude	F_{amp}	N	10 000
Excitation angular velocity	ω	$\frac{1}{\mathrm{s}}$	40π
System stiffness	k_p	$\frac{\mathrm{N}}{\mathrm{m}}$	1000
Convergence criterion	ϵ	–	0,001

Table 7: Example of the iterative procedure for a single degree-of-freedom friction support using equivalent energy dissipation method. In the table x_i and v_i are the initial values of maximum displacement and velocity for the iteration step, x_{i+1} and v_{i+1} are the resulting maximum displacement and velocity and k_{eq} and c_{eq} are the equivalent stiffness and damping.

$x_i\,[\mathrm{m}]$, $v_i\,\left[\frac{\mathrm{m}}{\mathrm{s}}\right]$	$k_{eq}\,\left[\frac{\mathrm{N}}{\mathrm{m}}\right]$	$c_{eq}\,\left[\frac{\mathrm{kg}}{\mathrm{s}}\right]$	$x_{i+1}\,[\mathrm{m}]$, $v_{i+1}\,\left[\frac{\mathrm{m}}{\mathrm{s}}\right]$	$\left\lvert\frac{x_{i+1}-x_i}{x_{i+1}}\right\rvert$	converged
$x_0 = 0{,}2000$ $v_0 = 5{,}0000$	0	12,4905	$x_1 = 0{,}0637$ $v_1 = 8{,}0081$	2,1384	no
$x_1 = 0{,}0637$ $v_1 = 8{,}0081$	0	7,7987	$x_2 = 0{,}0637$ $v_2 = 8{,}0083$	0,0000	yes

Table 8: Example of the iterative procedure for a single degree-of-freedom friction support using Jacobsen's method. In the table x_i and v_i are the initial values of maximum displacement and velocity for the iteration step, x_{i+1} and v_{i+1} are the resulting maximum displacement and velocity and k_{eq} and c_{eq} are the equivalent stiffness and damping.

$x_i\,[\mathrm{m}]$, $v_i\left[\frac{\mathrm{m}}{\mathrm{s}}\right]$	$k_{eq}\left[\frac{\mathrm{N}}{\mathrm{m}}\right]$	$c_{eq}\left[\frac{\mathrm{kg}}{\mathrm{s}}\right]$	$x_{i+1}\,[\mathrm{m}]$, $v_{i+1}\left[\frac{\mathrm{m}}{\mathrm{s}}\right]$	$\left\lvert\frac{x_{i+1}-x_i}{x_{i+1}}\right\rvert$	converged
$x_0 = 0{,}2000$ $v_0 = 5{,}0000$	245,2500	12,4905	$x_1 = 0{,}0638$ $v_1 = 8{,}0206$	2,1335	no
$x_1 = 0{,}0638$ $v_1 = 8{,}0206$	768,4972	7,7865	$x_2 = 0{,}0640$ $v_2 = 8{,}0477$	0,0034	no
$x_2 = 0{,}0640$ $v_2 = 8{,}0477$	765,9071	7,7603	$x_3 = 0{,}0640$ $v_3 = 8{,}0476$	0,0000	yes

The convergence of the iteration for these parameter values is fast for both methods. For the equivalent energy dissipation method a third iteration is needed only if the convergence criterion is changed to $\epsilon = 0,00001$. Comparing the values of c_{eq} with the resulting displacements during iteration in Tables 7 and 8, it can be observed that the displacements are not sensitive to variations in damping. Comparison of the results for the two methods is presented in Table 9.

Table 9: Iterative procedure results for a single degree-of-freedom friction support using different methods to determine equivalent stiffness k_{eq} and damping c_{eq}. In the table x and v are the maximum displacement and velocity of the system.

Method	$k_{eq}\left[\frac{\mathrm{N}}{\mathrm{m}}\right]$	$c_{eq}\left[\frac{\mathrm{kg}}{\mathrm{s}}\right]$	$x\,[\mathrm{m}]\,, v\left[\frac{\mathrm{m}}{\mathrm{s}}\right]$	Number of iterations
Eq. energy dissipation	0	7,7987	$x = 0{,}0637$ $v = 8{,}0083$	1
Jacobsen	765,9071	7,7603	$x = 0{,}0640$ $v = 8{,}0476$	2

These examples of gap and friction supports are limited on a single degree-of-freedom system and sinusoidal excitation. The analysis method was analytical solving of the equation of motion. In the general case, the system is much more complicated than a single degree-of-freedom system, the excitation might be other than sinusoidal and the analysis method could be some other than solving the equations of motion analytically. An analytical formula for iteration $x_{i+1} = f(x_i)$ could be very hard or impossible to derive in the general case.

3.3.3 Convergence

It is desirable that the iteration converges to some finite value as number of iterations i increases. The convergence of an iteration defined by $x_{i+1} = f(x_i)$ can be investigated with a convergence condition, for example with [39]

$$|f'(x_\infty)| < 1 \tag{44}$$

where x_∞ is the solution of the iteration. An iteration defined by $x_{i+1} = f(x_i)$ will converge to the solution x_∞ if the absolute value of its derivative at the solution is less than 1 and if inital guess x_0 is sufficiently close to x_∞ [39].

In the case of gap support, for values of loading, support stiffness and gap size that are of the same order of magnitude than the real-world supports, the iteration without under-relaxation was found divergent with the studied methods. In the example of Section 3.3.1 the absolute value of derivative of Equation (35) is over one, $|f'(x_\infty)| > 1$, and the iteration is divergent. This is why additional techniques are required to find the solution. In Section 3.3.1 the under-relaxation method was used. If the solution x_∞ is relatively large compared to gap size the condition of Equation (44) is satisfied.

For the friction support the iteration was found to converge in the example of Section 3.3.2. The absolute value of the derivative is under one, $|f'(x_\infty)| < 1$ and simple iteration was sufficient to find the solution. This suggests convergence for practical values of problem parameters. The limit $|f'(x_\infty)| = 1$ is encountered only if the resulting displacement is unrealistically small.

The expression $|f'(x_\infty)| < 1$ suggests that there could be a way to define an analytical expression of the convergence condition in a practical form, for example that x is smaller or larger to some finite value that depends on problem parameters. This kind of expression would tell us when simple iteration is enough to find the solution, or when additional techniques are needed. However, even for the single degree-of-freedom systems of Sections 3.3.1 and 3.3.2 the expressions become such that x cannot be solved analytically. The conclusion of these trials to find an analytical expression is that the point of $|f'(x)| = 1$ exists in the studied cases but it depends on all the problem parameters.

3.3.4 Initial guess and error

In iterative procedures it is evident that a good initial guess close to the solution leads to the converged solution faster than a distant guess. In this section, the initial guesses are investigated to find out if the guess should be smaller or greater than the actual solution. Basic engineering judgement can be used to estimate the possible domain of solution, but additional information is required to select a good initial guess. The initial guesses are examined by investigating the errors of the initial guess and the first iterate relative to the converged solution of the linear system.

The relative error of the initial guess x_0 is given by

$$x_0^{(err)} = \frac{x_0 - x_\infty}{x_\infty} \tag{45}$$

where x_∞ is the solution of the iterative procedure. The relative error of the next iterate is given by

$$x_1^{(err)} = \frac{x_1 - x_\infty}{x_\infty} = \frac{f(x_0) - x_\infty}{x_\infty} \tag{46}$$

The plot $x_1^{(err)}$ versus $x_0^{(err)}$ is of key interest when considering the characteristics of a good initial guess. To illustrate this, numerical examples are presented for gap and friction supports.

Gap support

Recall the example of Section 3.3.1 of a single degree-of-freedom gap support using Caughey's method to calculate the equivalent stiffness. Equation (35) of the form $x_{i+1} = f(x_i)$ was used along with $\hat{x}_{i+1} = x_i + (x_{i+1} - x_i)\alpha$ to perform the iteration. Equation (46) is slightly modified for this example:

$$x_1^{(err)} = \frac{\hat{x}_1 - x_\infty}{x_\infty} \tag{47}$$

The numerical values of the example of Section 3.3.1 are used. The plot $x_1^{(err)}$ versus $x_0^{(err)}$ for different values of α for gap support is presented in Figure 20. Please note that $x_1^{(err)}$ is plotted using Equation (47) which uses $\hat{x}_1$ and is strongly dependent on α. Also, if resulting displacement x_1 is smaller than the gap d, the x_1 is given the value of d so that the equivalent stiffness can be calculated.

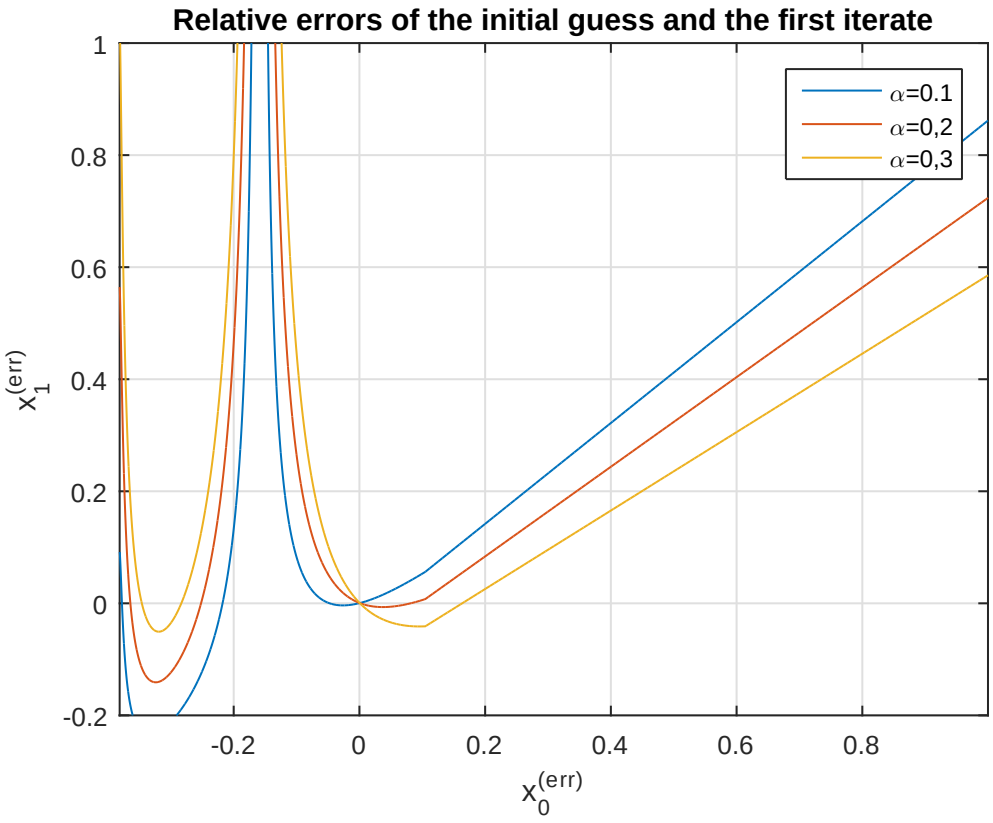

Figure 20: Relative error of the first iterate $x_1^{(err)}$ plotted against relative error of the initial guess $x_0^{(err)}$ for different values of relaxation parameter α for a gap support. The relative errors are measured relative to the converged solution.

Figure 20 should be interpreted so that, for example, if the relative error of initial guess is $+40\,\%$, $x_0^{(err)} = 0{,}4$, then after one iteration the relative error is $+24{,}37\,\%$, or $x_1^{(err)} = 0{,}2437$, for $\alpha = 0{,}2$. As seen from Figure 20 the error grows strongly if the initial guess is lower than the actual result. This depends on problem parameters since the peak is located where the system is at resonance with the excitation. On the other hand, if the initial guess is larger than the actual result, the next iterate still has some amount of error but the error growth rate with increasing $x_0^{(err)}$ is not as high as on the lower side.

The sharp turn at $x_0^{(err)} = 0{,}1049$ is the point at and above which the initial guess x_i is sufficiently large so that the resulting displacement x_1 is below the gap value d and x_1 is assigned the value of d. The multiple zero crossings are a result of the use of the method $\hat{x}_{i+1} = x_i + (x_{i+1} - x_i)\alpha$ to determine the initial value for the next iteration step. As an example for $\alpha = 0{,}3$: if the error of the initial guess is $x_0^{(err)} = 0{,}1635$ the resulting displacement x_1 is smaller than the solution (now also smaller than d), but the value for $\hat{x}_1$ becomes exactly the solution, thus its error is 0. Based on the smaller error growth rate on the domain above the solution, it can be concluded that an initial guess on the larger side is preferred. Errors obtained using secant stiffness or equivalent energy approach show the same behaviour as in

Figure 20.

Friction support

The plot for $x_1^{(err)}$ versus $x_0^{(err)}$ for friction support is presented in Figure 21. For a friction support Equations (45) and (46) are directly used to calculate the relative error of initial guess and first iterate. Equivalent energy dissipation method is used with the parameter values of example of Section 3.3.2. Equation (29) is used to calculate the equivalent damping so that the displacement is the only iteration variable.

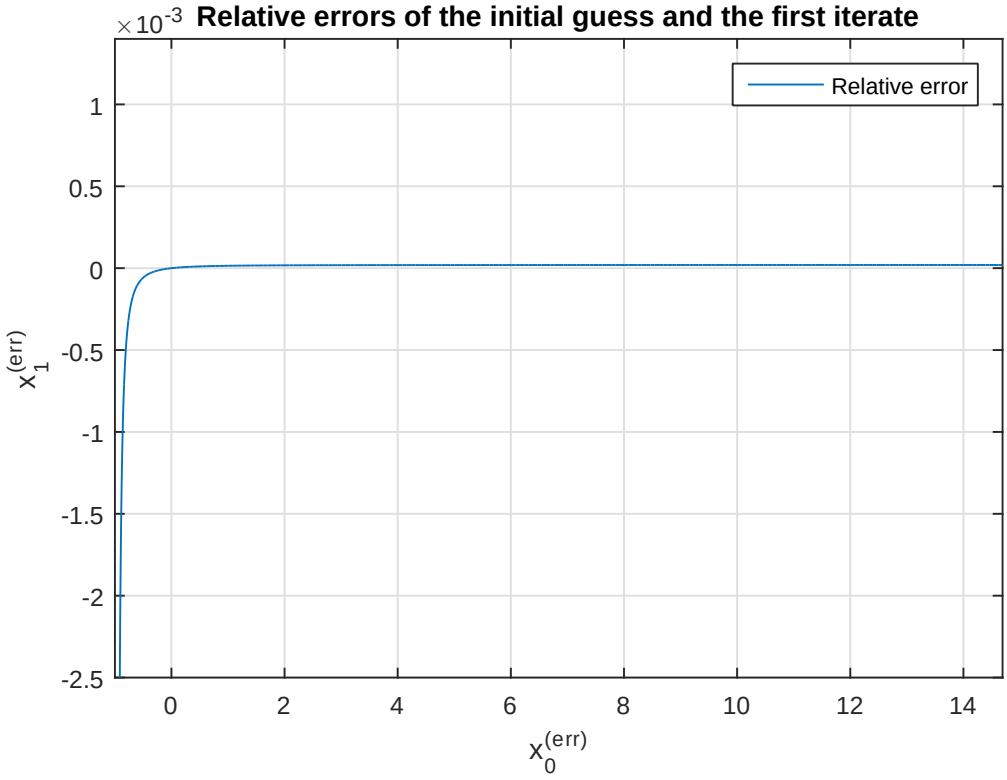

Figure 21: Relative error of the first iterate $x_1^{(err)}$ plotted against relative error of the initial guess $x_0^{(err)}$ for a friction support. The relative errors are measured relative to the converged solution.

For the friction support the relative error seems to approach negative infinity if the initial guess is significantly smaller than the solution i.e. the initial guess approaches zero. The relative error of first iterate seems not to grow significantly even if the relative error of initial guess is remarkably high (several hundred percents). It is recommended to pay special attention to the scale of the vertical axis, where the relative errors of the first iterate are generally very small. This is consistent with the fast convergence of the iteration in Section 3.3.2. Thus, it is concluded, that the initial guess should be larger than the expected solution in the case of the friction support.

3.4 Multiple degree-of-freedom systems

In general piping systems are multiple degree-of-freedom systems. The equation of motion for a multiple degree-of-freedom system is

$$\mathbf{M}\ddot{\mathbf{x}} + \mathbf{C}\dot{\mathbf{x}} + \mathbf{K}\mathbf{x} = \mathbf{F}(t) \tag{48}$$

where $\mathbf{M}$, $\mathbf{C}$, $\mathbf{K}$ represent the mass, damping and stiffness matrices, $\mathbf{F}(t)$ the excitation force vector and $\mathbf{x}$ the displacement vector of the system with the dot denoting derivation with respect to time. Piping supports affect the damping and stiffness matrices of the system. The number of degrees of freedom is very large in the general case and computer codes are used to analyse these systems.

In general, in a piping system there are n number of supports which act in various directions. Regarding gap supports, each support usually acts in two orthogonal directions and for both directions a nonlinear force-displacement relationship such as in Figure 3 can be obtained. The supports are replaced by equivalent springs with equivalent stiffnesses determined using the iterative procedure described in Section 3.1. The same applies for a friction support: the supports are replaced by equivalent spring-damper systems with equivalent properties determined using the iterative procedure.

In this study, each support direction is linearized individually. This means that for a single support direction, the equivalent properties are based on the displacement and velocity at support location in that direction only. Other directions are linearized based only on their displacements and velocities.

This individual approach where each support direction is linearized individually could be problematic since the system is coupled. All supports affect the system, and changing properties of one support changes the response in the whole system and consequently in all other support locations. The properties of all supports are changed on each iteration step and the response of the whole system may change considerably between iterations. Thus the multiple degree-of-freedom system could be expected to be more unstable than a single degree-of-freedom system meaning that it requires more iterations to find the converged solution.

For example, consider a system with four gap supports, each support acting in one direction and the system being loaded with a dynamic loading. The system is linearized by susbstituting equivalent springs to the model. An inital guess is given for all the supports and the iteration is started. After i iterations three supports have converged. The properties of the unconverged support are modified and consequently the responses are changed at other three support locations. The three other supports are no longer converged and more iterations are needed to find convergence of all supports. The iteration is converged to the solution only when all supports have found a convergent solution at the same time.

Before applying linearization on a real piping system in the next section, the linearization of two simplified multiple degree-of-freedom systems is studied. A gap support system and a friction support system, both with four supports, are used to demonsrate and examine the procedure. These provide understanding of the characteristic behaviour of these systems and indicate how the linearization can be applied to even more complicated real-world systems.

3.4.1 Gap supports

Figure 22 shows a two-dimensional beam system used here to study the linearization of a multiple degree-of-freedom system with four gap supports. The system consists of ten Bernoulli beam elements of equal length and equal stiffness. The beam system is simply supported at its end points. Each gap support is symmetric so that gaps and stiffnesses are equal on both sides of the beam and they act on nodes shown in the figure. A sinusoidal force is acting in the middle of the beam at node 6. Mass of the beam and moments of inertia are lumped to the nodes. The cross-section is shown in Figure 23. This example problem shows that a solution can be found if the supports are treated individually.

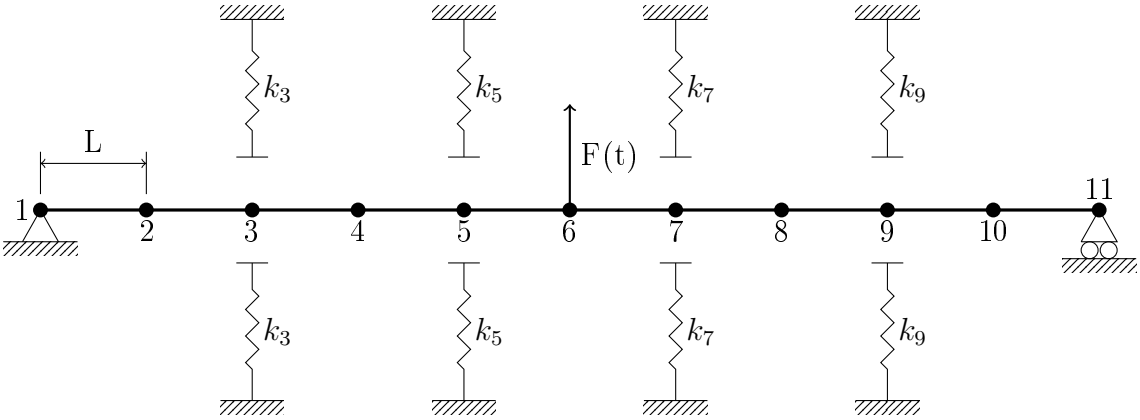

Figure 22: Example multiple degree-of-freedom system consisting of a beam and four gap supports. Length of one beam element is L, $F(t)$ is the applied loading and k_3, k_5, k_7 and k_9 are the support stiffnesses. Node numbering is also shown.

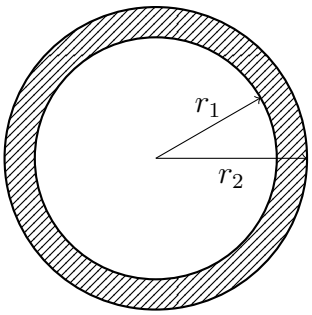

Figure 23: Cross-section of the beam. r_1 is the inner radius and r_2 is the outer radius of the beam.

The system has 11 nodes and 20 degrees of freedom. No damping is present and the equation of motion becomes

$$\mathbf{M}\ddot{\mathbf{x}} + \mathbf{K}\mathbf{x} = \mathbf{F}(t) \tag{49}$$

For clarity, the mass and stiffness matrices and excitation force vector are presented only in Appendix C. The values given for the parameters are shown in Table 10.

Table 10: Parameter values used in the multiple degree-of-freedom gap support system example.

Parameter	Symbol	Unit	Value
Inner radius	r_1	m	0,145
Outer radius	r_2	m	0,16
Beam element length	L	m	3
Density	ρ	$\frac{\text{kg}}{\text{m}^3}$	7850
Young's modulus	E	GPa	204
Applied loading	$F(t)$	N	$F_{amp} \sin \omega t$
Force amplitude	F_{amp}	N	500 000
Excitation angular velocity	ω	$\frac{1}{\text{s}}$	40π
Convergence criterion	ϵ	–	0,005
Support stiffness	k_3	$\frac{\text{N}}{\text{m}}$	$1{,}6 \cdot 10^9$
Support stiffness	k_5	$\frac{\text{N}}{\text{m}}$	$3{,}3 \cdot 10^9$
Support stiffness	k_7	$\frac{\text{N}}{\text{m}}$	$2{,}5 \cdot 10^9$
Support stiffness	k_9	$\frac{\text{N}}{\text{m}}$	$2{,}9 \cdot 10^9$
Gap size	d_3	m	0,04
Gap size	d_5	m	0,06
Gap size	d_7	m	0,05
Gap size	d_9	m	0,03

The dimensions, material properties and gap stiffnesses are of the same order of magnitude as in the real-world system presented in Section 4. The supports were replaced by equivalent springs and an initial guess of 5 mm greater than the gap size was given for displacements at support locations. The response of the system was found using forward Euler explicit time stepping scheme. Caughey's method was used to calculate the equivalent stiffnesses, with the remark that if the resulting displacement was smaller than the gap size, the result was assigned the value of the gap. This was to make sure the equivalent stiffness could be calculated. Each support was linearized individually.

The value of the relaxation parameter α should be chosen so that a solution satifying the convergence criterion can be obtained. Trial and error showed that with a too large value of α, a solution cannot be found. With a smaller value of α a solution was obtained, but with a great number of iterations. These gave motivation to change the value of α during the iteration in order to reduce the number of iterations required to find the solution.

Figure 24 shows the progress of the iterations where the value of α was kept constant at 0,04 and 0,004 and where the value was varied between the iterations.

Attention must be paid to the horizontal axes of the figures as they are of unequal magnitudes.

First, the value of α is kept constant at 0,04 and the progress of the iteration is shown in Figure 24(a). The results are oscillating around the solution but not converging and the process is stopped at 80 iterations. The iteration is unstable and cannot reach a solution satisfying the convergence criterion of 0,005.

To stabilize the iteration, the value of α is changed to 0,004 the results of which are presented in Figure 24(b). The starting point for the next iteration is close to the previous starting point, hence stabilizing the iteration but also requiring more rounds to obtain a solution. A solution satisfying the convergence criterion is found after 332 iteration rounds. The process is slower than with $\alpha = 0{,}04$ but once all the resulting displacements x_{i+1} reach the right order of magnitude, the solution is obtained. The converged values are shown in Table 11 below.

Table 11: Converged results of iteration using $\alpha = 0{,}004$. In the table $k_{eq}^{(3)}$, $k_{eq}^{(5)}$,$k_{eq}^{(7)}$ and $k_{eq}^{(9)}$ are the equivalent stiffnesses and $x^{(3)}$, $x^{(5)}$, $x^{(7)}$ and $x^{(9)}$ are the maximum displacements of the system at support locations.

Stiffness $\left[10^7 \frac{\mathrm{N}}{\mathrm{m}}\right]$		**Displacement** [m]	
$k_{eq}^{(3)}$	2,5893	$x^{(3)}$	0,0423
$k_{eq}^{(5)}$	2,4395	$x^{(5)}$	0,0622
$k_{eq}^{(7)}$	2,8294	$x^{(7)}$	0,0525
$k_{eq}^{(9)}$	3,2321	$x^{(9)}$	0,0314

In the above examples α is kept constant. Comparing results in Figures 24(a) and 24(b), it can be observed that with $\alpha = 0{,}04$ the right order of magnitude of results x_{i+1} is reached faster, but a converged solution cannot be obtained. In turn, with $\alpha = 0{,}004$ a solution is found but with a great number of iterations. These results give motivation to change the value of α between iterations so that the right order of magnitude is reached rapidly, but in a way that a converged solution is obtained.

To demonstrate this, an example is presented where α is large when the relative difference between x_i and x_{i+1} is large and as the relative difference gets smaller, also α becomes smaller. The values used in this example are presented in Table 12.

Table 12: The values of relaxation parameter α during the iteration. In the table x_i is the initial value of maximum displacement for the iteration step and x_{i+1} is the resulting maximum displacement.

Relative difference	**Value of α**
$0{,}05 < \left\lvert \frac{x_{i+1}-x_i}{x_i} \right\rvert$	$\alpha = 0{,}1$
$0{,}03 < \left\lvert \frac{x_{i+1}-x_i}{x_i} \right\rvert \leq 0{,}05$	$\alpha = 0{,}02$
$\left\lvert \frac{x_{i+1}-x_i}{x_i} \right\rvert \leq 0{,}03$	$\alpha = 0{,}004$

The values of relative difference and α are for illustration only, other values could lead to faster convergence for this problem. The progress of the iteration is shown in Figure 24(c). A converged solution is found after 26 iterations. This example demonstrates that the number of iterations is greatly dependent on the value of α. One should keep in mind that under-relaxation method was used here to stabilize the iteration and to obtain a converged solution, other methods exist and could lead to faster convergence.

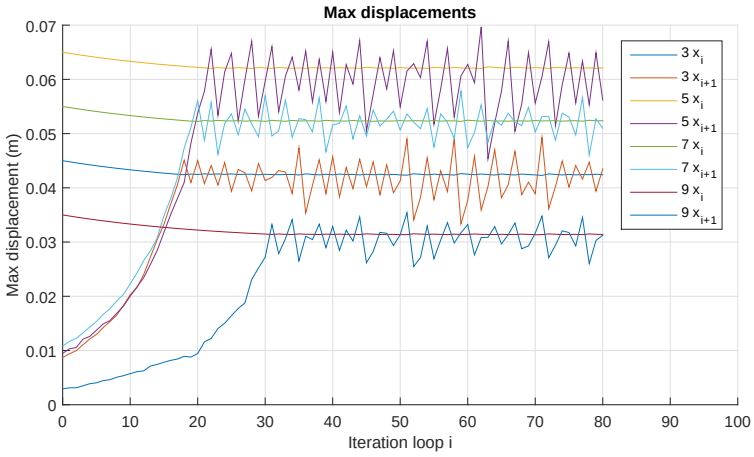

(a)

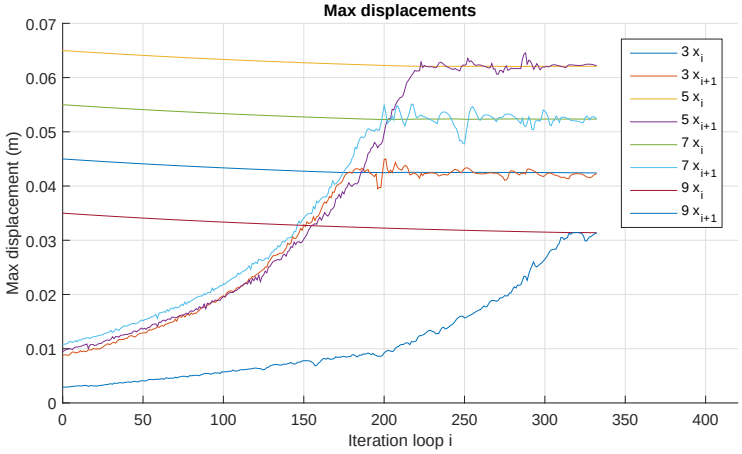

(b)

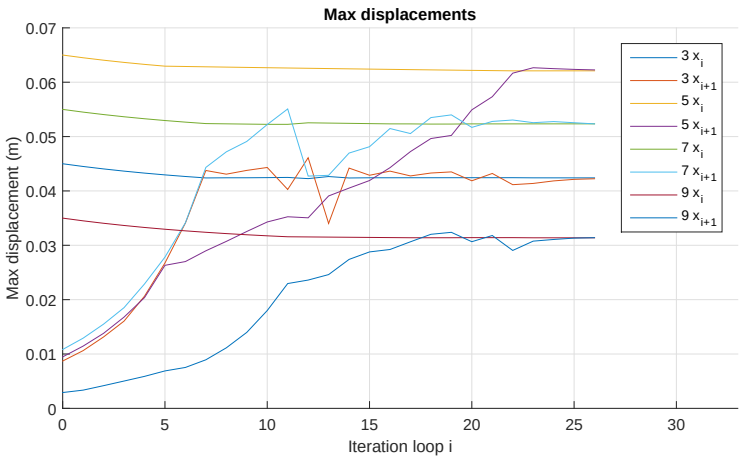

(c)

Figure 24: Maximum displacement results during the iteration using a) $\alpha = 0{,}04$ b) $\alpha = 0{,}004$ and c) varied α. Attention should be paid to the horizontal axes of the figures. Supports are indicated with numbers 3, 5, 7 and 9, respectively. Iteration loop number is denoted with i and x_i is the initial value of maximum displacement for the iteration step and x_{i+1} is the resulting maximum displacement.

The maximum displacements of equivalent linear system and the original nonlinear system are compared in Table 13. The difference is calculated relative to the nonlinear system.

Table 13: Comparison of the linear and nonlinear system maximum displacements. In the table $x^{(3)}$, $x^{(5)}$, $x^{(7)}$ and $x^{(9)}$ are the maximum displacements of the system at support locations.

	Linear system displacement [m]	**Nonlinear system displacement** [m]	**Difference**
$x^{(3)}$	0,0423	0,0633	−33 %
$x^{(5)}$	0,0622	0,0759	−18 %
$x^{(7)}$	0,0525	0,0680	−23 %
$x^{(9)}$	0,0314	0,0457	−31 %

As the table shows, in this case the maximum displacements of the linear system are smaller than in the nonlinear system.

More generally, this example problem shows that a solution can be found if the supports are treated individually. The example indicates the behaviour of a real-world system and brings up the difficulties that might be encountered there. These include the oscillation of the results around the solution and that numerous iterations might be needed to find the solution.

3.4.2 Friction supports

Figure 25 shows a one-dimensional bar system used here to study the linearization of a multiple degree-of-freedom system with four friction supports. The structure is divided into ten axial bar elements of equal length and equal stiffness. Nodes of the elements are shown in the figure and each node has one degree-of-freedom, translation in the axial direction. The beam is clamped at the ends and the loading is a sinusoidal displacement applied at the ends. The friction supports are acting on nodes shown in the figure. Mass of the beam is lumped to the nodes. The cross-section is the same as in the gap support example and it is shown in Figure 23.

The system has 11 nodes and 11 degrees of freedom, of which two are controlled by the aforementioned loading. Appendix C gives the stiffness and mass matrices of the system. The values given for the parameters are shown in Table 14. Weight of the beam is distributed uniformly, so that each support carries a mass of $2m$ when mass of one element is m.

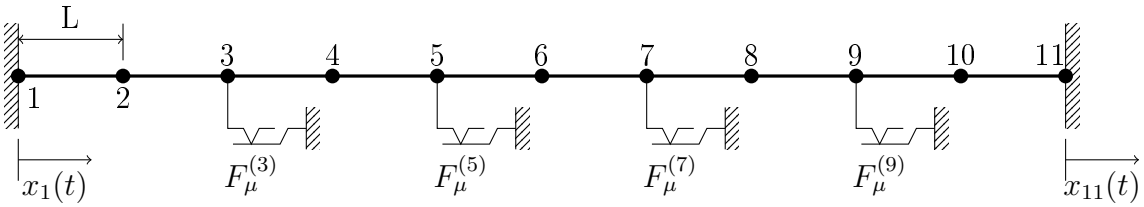

Figure 25: Example multiple degree-of-freedom friction support system. Length of one bar element is L, $x_1(t)$ and $x_{11}(t)$ are the applied displacement loadings and $F_\mu^{(3)}$, $F_\mu^{(5)}$, $F_\mu^{(7)}$ and $F_\mu^{(9)}$ are the support friction forces. Node numbering is also shown.

Table 14: Parameter values used in the multiple degree-of-freedom friction support system example.

Parameter	**Symbol**	**Unit**	**Value**
Inner radius	r_1	m	0,145
Outer radius	r_2	m	0,16
Bar element length	L	m	10
Density	ρ	$\frac{\text{kg}}{\text{m}^3}$	7850
Young's modulus	E	GPa	204
Excitation angular velocity	ω	$\frac{1}{\text{s}}$	80π
Forced displacement	$x_1(t)$	m	$0{,}1\sin(\omega t)$
Forced displacement	$x_{11}(t)$	m	$0{,}1\sin(\omega t)$
Convergence criterion	ϵ	–	0,005
Gravitational acceleration	g	$\frac{\text{m}}{\text{s}^2}$	9,81
Support force	$F_n^{(3)}$	N	$2mg$
Support force	$F_n^{(5)}$	N	$2mg$
Support force	$F_n^{(7)}$	N	$2mg$
Support force	$F_n^{(9)}$	N	$2mg$
Coefficient of friction	μ_3	–	0,6
Coefficient of friction	μ_5	–	0,4
Coefficient of friction	μ_7	–	0,5
Coefficient of friction	μ_9	–	0,3

For the linearization the supports are replaced by spring-damper systems and initial guesses of $x_0 = 0{,}5\,\text{m}$ and $v_0 = 20\,\frac{\text{m}}{\text{s}}$ are given for all supports. The response of the system was found using forward Euler explicit time stepping scheme. The

equivalent energy dissipation method is used to determine equivalent stiffness and damping. Each support is considered an individual in the iteration. The value of α is kept constant at 1 so the iteration is reduced to a simple iteration. The progress of the iteration is shown in Figure 26.

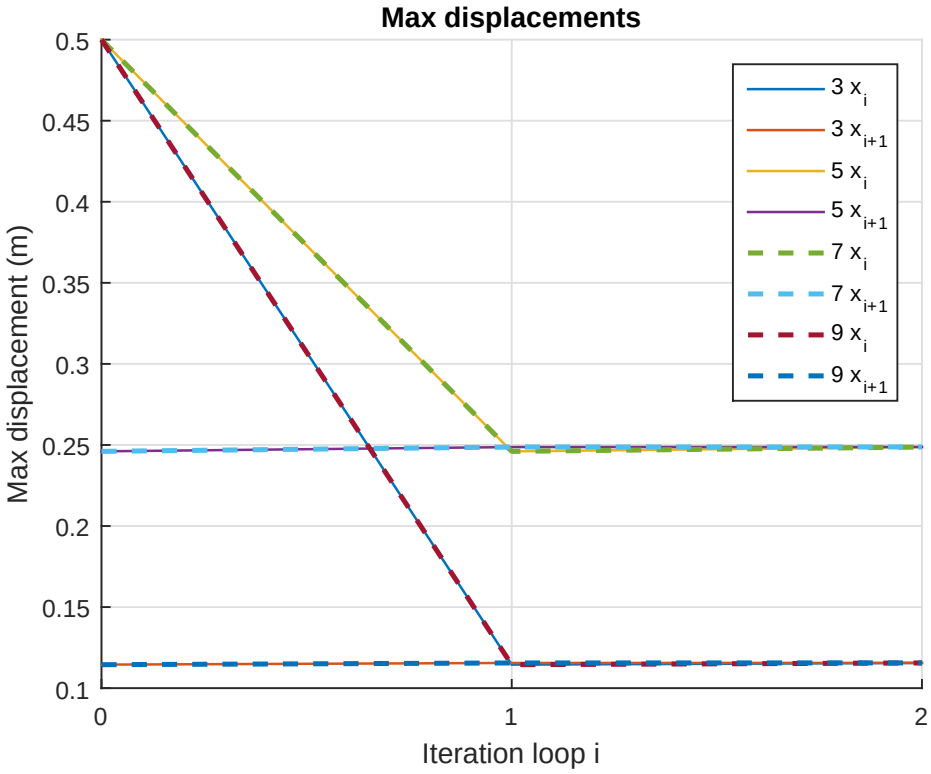

(a)

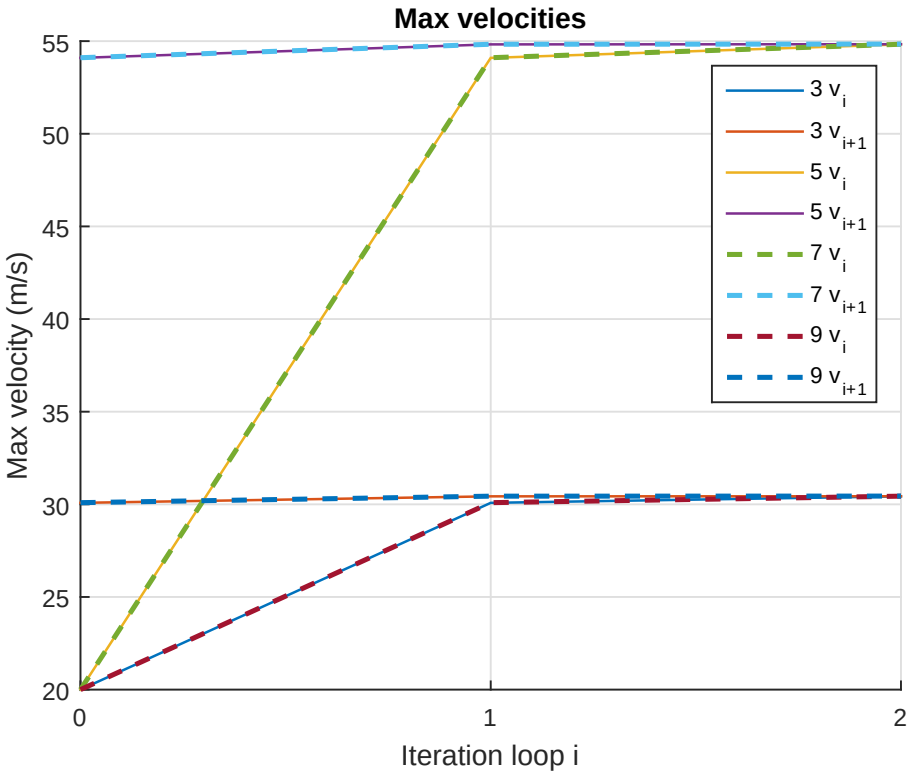

(b)

Figure 26: The graphs show a) maximum displacements and b) maximum velocities during the iteration for friction supports. Supports are indicated with numbers 3, 5, 7 and 9 and dashed lines are used to distinguish the results. Iteration loop number is denoted with i and x_i and v_i are the initial values of maximum displacement and velocity for the iteration step and x_{i+1} and v_{i+1} are the resulting maximum displacement and velocity.

The iteration converges after two rounds for equivalent energy dissipation method. The results of supports 3 and 9 are practically congruent, therefore dashed lines are used for support 9 results. Same behaviour is observed with supports 5 and 7. The converged values are shown in Table 15 below. For comparison, in Table 16 the converged values are shown for Jacobsen's method, which converged also after 2 iterations.

Table 15: Converged results of iteration using equivalent energy dissipation method. In the table $k_{eq}^{(3)}$, $k_{eq}^{(5)}$,$k_{eq}^{(7)}$ and $k_{eq}^{(9)}$ are the equivalent stiffnesses, $c_{eq}^{(3)}$, $c_{eq}^{(5)}$,$c_{eq}^{(7)}$ and $c_{eq}^{(9)}$ are the equivalent dampings, $x^{(3)}$, $x^{(5)}$, $x^{(7)}$ and $x^{(9)}$ are the maximum displacements of the system at support locations and $v^{(3)}$, $v^{(5)}$, $v^{(7)}$ and $v^{(9)}$ are the maximum velocities of the system at support locations.

Stiffness $\left[\frac{\mathrm{N}}{\mathrm{m}}\right]$		**Damping** $\left[\frac{\mathrm{kg}}{\mathrm{s}}\right]$	
$k_{eq}^{(3)}$	0	$c_{eq}^{(3)}$	556,2162
$k_{eq}^{(5)}$	0	$c_{eq}^{(5)}$	205,6434
$k_{eq}^{(7)}$	0	$c_{eq}^{(7)}$	257,0282
$k_{eq}^{(9)}$	0	$c_{eq}^{(9)}$	278,0656
Displacement [m]		**Velocity** $\left[\frac{\mathrm{m}}{\mathrm{s}}\right]$	
$x^{(3)}$	0,1159	$v^{(3)}$	30,4081
$x^{(5)}$	0,2489	$v^{(5)}$	54,8320
$x^{(7)}$	0,2489	$v^{(7)}$	54,8375
$x^{(9)}$	0,1159	$v^{(9)}$	30,4127

Table 16: Converged results of iteration using Jacobsen's method. In the table $k_{eq}^{(3)}$, $k_{eq}^{(5)}$,$k_{eq}^{(7)}$ and $k_{eq}^{(9)}$ are the equivalent stiffnesses, $c_{eq}^{(3)}$, $c_{eq}^{(5)}$,$c_{eq}^{(7)}$ and $c_{eq}^{(9)}$ are the equivalent dampings, $x^{(3)}$, $x^{(5)}$, $x^{(7)}$ and $x^{(9)}$ are the maximum displacements of the system at support locations and $v^{(3)}$, $v^{(5)}$, $v^{(7)}$ and $v^{(9)}$ are the maximum velocities of the system at support locations.

Stiffness $\left[10^4 \frac{\mathrm{N}}{\mathrm{m}}\right]$		**Damping** $\left[\frac{\mathrm{kg}}{\mathrm{s}}\right]$	
$k_{eq}^{(3)}$	11,496	$c_{eq}^{(3)}$	555,7157
$k_{eq}^{(5)}$	3,5605	$c_{eq}^{(5)}$	205,6386
$k_{eq}^{(7)}$	4,4503	$c_{eq}^{(7)}$	257,0130
$k_{eq}^{(9)}$	5,7479	$c_{eq}^{(9)}$	277,7687
Displacement [m]		**Velocity** $\left[\frac{\mathrm{m}}{\mathrm{s}}\right]$	
$x^{(3)}$	0,1156	$v^{(3)}$	30,4354
$x^{(5)}$	0,2488	$v^{(5)}$	54,8335
$x^{(7)}$	0,2488	$v^{(7)}$	54,8409
$x^{(9)}$	0,1156	$v^{(9)}$	30,4450

The convergence is fast for both methods. The equivalent damping values, displacements and velocities are nearly equal for both methods. The stiffness values are based on maximum displacements and damping values on maximum velocities. Even though displacements and velocities are practically equal for supports 3 and 9, as well as for 5 and 7, the equivalent stiffnesses and dampings are different. This is due to the different coefficients of friction of the supports, see Table 14.

To compare the equivalent linear systems with the original nonlinear system, maximum displacements and velocities are shown in Tables 17 and 18.

Table 17: Comparison of the maximum displacements of linear and nonlinear systems. The differences are calculated based on the nonlinear result. In the table $x^{(3)}$, $x^{(5)}$, $x^{(7)}$ and $x^{(9)}$ are the maximum displacements of the system at support locations.

	Nonlinear system [m]	**Jacobsen's method** [m]		**Eq. energy dissipation** [m]	
$x^{(3)}$	0,1147	0,1156	+0,78 %	0,1159	+1,0 %
$x^{(5)}$	0,2471	0,2488	+0,69 %	0,2489	+0,73 %
$x^{(7)}$	0,2472	0,2488	+0,65 %	0,2489	+0,69 %
$x^{(9)}$	0,1147	0,1156	+0,78 %	0,1159	+1,0 %

Table 18: Comparison of the maximum velocities of linear and nonlinear systems. The differences are calculated based on the nonlinear result. In the table $v^{(3)}$, $v^{(5)}$, $v^{(7)}$ and $v^{(9)}$ are the maximum velocities of the system at support locations.

	Nonlinear system $\left[\frac{\mathrm{m}}{\mathrm{s}}\right]$	**Jacobsen's method** $\left[\frac{\mathrm{m}}{\mathrm{s}}\right]$		**Eq. energy dissipation** $\left[\frac{\mathrm{m}}{\mathrm{s}}\right]$	
$v^{(3)}$	30,2604	30,4354	+0,58 %	30,4081	+0,49 %
$v^{(5)}$	54,5695	54,8335	+0,48 %	54,8320	+0,48 %
$v^{(7)}$	54,6034	54,8409	+0,43 %	54,8375	+0,43 %
$v^{(9)}$	30,2577	30,4450	+0,62 %	30,4127	+0,51 %

The maximum displacements and velocities for the equivalent linear systems are all close to the nonlinear system, all being slightly higher in the linear system. This indicates that the linearization can be well applied to friction supports and that the correspondence is good.

This example demonstrates, that the linearization procedure can be applied to a multiple degree-of-freedom friction support problem. Solution was found with simple iteration and convergence was fast. The example indicates the behaviour of a real-world system and application of the linearization there. It is concluded that linearization of friction supports is straightforward.

4 Application of the methods

As already mentioned in Section 1, the dynamic analyses of piping systems are usually performed using the finite element method. Several finite element computer programs are available for the analyses of stuctural systems. In this section it is demonstrated that the linearization can be applied also if the dynamic analyses are made using a finite element computer program. The linearization procedure is applied to a real piping system whose finite element model is shown in Figures 27, 28 and 29.

4.1 Description of model

The example system system of Figures 27, 28 and 29 is a part of a typical nuclear power plant piping system consisting of a pipe and four gap supports. The lower end of the pipe is simply supported with displacements restricted in all directions but allowing rotations. The upper end is clamped restricting displacements and rotations in all directions. Each support is clamped from two points. The highest support restricts the vertical motion but this does not affect the linearization procedure. The coordinate system is shown in the figures and it is used to define gap directions. Support numbering is shown in Figure 27.

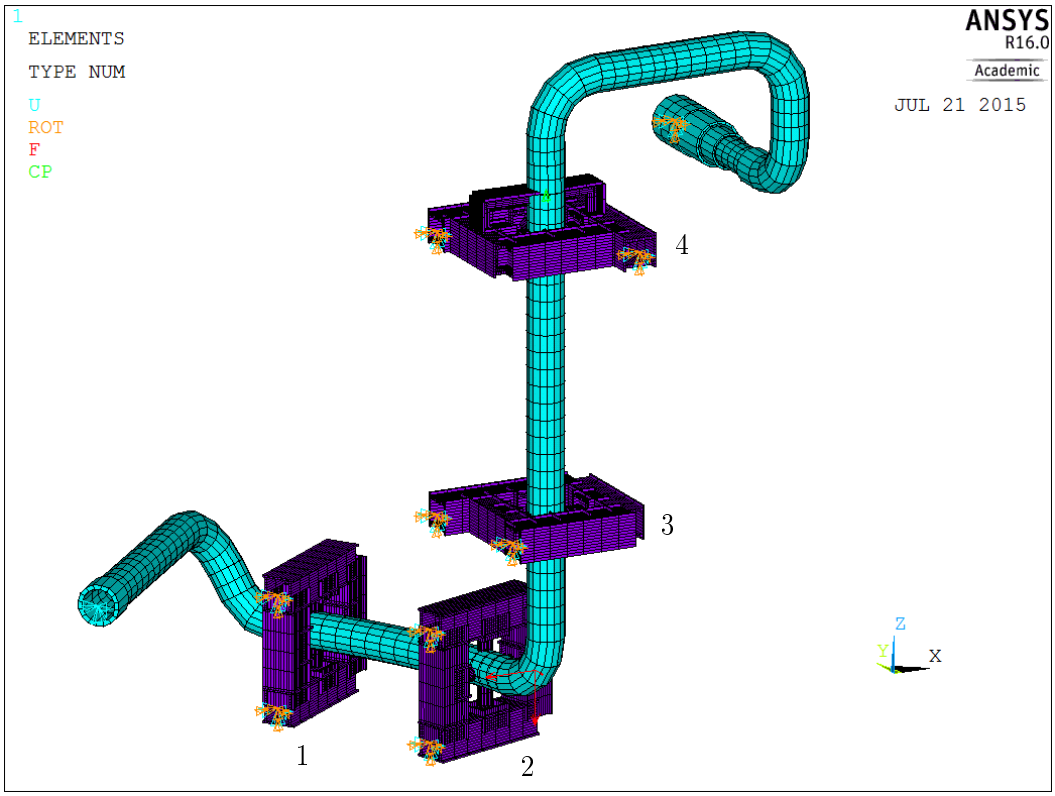

Figure 27: Visualization of the piping system. The pipe is modeled with pipe elements and the supports with beam elements. Support numbering and the coordinate system used are shown.

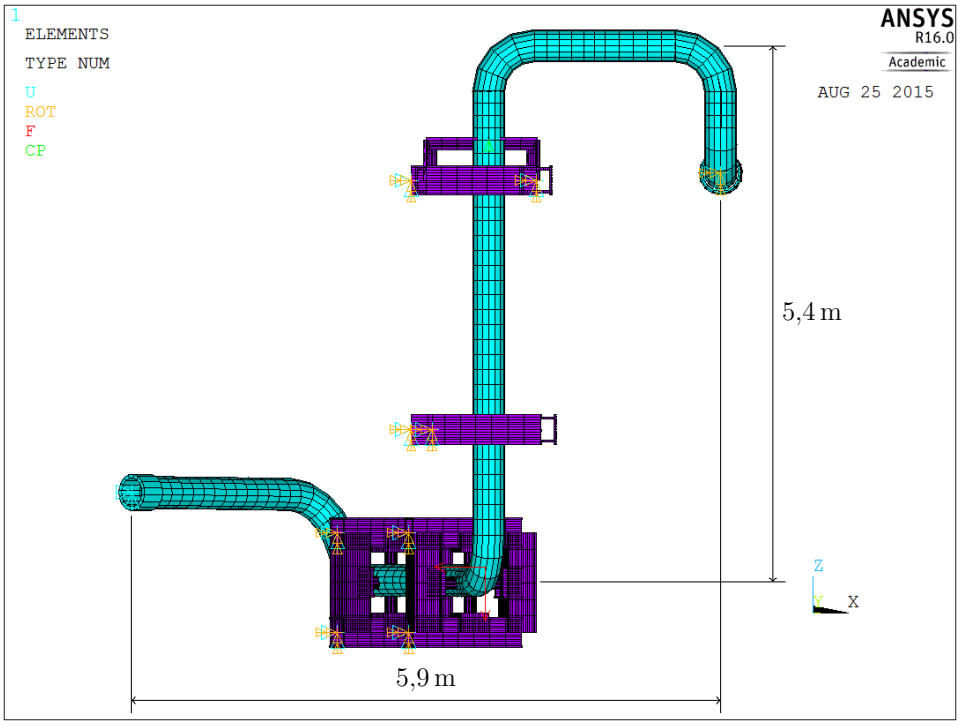

Figure 28: Visualization of the piping system presenting the main dimensions, view from the side.

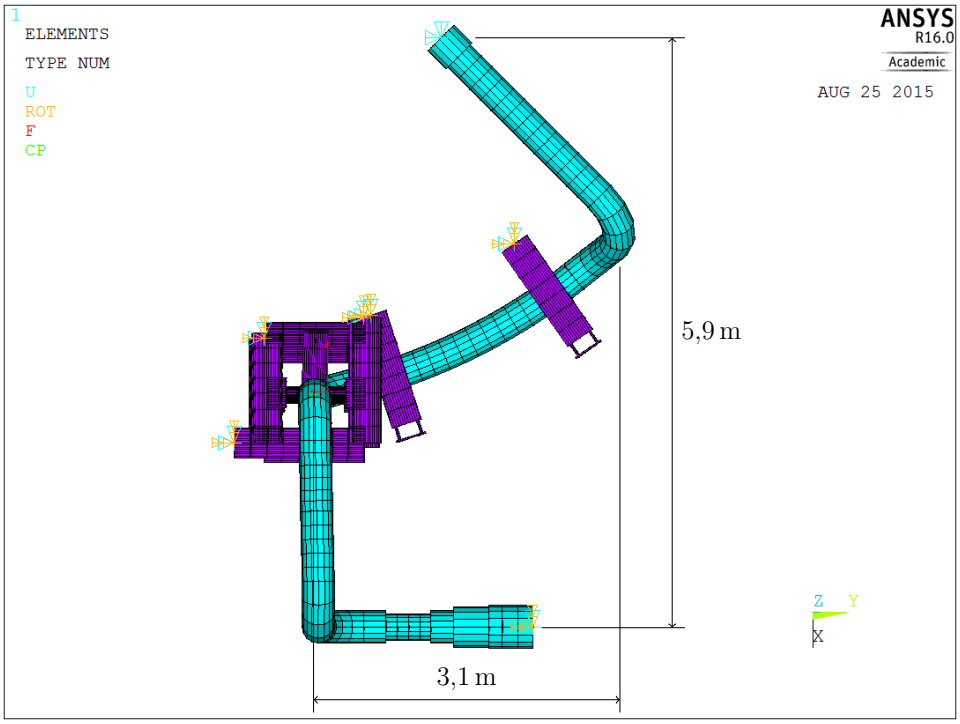

Figure 29: Visualization of the piping system presenting the main dimensions, view from the above.

The modeling and the analyses were made using ANSYS Mechanical APDL 16.0 finite element software. The pipe model consists of pipe elements called ELBOW290 in the program. The supports consist of Timoshenko beam elements which are called BEAM188. The used pipe material was a metal alloy and the supports were made of steel.

The system is loaded with a 15 Hz sinusoidal point force on the pipe. The force is located in the corner between supports 2 and 3 and its components can be seen as red arrows in Figure 27. The force components are

$$\begin{aligned} F_x &= 750000 \cdot 0{,}95 \sin(30\pi t) \\ F_y &= 750000 \cdot 0{,}31 \sin(30\pi t) \\ F_z &= 750000 \sin(30\pi t) \end{aligned} \tag{50}$$

The multiplications 0,95 and 0,31 for the x and y directions originate from the support 2 gap direction so that the resulting force amplitude in the xy-plane is 750 kN in the direction of the gap. The loading is an example loading that is chosen so that all gaps are closing in the nonlinear model.

4.2 Supports

The supports of the model are steel structures which consist of beams. In terms of Section 2.1 the supports are rigid restraints which limit the movements of the pipe in a plane perpendicular to the pipe axis, as can be seen in Figure 27. The movement of the pipe is limited by boxing the pipe inside the structure. The supports are clamped to the adjacent building structures. Referring to Section 2.1 no supports are however infinitely rigid and a finite stiffness can be determined. The stiffnesses for the supports of the model are determined later in this section. There is a clearance between the support and the pipe which introduces a gap. Thus the supports are gap supports.

Each support acts in two orthogonal directions, which are defined by unit vectors that point to the positive direction of gaps. A schematic figure of a gap support is presented in Figure 30 illustrating the unit vectors and notations used.

Each support direction is linearized individually. The equivalent stiffness for a direction is based only on the displacement in that direction. The nonlinear support gaps d_1 and d_2 are illustrated in Figure 30 and their significance in the support force-displacement behaviour is visible in Figure 31. The nonlinear support stiffnesses after gap closure are determined in the gap direction, k_1 being the stiffness when d_1 is closed and k_2 when d_2 is closed as depicted in Figure 31.

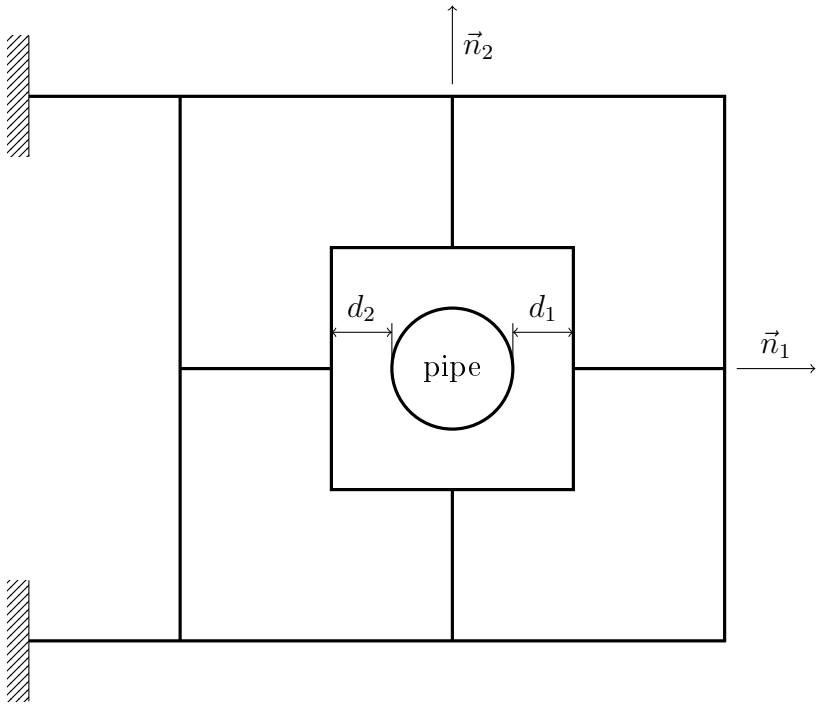

Figure 30: Schematic figure of a gap support illustrating notations used. In the figure $\vec{n}_1$ and $\vec{n}_2$ are unit vectors that point to the positive direction of the gaps and d_1 and d_2 are gap sizes in the positive and negative directions.

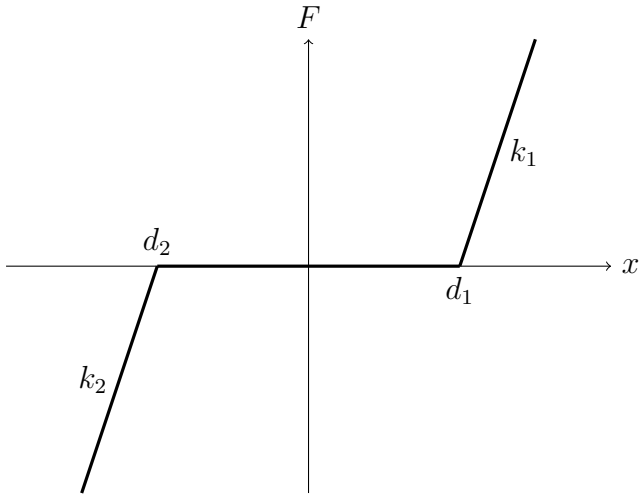

Figure 31: Nonlinear force-displacement behaviour of gap support with notations used. Reaction force of support is denoted with F, displacement of system with x, gap sizes in the positive and negative directions with d_1 and d_2 and support stiffnesses on the positive and negative sides with k_1 and k_2.

For each support direction as in Figure 30, a force-displacement relatioship of Figure 31 can be constructed. Since one support acts in two directions, for a system

of four supports there are eight directions. Thus in this example eight items are linearized at the same time.

The stiffnesses k_1 and k_2 for each support direction were determined in the ANSYS finite element program by giving a displacement to the support at the pipe location and observing the resulting force. The gap directions, stiffnesses and gap magnitudes of the supports are presented in Table 19. Gap directions are indicated in the global coordinate system depicted in Figure 27.

Table 19: Properties of gap supports. In the table $\vec{n}_1$ and $\vec{n}_2$ are unit vectors that point to the positive direction of the gaps, k_1 and k_2 are support stiffnesses on the positive and negative sides and d_1 and d_2 are gap sizes in the positive and negative directions.

Support no.	Type	Gap direction	k_1 $\left[\frac{\text{N}}{\text{mm}}\right]$	k_2 $\left[\frac{\text{N}}{\text{mm}}\right]$	d_1 [mm]	d_2 [mm]
1	Gap	$\vec{n}_1 = (0{,}82;0{,}58;0)$	3257000	3257000	29	-29
		$\vec{n}_2 = (0,0,1)$	1383000	1383000	29	-29
2	Gap	$\vec{n}_1 =(0{,}95;0{,}31;0)$	3213000	3213000	29	-29
		$\vec{n}_2 =(0,0,1)$	1395000	1395000	29	-29
3	Gap	$\vec{n}_1 =(1,0,0)$	2879000	2879000	28	-28
		$\vec{n}_2 =(0,1,0)$	1298000	1298000	28	-28
4	Gap	$\vec{n}_1 =(1,0,0)$	2557000	2557000	28	-28
		$\vec{n}_2 =(0,1,0)$	2893000	2893000	29	-29

As seen in Table 19 each support direction is symmetric, i.e. stiffnesses and gap magnitudes are equal on both sides, $|d_1| = |d_2|$ and $k_1 = k_2$. The stiffness values are very high in general.

4.3 Selection of method and iteration parameters

The equivalent stiffnesses were calculated using Caughey's method as in [6, 20, 23, 24]. The calculation formula was presented in Section 3.2.1 and it is [20]

$$k_{eq} = \frac{k_1}{\pi}(\pi - 2\theta - \sin 2\theta)$$

where

$$\theta = \arcsin \frac{d}{x_i}$$

and x_i is the maximum displament at support location. The iterative procedure is expected to be divergent due to high stiffness values and therefore under-relaxation method is used. Recalling from Section 3.1, the starting point for the next iteration

is modified according to the formula

$$\hat{x}_{i+1} = x_i + (x_{i+1} - x_i)\alpha$$

where x_i is the starting point of the iteration and x_{i+1} the resulting displacement. Relaxation parameter α is kept constant and is chosen to be 0,01. Convergence is checked using

$$\left| \frac{x_{i+1} - x_i}{x_{i+1}} \right| < \epsilon$$

where ϵ is chosen to be 0,005. Initial guesses for the supports are shown in Table 20. The initial guesses were made after a few test analyses and hence they are quite accurate.

Table 20: Initial guesses for the supports of the real piping system. In the table $\vec{n}_1$ and $\vec{n}_2$ are unit vectors that point to the positive direction of the gaps.

Support no.	Type	Gap direction	Initial guess x_0 [mm]
1	Gap	$\vec{n}_1$	29,15
		$\vec{n}_2$	32,05
2	Gap	$\vec{n}_1$	30,3
		$\vec{n}_2$	34,5
3	Gap	$\vec{n}_1$	29,7
		$\vec{n}_2$	34,1
4	Gap	$\vec{n}_1$	28,15
		$\vec{n}_2$	30,9

4.4 Results of the iteration

In this section, the results of the iteration procedure and the equivalent linear system are presented for the problem described in Sections 4.1, 4.2 and 4.3. The progress and results of the iteration are presented in Figure 32.

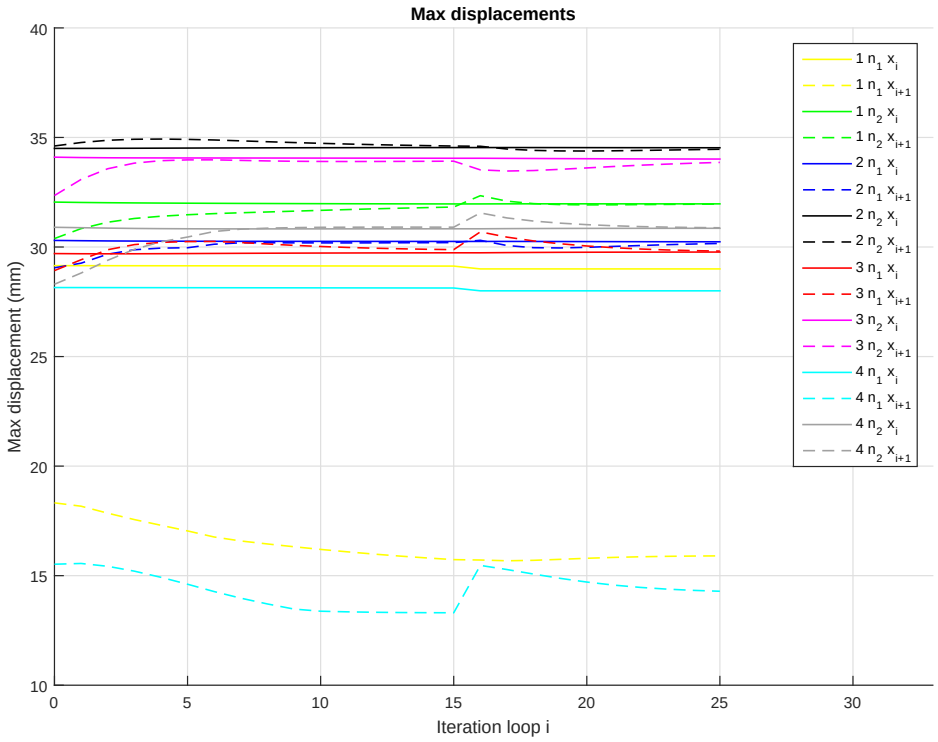

Figure 32: Progress and results of the iteration. Initial values (starting points) for the iteration rounds are presented as solid lines and the corresponding results as dashed lines. Supports are indicated with numbers 1, 2, 3 and 4, respectively, and $\vec{n}_1$ and $\vec{n}_2$ are unit vectors that point to the positive direction of the gaps. Iteration loop number is denoted with i and x_i is the initial value of maximum displacement for the iteration step and x_{i+1} is the resulting maximum displacement.

As seen in Figure 32, the initial guesses are very good and the right order of magnitude of results is obtained fast. At 15 iterations, all supports have found a converged solution, except support no. 1 in the $\vec{n}_1$ direction and support no. 4 in the $\vec{n}_1$ direction. The displacements for these two directions are such that the gaps (29 mm and 28 mm) are not closing and the starting points of the iteration are appoaching the gap magnitude, and hence the equivalent stiffnesses are approaching zero. The linearized model thus predicts that gaps are left open for these two directions.

For the 16th iteration, the starting points for all other supports are kept the same as in the 15th iteration but for the two directions where the gaps are not closing, the starting points are assigned the magnitude of the gaps, making $k_{eq} = 0$ in their

directions. This is why a leap is observed in the results at 16th iteration. After this, the iteration is continued until convergence is reached again, at 25 iterations. The two support directions where $k_{eq} = 0$ are still predicted to have zero stiffness and other support directions have found converged solutions. The converged values for equivalent stiffnesses and displacements are shown in Table 21.

Table 21: Converged values of iteration. In the table $\vec{n}_1$ and $\vec{n}_2$ are unit vectors that point to the positive direction of the gaps, k_{eq} is the equivalent stiffness and x is the maximum displacement of the system at support location to the indicated direction.

Support no.	Gap direction	k_{eq} $\left[\frac{\text{N}}{\text{mm}}\right]$	x [mm]
1	$\vec{n}_1$	0	15,903
	$\vec{n}_2$	46333	31,960
2	$\vec{n}_1$	31771	30,162
	$\vec{n}_2$	104686	34,461
3	$\vec{n}_1$	49631	29,814
	$\vec{n}_2$	112741	33,861
4	$\vec{n}_1$	0	14,288
	$\vec{n}_2$	50686	30,878

The values in Table 21 represent the linearized values of the system, and thereby an equivalent linear system for the problem is obtained. The equivalent linear system is then further analysed and compared with the nonlinear system.

4.5 Comparison of nonlinear and linearized systems

The equivalent linear system and the original nonlinear system are investigated to compare maximum displacements at support locations, maximum support forces, support force-displacement relationships and bending moments in the pipe at support locations. In addition, the lowest natural frequencies are shown for both systems.

The results were obtained by time history analysis using the ANSYS Mechanical APDL 16.0 finite element program. The analysis type was full transient analysis with 3 seconds of analysis time. The time step size was 0,0001 s. The maximum absolute displacements of nonlinear and linear systems are presented in Table 22.

Table 22: Nonlinear and linear system maximum absolute displacements at support locations. Support 1 $\vec{n}_1$ and support 4 $\vec{n}_1$ directions had zero stiffnesses in the linear system. In the table $\vec{n}_1$ and $\vec{n}_2$ are unit vectors that point to the positive direction of the gaps and x is the maximum displacement of the system at support location to the indicated direction.

Support no.	Gap direction	Nonlinear x [mm]	Linear x [mm]	Difference
1	$\vec{n}_1$	31,195	15,903	−49 %
	$\vec{n}_2$	32,003	31,960	−0,13 %
2	$\vec{n}_1$	31,803	30,162	−5,2 %
	$\vec{n}_2$	30,175	34,461	+14 %
3	$\vec{n}_1$	31,806	29,814	−6,3 %
	$\vec{n}_2$	31,958	33,861	+6,0 %
4	$\vec{n}_1$	30,611	14,288	−53 %
	$\vec{n}_2$	31,253	30,878	−1,2 %

Maximum absolut support forces are presented in Table 23. The nonlinear forces are calculated based on the maximum absolute displacements and values of k_1 in Table 19. This is to exclude the effect of dynamic impact forces that are present in the nonlinear results, since the supports have mass.

Table 23: Nonlinear and linear system maximum absolute support forces. In the table $\vec{n}_1$ and $\vec{n}_2$ are unit vectors that point to the positive direction of the gaps and F is the maximum absolute support force in the indicated direction.

Support no.	Gap direction	Nonlinear F [10^6N]	Linear F [10^6N]	Difference
1	$\vec{n}_1$	7,148	0	−100 %
	$\vec{n}_2$	4,153	1,481	−64 %
2	$\vec{n}_1$	9,005	0,979	−89 %
	$\vec{n}_2$	1,639	3,608	+120 %
3	$\vec{n}_1$	10,960	1,480	−86 %
	$\vec{n}_2$	5,137	3,818	−26 %
4	$\vec{n}_1$	6,676	0	−100 %
	$\vec{n}_2$	6,517	1,565	−76 %

Two typical support force-displacement relationships are presented in Figures 33 and 34. All the force-displacement relationships are presented in Appendix D.

The nonlinear and linear solutions are presented in the same graph for each support direction. The results are shown as obtained from the finite element program. The linear results are on the same line, as expected, but the nonlinear results show some scatter. This is due to the dynamics, since the supports have mass and the high peaks observed are impact forces. Therefore, the nonlinear supporting forces are shown also without the effect of the impact forces. These have been obtained by calculating the force based on the displacements and values of k_1 in Table 19.

After the force-displacement relationships, two typical beam bending moment resultant magnitudes are presented in Figures 35 and 36. All the bending moments are presented in Appendix D. The results are shown as functions of time for three first seconds of the analysis. Bending moment magnitudes are measured at support locations, and as only magnitudes are considered, the values are nonnegative. Directions are not considered here. Maximum values of nonlinear and linear systems are shown in Table 24. Bending moments are investigated instead of stresses, since bending stresses follow directly from the bending moments.

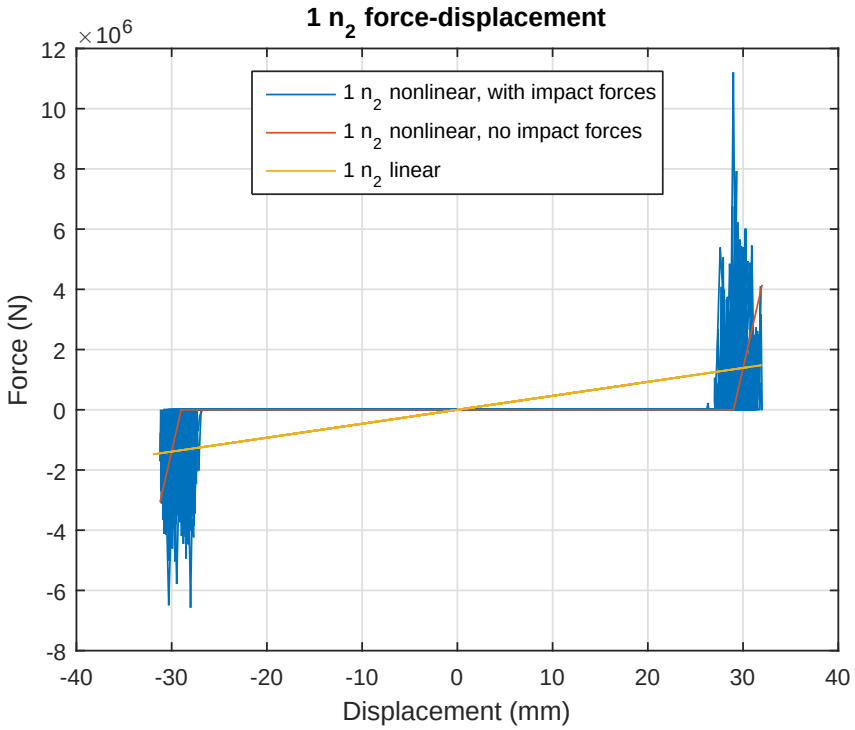

Figure 33: Support 1 force-displacement relationship in the n_2-direction for the nonlinear support with and without impact forces and for the linear support.

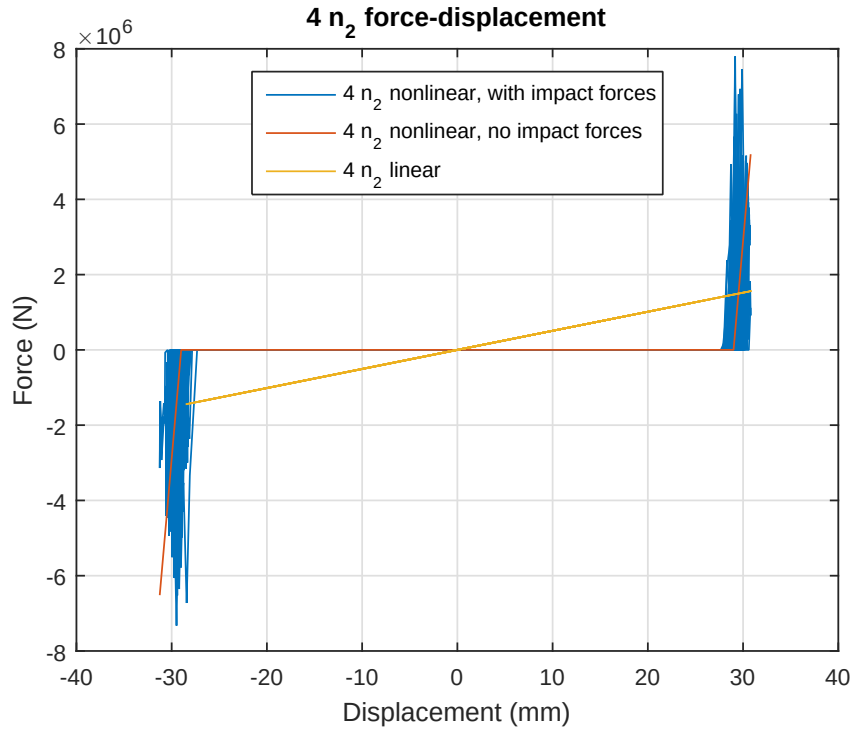

Figure 34: Support 4 force-displacement relationship in the n_2-direction for the nonlinear support with and without impact forces and for the linear support.

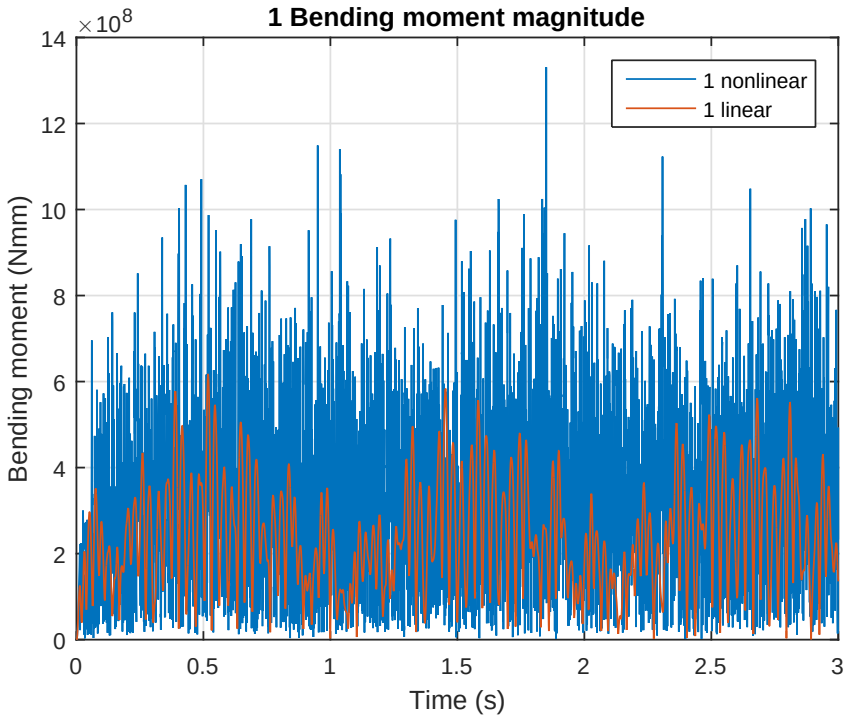

Figure 35: Support 1 bending moment magnitude as function of time for the nonlinear and linear cases.

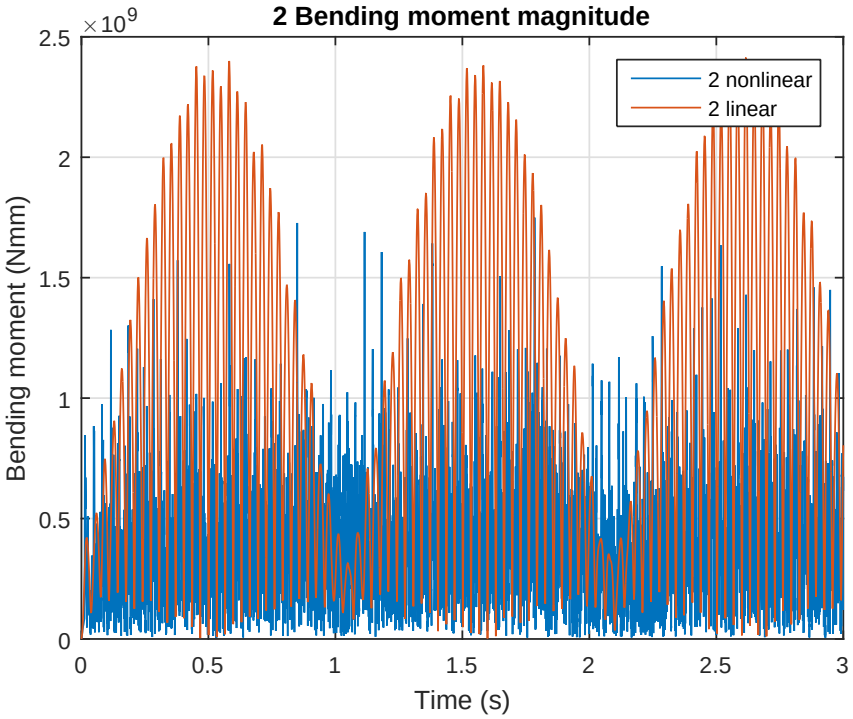

Figure 36: Support 2 bending moment magnitude as function of time for the nonlinear and linear cases.

Table 24: Nonlinear and linear system maximum bending moment magnitudes.

Support no.	Nonlinear M [10^9Nmm]	Linear M [10^9Nmm]	Difference
1	1,331	0,617	−54 %
2	1,750	2,414	+38 %
3	1,384	3,065	+121 %
4	1,317	0,617	−53 %

The lowest natural frequencies of both systems are shown in Table 25. The nonlinear system frequencies are calculated gaps open i.e. with a completely free pipe without supports. The linear system has equivalent springs attached to the pipe at support locations thus changing the natural frequencies.

Table 25: Lowest natural frequencies of nonlinear and linear systems.

Frequency	Nonlinear [Hz]	Linear [Hz]
1	5,9444	15,956
2	7,7169	18,618
3	9,4658	22,522
4	11,147	24,625
5	18,863	31,213
6	27,451	38,603
7	33,199	40,040
8	37,524	47,138
9	39,418	53,523
10	51,047	58,387

The results of the linearization procedure were presented in Section 4.4. The initial guesses were very good and an equivalent linear system was obtained. During the iteration process, however, displacements in two support directions were such that the equivalent stiffnesses approached zero. The stiffnesses were assigned the value of zero once all other supports had found a converged solution. A rule could be developed for handling of these situations, since in these cases it is evident that the equivalent stiffness will approach zero, but to arrive even close would take numerous iterations. The key characteristic is that the displacement is lower than the gap magnitude, even though other supports have found a converged solution and the equivalent stiffness is approaching zero. Also, in these cases convergence cannot be attained in the sense that starting point and result are close to each other.

An equivalent linear system for the problem was obtained, and comparison to the original nonlinear system was made. The maximum displacements were presented in Table 22. The nonlinear displacements were all of the order of 30−32 mm whereas for the equivalent linear system the displacements ranged from 14 mm to over 34 mm. Relative differences were high for the directions where equivalent stiffnesses were zero. Otherwise the relative differences were not as high, but exact matches were not observed.

Maximum support forces in Table 23 showed a clear trend the linear forces being always lower than the nonlinear forces, except for support 2 in the $\vec{n}_2$ direction. The support directions where $k_{eq} = 0$ produce no supporting force. No clear relation can be observed between the linear and nonlinear maximum forces, such as the nonlinear forces being n times the linear forces. The force-displacement relationships show clearly the difference between the nonlinear and equivalent linear systems. The impact forces of nonlinear system show as high peaks and cannot be modelled by the linear system. The time step size affects considerably to the force peaks. Also, one can observe the Caughey's method which was used for linearization. The mean-squared error is minimized between the linear and nonlinear force-displacement relationships at the maximum linear displacement.

Observing the bending moment magnitudes of supports 1, 2, 3 and 4, it is seen that bending moments in the nonlinear system are more stable than in the linear system. Nonlinear system shows rather constant behaviour while in the linear system an oscillating behaviour with a period of about 1 second repeats over and over again. This was also noticed in the time histories of displacements. This oscillation could be due to the loading frequency that is close to the lowest natural frequency of the linear system.

The maximum values of bending moment magnitudes of supports 1 and 4 are smaller in the linear system, whereas for supports 2 and 3 they are higher in the linear system. The point force was applied between supports 2 and 3 but in the nonlinear system the maximum values are nearly the same for all supports. In the linear system, the maximum values are considerably higher close to the point force.

The linear system natural frequencies are higher than the nonlinear system natural frequencies. Adding springs to the system changes the stiffness matrix and therefore the natural frequencies. It should be remembered that the equivalent stiffnesses are changed during the iteration, and hence at every iteration step the natural frequencies are different. The values presented in Table 25 are the frequencies of the converged equivalent linear system.

5 Discussion

5.1 Linearization procedure

The ultimate purpose of linearization of piping supports in dynamic analyses is to be able to perform the dynamic analyses faster than with nonlinear modeling. Nonlinear dynamic systems are solved using time-history analysis whereas for linear systems also other methods are available, such as response spectrum analysis. In addition, cases where the loading is defined as a spectrum can be analysed without converting the loading to the time domain. Potential time savings make linearization an attractive option to perform the dynamic analyses.

The linearization method presented in this study is based on maximum displacements and velocities of the system, and is therefore applicable to any dynamic analysis method where these quantities can be obtained. In this study, analytical solving of the equation of motion was used for single degree-of-freedom systems in Section 3.3 and time history analysis was used for multiple degree-of-freedom systems in Sections 3.4 and 4.4.

For gap supports, the methods presented require the displacement to be greater or equal to the gap magnitude to be able to calculate the equivalent stiffness. If the displacement is smaller than the gap, the equivalent stiffness should be zero. For friction supports, the maximum displacement and velocity need to be nonzero. The properties of the original support need to be known, such as gap magnitude and support stiffness for gap supports and surface normal force and coefficient of friction for friction supports.

The linearization is dependent on the applied loading. Each different load case will have a different equivalent linear system, provided that equivalent properties are nonzero. Thus the linearization will have to be performed to each load case separately.

The support nonlinearities considered in this study were nonlinearities arising from gap and friction. Other nonlinearities, such as plastic material behaviour of supports, affect the support force-displacement behaviour. The principles for linearization of these other nonlinearities remain the same as with the methods presented in this study. Consider for example a gap support with plastic material behaviour so that the hysteresis loop is stabilized. Even though the force-displacement behaviour is different, for a maximum displacement, minimization of mean squared error can be made (Caughey's method), a secant from the origin can be drawn (secant stiffness) or elastic energy stored can be calculated (equivalent energy approach) to determine the equivalent stiffness. Systems with plasticity exhibit hysteretic characteristics and an equivalent damping is usually determined along with stiffness [29]. More generally, the support force-displacement relationship is to be linearized, and many methods exist and can be used to do it.

The linearization methods presented in this study are based on minimization of mean squared error between linear and nonlinear systems, secant stiffness and equivalent energy approach for gap supports, and equivalent energy dissipation method and Jacobsen's method for friction supports. Different methods result in different

equivalent linear systems, based on their definition. For example, for a given load case, the secant stiffness will result in a high stiffness and small displacement whereas the equivalent energy approach will result in a low stiffness and large displacement. There are also other methods to determine the equivalent properties, and more methods can be developed. For example, for a gap support, an equivalent stiffness could be determined by fitting a straight line to the force-displacement relationship at displacement x_i using the method of least squares.

The question arises whether some method is better than the other for linearization. The goodness of an equivalent linear system is somewhat difficult to define, and it is dependent on what we want to measure. We could measure the error between the nonlinear and equivalent linear systems, but then some methods result in more accurate displacements, whereas other methods give more accurate bending moments. Also, depending on the loading, some methods could give results closer to nonlinear solution than the others. Comparing the methods to find the best way to determine an equivalent linear system was however beyond the scope of this study.

This study focused on the linearization methods and the procedure to determine the equivalent linear system. Difficulties were encountered when applying the iterative procedure to gap supports, first with the single degree-of-freedom system, then with the multiple degree-of-freedom system and ultimately with the real-world system. The difficulty is that the iterative procedure is highly divergent, and additional techniques are needed to get the iteration convergent and arrive at the solution. The divergence arises from the fact that the relation of maximum displacement to the gap magnitude, $\frac{x_i}{d}$, is close to 1. The maximum displacement is a function of all the problem parameters, but the main reason for the relation to be close to 1 are the stiff gap supports i.e. very high values of k_1. During the iteration, even a small variation in $\frac{x_i}{d}$ will result in a remarkable change in the equivalent stiffness.

Based on these remarks, it is concluded that for gap supports the iterative procedure converges best if the relation $\frac{x_i}{d}$ is large. The iteration is relatively stable and the equivalent linear system is obtained with reasonable amount of iterations. The relation $\frac{x_i}{d}$ becomes large when the support stiffness is low and loading amplitude is high. It is thus concluded that with large $\frac{x_i}{d}$ the linearization procedure can be well applied for gap supports.

The additional technique used in this study to get the iteration convergent was the under-relaxation method. The dominating parameter in the under-relaxation method is the relaxation parameter α and with a constant value the solution is obtained with numerous iterations. Even by simply changing the α between iterations the procedure was considerably faster. Other methods exist besides under-relaxation, and by focusing on numerical mathematics the convergence can be made faster. This way a good method and good iteration parameters can be chosen. The most important observation is that the starting point for the next iteration must be chosen wisely based on the previous results.

For systems where all gaps are not predicted to be closing, a first analysis could be made without any supports to see which gaps are clearly closing. This analysis would also give a hint of possible initial guesses. If the displacement is only slightly larger than the gap magnitude, during the iteration $\frac{x_i}{d}$ is close to 1 and the procedure

becomes highly unstable. Iteration parameters must be well adapted and finding the solution could take numerous iterations. In these cases, the gaps have only a small effect on the system, and it could be better to neglect the gap in the analysis, i.e. set $k_{eq} = 0$ to avoid difficulties in convergence during the iteration. This introduces however some error to the solution.

Friction supports, on the other hand, show no problems with convergence during the iteration based on the results of this study. The convergence was fast for both single and multiple degree-of-freedom systems and the solution was found by simple iteration. The friction supports did not affect the system displacements and velocities as significantly as gap supports in the examples of this study. However, the support normal force was kept constant, which in a real system can vary as a function of time. Linearization of friction supports lack the application to a real-world example in this study. It is concluded that linearization can be well applied to friction supports, provided that the surface normal force is constant.

In this study, the linearization was performed individually for each support direction for multiple degree-of-freedom systems with several supports. However, the system is coupled, and for this reason a coupled linearization might perform better. In coupled linearization the starting point for the next iteration of a support direction is based on displacements at all support locations of the system, instead of the displacement in that support direction only. Coupled linearization would take the system into account as a whole and faster convergence could be attained. However, defining a mathematical formula that relates the starting point of iteration for a support direction and displacements at all support locations of the system might prove to be difficult.

The gap supports studied in this thesis were symmetrical. Gaps were equal on both sides of the pipe and nonlinear support stiffnesses had the same value on positive and negative sides. The gaps can be unequal and stiffnesses might also vary. The mean value of the loading can be nonzero so that the pipe is oscillating around a point other than the initial equilibrium position. Furthermore, the initial equilibrium position of the system might be such that the pipe is in contact with one side of the support, with some initial supporting force. Moreover, a support to be linearized could be one-sided so that the actual support limits the pipe movement in only one side. Linearization of these unsymmetrical supports should be started by considering their force-displacement relationship and finding a method to calculate the equivalent stiffness and possible damping. One possible method is the min-max stiffness presented in this study, but linearization of unsymmetrical supports requires further investigation.

The linearization methods presented in this study are based on maximum displacement and velocity. The converged solution is obtained once the resulting maximum displacement is close enough to the starting point. The parameter examined could be something else than displacement. The linearization could be performed by relating the equivalent stiffness (and damping) to some other parameter, for example to bending moment, stress or force, depending on the parameter of interest. These approaches would result in different equivalent linear systems, which possibly represent the original nonlinear system better than displacement-based linearization.

Smaller error might be attained for example for bending moments and stresses.

5.2 Application of the methods

Based on the results of Section 4.4, and the comparison between linear and nonlinear systems in Section 4.5, the following is concluded on how well the equivalent linear system obtained represents the original nonlinear system:

- Maximum displacements are of the same order of magnitude, though large differences occur at single locations.
- Maximum forces are generally smaller in the linear system, and impact forces of nonlinear model cannot be modelled linearly.
- Bending moments in the pipe differ significantly, and in the linear system are both higher and smaller than in the nonlinear system.

In this study, the equivalent linear system correspondence to the nonlinear system is not precise. Using other methods to calculate the equivalent stiffness, such as secant stiffness or equivalent energy approach, lead to different equivalent linear systems that might be closer to the original nonlinear system. In the linearization the system is changed, adding springs affect the system stiffness matrix and thus its natural frequencies. Periodic oscillation is observed in the linear system, which is not present in the nonlinear system. One of the natural frequencies of the linear system is close to the frequency of the loading, and this could be the reason for the oscillation. However, the iteration converged to this kind of solution. The question arises whether the resulting natural frequencies of the linear system are always somehow related to the loading.

The load case was a sinusoidal point force applied to the pipe, which was chosen so that all gaps are closing in the nonlinear model. Other types of load cases could lead to better correspondence between the systems, however, the method should be well applicable to all load cases, including this one.

One of the most important goals of the linearization of piping supports, as presented in Sections 1 and 3, is to obtain an equivalent linear system so that the computational-intensive nonlinear problem is never solved. If we follow the procedure presented in this thesis and obtain an equivalent linear system, can we be sure that it represents well the original nonlinear system? In other words, can we be sure of the accuracy of the linear system, based only on the resulting linear system, as the nonlinear problem is not solved? In this study, the linearized system predicts that two gaps are left open and differences are found in support forces and pipe bending moments. On the other hand, displacements are of the same order of magnitude and a clear pattern is observed in the support forces. Thus, based on the linearized system, we can say that most displacements are of the same order of magnitude, the forces are generally too low and the bending moments vary significantly. An equivalent linear system can be obtained but it does not guarantee that the whole system behaviour is well modelled.

The example real-world system used in this study is a part of an actual piping system. The system is not a simplified model, such as a straight pipe, but a diverse system with bends and supports in various directions. Thus the conclusions drawn here are well applicable to similar and even to more complicated real-world systems.

5.3 Further work

Practical implementation of linearization can follow the procedure described in this thesis. A computer code can be created to run the procedure, as was done in this thesis for the single and multiple degree-of-freedom examples in Sections 3.3 and 3.4. In the case of gap supports, if the loading is such that many gaps will not be closing, it might be reasonable to assign the value of the gap for the initial guess, making $k_{eq} = 0$ for all supports. Then the procedure can be followed. The supports where the displacement is smaller than the gap magnitude, will remain to have $k_{eq} = 0$, and for the others an equivalent stiffness is found by the procedure. If the under-relaxation method is used in the iteration, the relaxation parameter should be simply varied to improve convergence. It is suggested the parameter to be large when difference between the starting point and the result is large, and to get smaller when the starting point and the result approach each other.

Many improvements can be made to the linearization procedure and methods. The following topics are recommended for investigation in order to further develop the linearization of piping supports:

- The linearization should be performed to a real-world gap support system using other methods than Caughey's method and the results should be compared. Furthermore, new methods to calculate the equivalent stiffness could be developed. It would be worthwhile to identify the methods and problem types that yield corresponding results with the nonlinear model.
- The method should be developed for unsymmetrical supports.
- Investigation could be made regarding load cases of other types than a sinusoidal point force and how different methods perform in them. It should be tried to identify load cases in which the linearization yields results corresponding to nonlinear model.
- Natural frequencies of the linear system should be investigated during the iteration. Also, the relation between loading frequency and the equivalent linear system natural frequencies could be investigated.
- It would be interesting to use other analysis methods, for example response spectrum analysis.
- The linearization should be performed to a real-world friction support system to further demonstrate the procedure for friction supports.
- It would be worthwhile to focus on numerical mathematics to find the best iterative method and parameters for linearization.

- It would be useful to investigate the possibility of coupled linearization, so that the displacements at all support locations affect the initial value of a single support for an iteration step.
- Other variables than displacement and velocity should be considered to be used for linearization.

References

[1] K. Escoe. *Piping and Pipeline Assessment Guide.* Elsevier, April 2006.

[2] J.N. Lillington. *The Future of Nuclear Power.* Elsevier, 2004.

[3] J.C. Wachel. Displacement method for determining acceptable piping vibration amplitudes. *PVP-Vol. 313-2, International Pressure Vessels and Piping Codes and Standards: Volume 2 - Current Perspectives*, 1995.

[4] L.-C. Peng and T.-L. Peng. *Pipe Stress Engineering.* ASME Press, Peng Engineering, Houston, Texas, USA, 2009.

[5] P. R. Smith and T. J. Van Laan. *Piping and Pipe Support Systems.* McGraw-Hill Book Company, 1987.

[6] Y. J. Park, C. H. Hofmayer, and N. C. Chokshi. Applications of equivalent linearization approaches to nonlinear piping systems. In *Transactions of the 14th International Conference on Structural Mechanics in Reactor Technology (SMiRT 14), Lyon, France, August 17-22, 1997.*

[7] L.-C. Peng. Treatment of support friction in pipe stress analysis. *ASME PVP - Vol. 169 Design and Analysis of Piping and Components*, 169, 1989.

[8] F. Steinwender, J. Lockau, and J. Rudolph. Experimental investigation of the load transfer behaviour of piping supports under high-frequency excitation. *Nuclear Engineering and Design*, 83(1):27–30, 1984.

[9] Y. M. Parulekar, G. R. Reddy, K. K. Vaze, a. K. Ghosh, H. S. Kushwaha, and R. Ramesh Babu. Seismic response analysis of RCC structure with yielding dampers using linearization techniques. *Nuclear Engineering and Design*, 239:3054–3061, 2009.

[10] J. Bonet and R. D. Wood. *Nonlinear continuum mechanics for finite element analysis 2nd edition.* Cambridge University Press, 2008.

[11] J. I. Burgaleta. Pipe Whip Restraint Gap Effect Analysis. In *Transactions of the 7th International Conference on Structural Mechanics in Reactor Technology (SMiRT 7), Chicago, Illinois, USA, August 22-26, 1983.*

[12] P. Wriggers. *Computational contact mechanics.* John Wiley & Sons Ltd., Chichester, 2002.

[13] S. M. Ma and K. J. Bathe. On finite element analysis of pipe whip problems. *Nuclear Engineering and Design*, 37, 1976.

[14] S. Ueda. Experimental and Analytical Results of 4 Inch Pipe Whip Tests Under BWR Conditions. In *Transactions of the 7th International Conference on Structural Mechanics in Reactor Technology (SMiRT 7), Chicago, Illinois, USA, August 22-26, 1983.*

[15] Robert L. Cloud Associates Inc. A Simplified Piping Support System With Seismic Limit Stops. *EPRI NP-6442 Project 2349-1 Interim Report July 1989.*

[16] S. Alkmyr. *Parameter study on nonlinear piping systems exposed to time history loading in ANSYS.* Master's thesis, Lund University, 2014.

[17] ANSYS Inc. ANSYS 16.0 Documentation, 2015.

[18] S. V. Bakre, R. S. Jangid, and G. R. Reddy. Response of piping system on friction support to bi-directional excitation. *Nuclear Engineering and Design*, 237:124–136, 2007.

[19] J. Axelsson and H. Viktorsson. *Influence of Support Stiffness in Dynamic Analysis of Piping Systems.* Master's thesis, Chalmers University of Technology, 2011.

[20] H. Murakami, T. Hirai, M. Nakata, T. Kobori, K. Mizukoshi, Y. Takenaka, and N. Miyagawa. Seismic analysis of equipment system with non-linearities such as gap and friction using equivalent linearization method. In *Transactions of the 10th International Conference on Structural Mechanics in Reactor Technology (SMiRT 10), Anaheim, California, USA, August 22-27, 1989.*

[21] J. Pop, Jr, S. Singh, and M. A. Pressburger. Response spectrum analysis of piping systems with elastic-plastic gap supports. *Nuclear Engineering and Design*, 181:131–144, 1998.

[22] J. H. Ferziger and M. Peric. *Computational Methods for Fluid Dynamics.* Springer, 2002.

[23] Y. J. Park and C. H. Hofmayer. Practical application of equivalent linearization approaches to nonlinear piping systems. In *Joint ASME/JSME pressure vessels and piping conference; Honolulu, HI (United States); 23-27 July 1995; BNL-NUREG–61620; CONF-950740–27*, 1995.

[24] Y. M. Parulekar, G. R. Reddy, K. K. Vaze, and K. Muthumani. Passive Control of Seismic Response of Piping Systems. *ASME Journal of Pressure Vessel Technology*, 128:364–369, 2006.

[25] T. K. Caughey. Equivalent Linearization Techniques. *The Journal of the Acoustical Society of America*, 35(11), 1963.

[26] H. Dwairi and M. Kowalsky. Investigation of Jacobsen's equivalent viscous damping approach as applied to displacement-based seismic design. In *13th World Conference on Earthquake Engineering, Vancouver, B.C., Canada, August 1-6, 2004*, number 228, 2004.

[27] H. Dwairi, M. J. Kowalsky, and J. M. Nau. Equivalent Damping in Support of Direct Displacement-Based Design. *Journal of Earthquake Engineering*, 11:512–530, 2007.

[28] A. C. Guyader. *A Statistical Approach to Equivalent Linearization with Applications to Performance-Based Engineering.* PhD thesis, California Institute of Technology, 2003.

[29] T. Liu. *Equivalent linearization analysis method for base-isolated buildings.* PhD thesis, University of Trento, 2014.

[30] A. Occhiuzzi. *Seismic ductility of base isolated structures.* Master's thesis, Massachusetts Institute of Technology, 1994.

[31] A. Yavas and S. Saylan. Effect of equivalent linearization in direct displacement based seismic design of bridge columns. In *13th World Conference on Earthquake Engineering, Vancouver, B.C., Canada, August 1-6, 2004*, number 2687, 2004.

[32] R. Zaharia and F. Taucer. Equivalent period and damping for EC8 spectral response of SDOF ring-spring hysteretic models. *European Commission, Joint Research Centre, Scientific and Technical Reports*, JRC 45403, 2008.

[33] K. Fujita, T. Kimura, and Y. Ohe. Seismic Response Analysis of Piping Systems With Nonlinear Supports Using Differential Algebraic Equations. *ASME Journal of Pressure Vessel Technology*, 126:91–97, 2004.

[34] W. D. Iwan. Predicting the earthquake response of resiliently mounted equipment with motion limiting constraints. In *Proceeding of the 6th World Conference on Earthquake Engineering, New Delhi, India*, pages 3292–3297, 1977.

[35] W. D. Iwan. The earthquake design and analysis of equipment isolation systems. *Earthquake Eng. Struct. Dyn.*, 6:523–534, 1978.

[36] Dr. N.S.V K. R. Roy. *Mechanical Vibrations of Elastic Systems.* Asian Books Private Limited, New Delhi, India, 2006.

[37] C. F. Beards. *Engineering Vibration Analysis with Application to Control Systems.* Edward Arnold, London, 1995.

[38] R. Majed and J. L. Raynaud. Prediction of the dynamic behavior of a non-linear structure with a dry friction. In *New Advances in Modal Synthesis of Large Structures: Non-linear Damped and Non-deterministic Cases: Proceedings of the international conference MV2, Lyon, France, 5-6 October 1995, Jezequel (ed.)*, pages 577–587. CRC Press, 1997.

[39] E. Süli and D. F. Mayers. *An Introduction to Numerical Analysis.* Cambridge University Press, Cambridge, 2003.

A Derivation of analytical expression of maximum displacement for linearized single degree-of-freedom gap support

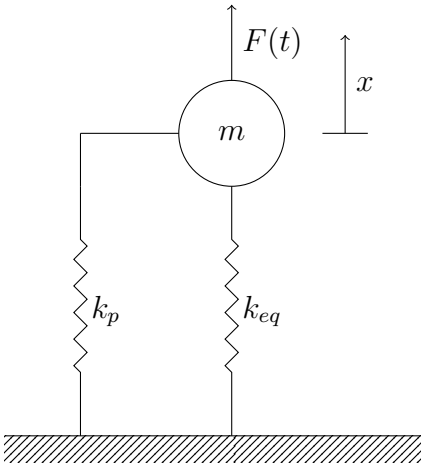

Figure A.1: Single degree-of-freedom system of linearized gap support. In the figure m is the mass of the system, k_p the system stiffness, k_{eq} the equivalent stiffness, $F(t)$ the applied loading and x the displacement of the system.

The system of Figure A.1 is studied and an analytical expression of maximum displacement is derived.

The equation of motion of the system of Figure A.1 is

$$-k_{eq}x - k_p x + F(t) = m\ddot{x} \tag{A.1}$$

where k_{eq} is the equivalent support stiffness, k_p system stiffness, $F(t)$ loading and m mass of the system. Assuming a harmonic excitation $F(t) = F_{amp}\sin(\omega t)$ and rearranging gives

$$m\ddot{x} + (k_{eq} + k_p)x - F_{amp}\sin(\omega t) = 0 \tag{A.2}$$

where F_{amp} is the force amplitude and ω the angular velocity of loading. Solving Equation (A.2) yields the displacement as a function of time

$$x(t) = \frac{F_{amp}/m}{\omega_n^2 - \omega^2}\sin(\omega t) - \frac{\omega F_{amp}/m}{(\omega_n^2 - \omega^2)\omega_n}\sin(\omega_n t) \tag{A.3}$$

where $\omega_n = \sqrt{\frac{k_{eq}+k_p}{m}}$ is the natural angular velocity of the linearized system. Examining Equation (A.3) it can be seen that the maximum absolute value of x occurs when the sine functions have the values $\sin(\omega t) = 1$ and $\sin(\omega_n t) = -1$ as in Equation (A.4) or when $\sin(\omega t) = -1$ and $\sin(\omega_n t) = 1$ as in Equation (A.5).

$$x_{max} = \left|\frac{F_{amp}/m}{\omega_n^2 - \omega^2} + \frac{\omega F_{amp}/m}{(\omega_n^2 - \omega^2)\omega_n}\right| \tag{A.4}$$

$$x_{max} = \left| -\frac{F_{amp}/m}{\omega_n^2 - \omega^2} - \frac{\omega F_{amp}/m}{(\omega_n^2 - \omega^2)\omega_n} \right| \tag{A.5}$$

Maximum amplitudes obtained using Equations (A.4) and (A.5) are the same, since Equation (A.5) can be rearranged as

$$x_{max} = \left| -\left(\frac{F_{amp}/m}{\omega_n^2 - \omega^2} + \frac{\omega F_{amp}/m}{(\omega_n^2 - \omega^2)\omega_n} \right) \right| \tag{A.6}$$

and remembering the basic formula that for any a, it holds that $|a| = |-a|$. Thus only Equation (A.4) is investigated here. Equation (A.4) can be rearranged further as

$$x_{max} = \left| \frac{F_{amp}/m}{\omega_n^2 - \omega^2} \left(1 + \frac{\omega}{\omega_n} \right) \right| \tag{A.7}$$

Substituting the expression of system natural angular velocity $\omega_n = \sqrt{\frac{k_{eq}+k_p}{m}}$ yields

$$x_{max} = \left| \frac{F_{amp}/m}{\frac{k_{eq}+k_p}{m} - \omega^2} \left(1 + \frac{\omega}{\sqrt{\frac{k_{eq}+k_p}{m}}} \right) \right| \tag{A.8}$$

B Derivation of analytical expressions of maximum displacement and velocity for linearized single degree-of-freedom friction support

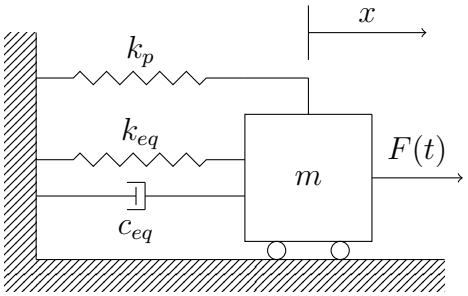

Figure B.1: Single degree-of-freedom system of linearized friction support. In the figure m is the mass of the system, k_p is the system stiffness, $F(t)$ is the applied loading, x is the displacement of the system and k_{eq} and c_{eq} are the equivalent stiffness and damping.

The system of Figure B.1 is studied and analytical expressions of maximum displacement and velocity amplitudes are derived in the steady-state vibration. Steady state of the vibration is reached after some time when transient effects have decayed and the system oscillates with the same frequency as the excitation.

The equation of motion for the system of Figure B.1 is

$$-k_p x - k_{eq} x - c_{eq}\dot{x} + F(t) = m\ddot{x} \tag{B.1}$$

Assuming a harmonic excitation $F(t) = F_{amp}\sin(\omega t)$ and rearranging gives

$$m\ddot{x} + c_{eq}\dot{x} + (k_p + k_{eq})x - F_{amp}\sin(\omega t) = 0 \tag{B.2}$$

where F_{amp} is the force amplitude and ω the angular velocity of the excitation. Solving Equation (B.2) with the initial conditions $x(0) = 0$ and $x'(0) = 0$ yields the displacement as a function of time:

$$x(t) = \frac{\omega_n^2 F_{amp}}{(k_p + k_{eq})\left[(\omega^2 - \omega_n^2)^2 + (2\xi\omega\omega_n)^2\right]}\left[2\xi\omega\omega_n\cos(\omega t) - (\omega^2 - \omega_n^2)\sin(\omega t)\right] + Ae^{-\xi\omega_n t} + Be^{-\xi\omega_n t} \tag{B.3}$$

where $\omega_n = \sqrt{\frac{k_p+k_{eq}}{m}}$, $\xi = \frac{c_{eq}}{2m\omega_n} = \frac{c_{eq}}{2\sqrt{m(k_p+k_{eq})}}$ and $A = A(\omega, \omega_n, F_{amp}, \xi, k_{eq}, k_p, t)$ and $B = B(\omega, \omega_n, F_{amp}, \xi, k_{eq}, k_p, t)$ are functions of parameters. A and B are however of less importance in this problem. In the beginning of the vibration, there are transient effects present but these decay after some time and the vibration becomes steady. The maximum displacement and velocity used for the calculation of equivalent properties is considered in the steady state of the vibration. The equation for

steady-state vibration is obtained from Equation (B.3) by letting the time to go to infinity, $t \to \infty$. The exponential terms vanish and we obtain for the steady-state vibration

$$x(t)_{ss} = \frac{\omega_n^2 F_{amp}}{(k_p + k_{eq})\left[(\omega^2 - \omega_n^2)^2 + (2\xi\omega\omega_n)^2\right]}\left[2\xi\omega\omega_n cos(\omega t) - (\omega^2 - \omega_n^2)sin(\omega t)\right] \tag{B.4}$$

The maximum value of Equation (B.4) is

$$x_{max} = \frac{\omega_n^2 F_{amp}}{(k_p + k_{eq})\sqrt{(\omega^2 - \omega_n^2)^2 + (2\xi\omega\omega_n)^2}} \tag{B.5}$$

The velocity is obtained by taking derivative of Equation (B.4) with respect to time

$$\dot{x}(t)_{ss} = \frac{\omega_n^2 F_{amp}}{(k_p + k_{eq})\left[(\omega^2 - \omega_n^2)^2 + (2\xi\omega\omega_n)^2\right]}\left[-2\xi\omega^2\omega_n sin(\omega t) - (\omega^2 - \omega_n^2)\omega cos(\omega t)\right] \tag{B.6}$$

and the maximum value for velocity becomes

$$v_{max} = \frac{\omega_n^2 F_{amp}}{(k_p + k_{eq})\left[(\omega^2 - \omega_n^2)^2 + (2\xi\omega\omega_n)^2\right]}\sqrt{(2\xi\omega^2\omega_n)^2 + ((\omega^2 - \omega_n^2)\omega)^2} \tag{B.7}$$

C Equations of motion for the example multiple degree-of-freedom systems of Section 3.4

Gap supports

The example multiple degree-of-freedom gap support system of Section 3.4.1 is presented in Figures C.1 and C.2.

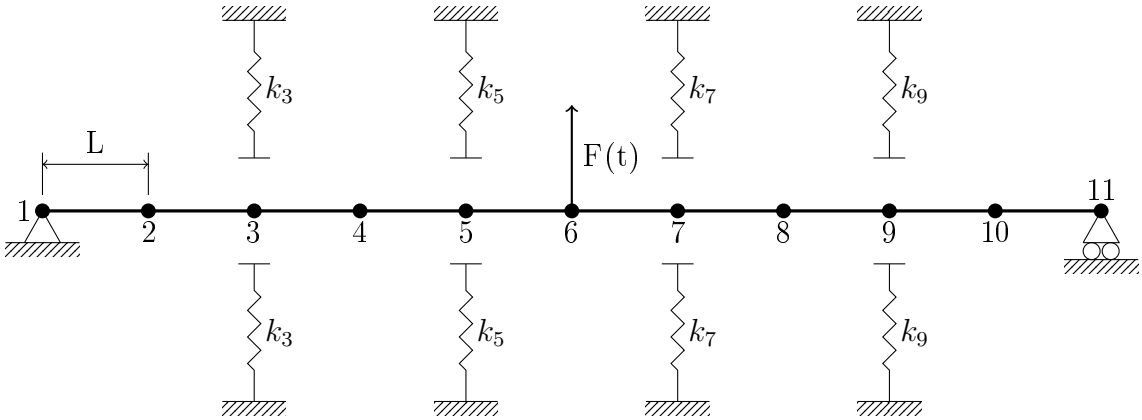

Figure C.1: Example multiple degree-of-freedom system consisting of a beam and four gap supports. Length of one beam element is L, $F(t)$ is the applied loading and k_3, k_5, k_7 and k_9 are the support stiffnesses. Node numbering is also shown.

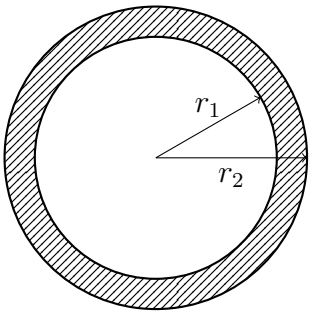

Figure C.2: Cross-section of the beam. r_1 is the inner radius and r_2 is the outer radius of the beam.

The system has 11 nodes and with the end nodes pinned 20 degrees of freedom. No damping is present and the equation of motion becomes

$$\mathbf{M}\ddot{\mathbf{x}} + \mathbf{K}\mathbf{x} = \mathbf{F}(t) \tag{C.1}$$

where

$$\mathbf{M} = \begin{bmatrix}
m_1 & 0 & 0 & 0 & 0 & 0 & 0 & 0 & 0 & 0 & 0 & 0 & 0 & 0 & 0 & 0 & 0 & 0 & 0 & 0 & 0 \\
0 & J_1 & 0 & 0 & 0 & 0 & 0 & 0 & 0 & 0 & 0 & 0 & 0 & 0 & 0 & 0 & 0 & 0 & 0 & 0 & 0 \\
0 & 0 & m_2 & 0 & 0 & 0 & 0 & 0 & 0 & 0 & 0 & 0 & 0 & 0 & 0 & 0 & 0 & 0 & 0 & 0 & 0 \\
0 & 0 & 0 & J_2 & 0 & 0 & 0 & 0 & 0 & 0 & 0 & 0 & 0 & 0 & 0 & 0 & 0 & 0 & 0 & 0 & 0 \\
0 & 0 & 0 & 0 & m_3 & 0 & 0 & 0 & 0 & 0 & 0 & 0 & 0 & 0 & 0 & 0 & 0 & 0 & 0 & 0 & 0 \\
0 & 0 & 0 & 0 & 0 & J_3 & 0 & 0 & 0 & 0 & 0 & 0 & 0 & 0 & 0 & 0 & 0 & 0 & 0 & 0 & 0 \\
0 & 0 & 0 & 0 & 0 & 0 & m_4 & 0 & 0 & 0 & 0 & 0 & 0 & 0 & 0 & 0 & 0 & 0 & 0 & 0 & 0 \\
0 & 0 & 0 & 0 & 0 & 0 & 0 & J_4 & 0 & 0 & 0 & 0 & 0 & 0 & 0 & 0 & 0 & 0 & 0 & 0 & 0 \\
0 & 0 & 0 & 0 & 0 & 0 & 0 & 0 & m_5 & 0 & 0 & 0 & 0 & 0 & 0 & 0 & 0 & 0 & 0 & 0 & 0 \\
0 & 0 & 0 & 0 & 0 & 0 & 0 & 0 & 0 & J_5 & 0 & 0 & 0 & 0 & 0 & 0 & 0 & 0 & 0 & 0 & 0 \\
0 & 0 & 0 & 0 & 0 & 0 & 0 & 0 & 0 & 0 & m_6 & 0 & 0 & 0 & 0 & 0 & 0 & 0 & 0 & 0 & 0 \\
0 & 0 & 0 & 0 & 0 & 0 & 0 & 0 & 0 & 0 & 0 & J_6 & 0 & 0 & 0 & 0 & 0 & 0 & 0 & 0 & 0 \\
0 & 0 & 0 & 0 & 0 & 0 & 0 & 0 & 0 & 0 & 0 & 0 & m_7 & 0 & 0 & 0 & 0 & 0 & 0 & 0 & 0 \\
0 & 0 & 0 & 0 & 0 & 0 & 0 & 0 & 0 & 0 & 0 & 0 & 0 & J_7 & 0 & 0 & 0 & 0 & 0 & 0 & 0 \\
0 & 0 & 0 & 0 & 0 & 0 & 0 & 0 & 0 & 0 & 0 & 0 & 0 & 0 & m_8 & 0 & 0 & 0 & 0 & 0 & 0 \\
0 & 0 & 0 & 0 & 0 & 0 & 0 & 0 & 0 & 0 & 0 & 0 & 0 & 0 & 0 & J_8 & 0 & 0 & 0 & 0 & 0 \\
0 & 0 & 0 & 0 & 0 & 0 & 0 & 0 & 0 & 0 & 0 & 0 & 0 & 0 & 0 & 0 & m_9 & 0 & 0 & 0 & 0 \\
0 & 0 & 0 & 0 & 0 & 0 & 0 & 0 & 0 & 0 & 0 & 0 & 0 & 0 & 0 & 0 & 0 & J_9 & 0 & 0 & 0 \\
0 & 0 & 0 & 0 & 0 & 0 & 0 & 0 & 0 & 0 & 0 & 0 & 0 & 0 & 0 & 0 & 0 & 0 & m_{10} & 0 & 0 \\
0 & 0 & 0 & 0 & 0 & 0 & 0 & 0 & 0 & 0 & 0 & 0 & 0 & 0 & 0 & 0 & 0 & 0 & 0 & J_{10} & 0 \\
0 & 0 & 0 & 0 & 0 & 0 & 0 & 0 & 0 & 0 & 0 & 0 & 0 & 0 & 0 & 0 & 0 & 0 & 0 & 0 & m_{11} \\
0 & 0 & 0 & 0 & 0 & 0 & 0 & 0 & 0 & 0 & 0 & 0 & 0 & 0 & 0 & 0 & 0 & 0 & 0 & 0 & J_{11}
\end{bmatrix} \tag{C.2}$$

and

$$\mathbf{K} = \frac{EI}{L^3} \begin{bmatrix}
12 & -6L & -12 & -6L & 0 & 0 & 0 & 0 & 0 & 0 & 0 & 0 & 0 & 0 & 0 & 0 & 0 & 0 & 0 & 0 & 0 \\
-6L & 4L^2 & 6L & 2L^2 & 0 & 0 & 0 & 0 & 0 & 0 & 0 & 0 & 0 & 0 & 0 & 0 & 0 & 0 & 0 & 0 & 0 \\
-12 & 6L & 24 & 0 & -12 & -6L & 0 & 0 & 0 & 0 & 0 & 0 & 0 & 0 & 0 & 0 & 0 & 0 & 0 & 0 & 0 \\
-6L & 2L^2 & 0 & 8L^2 & 6L & 2L^2 & 0 & 0 & 0 & 0 & 0 & 0 & 0 & 0 & 0 & 0 & 0 & 0 & 0 & 0 & 0 \\
0 & 0 & -12 & 6L & 24 & 0 & -12 & -6L & 0 & 0 & 0 & 0 & 0 & 0 & 0 & 0 & 0 & 0 & 0 & 0 & 0 \\
0 & 0 & -6L & 2L^2 & 0 & 8L^2 & 6L & 2L^2 & 0 & 0 & 0 & 0 & 0 & 0 & 0 & 0 & 0 & 0 & 0 & 0 & 0 \\
0 & 0 & 0 & 0 & -12 & 6L & 24 & 0 & -12 & -6L & 0 & 0 & 0 & 0 & 0 & 0 & 0 & 0 & 0 & 0 & 0 \\
0 & 0 & 0 & 0 & -6L & 2L^2 & 0 & 8L^2 & 6L & 2L^2 & 0 & 0 & 0 & 0 & 0 & 0 & 0 & 0 & 0 & 0 & 0 \\
0 & 0 & 0 & 0 & 0 & 0 & -12 & 6L & 24 & 0 & -12 & -6L & 0 & 0 & 0 & 0 & 0 & 0 & 0 & 0 & 0 \\
0 & 0 & 0 & 0 & 0 & 0 & -6L & 2L^2 & 0 & 8L^2 & 6L & 2L^2 & 0 & 0 & 0 & 0 & 0 & 0 & 0 & 0 & 0 \\
0 & 0 & 0 & 0 & 0 & 0 & 0 & 0 & -12 & 6L & 24 & 0 & -12 & -6L & 0 & 0 & 0 & 0 & 0 & 0 & 0 \\
0 & 0 & 0 & 0 & 0 & 0 & 0 & 0 & -6L & 2L^2 & 0 & 8L^2 & 6L & 2L^2 & 0 & 0 & 0 & 0 & 0 & 0 & 0 \\
0 & 0 & 0 & 0 & 0 & 0 & 0 & 0 & 0 & 0 & -12 & 6L & 24 & 0 & -12 & -6L & 0 & 0 & 0 & 0 & 0 \\
0 & 0 & 0 & 0 & 0 & 0 & 0 & 0 & 0 & 0 & -6L & 2L^2 & 0 & 8L^2 & 6L & 2L^2 & 0 & 0 & 0 & 0 & 0 \\
0 & 0 & 0 & 0 & 0 & 0 & 0 & 0 & 0 & 0 & 0 & 0 & -12 & 6L & 24 & 0 & -12 & -6L & 0 & 0 & 0 \\
0 & 0 & 0 & 0 & 0 & 0 & 0 & 0 & 0 & 0 & 0 & 0 & -6L & 2L^2 & 0 & 8L^2 & 6L & 2L^2 & 0 & 0 & 0 \\
0 & 0 & 0 & 0 & 0 & 0 & 0 & 0 & 0 & 0 & 0 & 0 & 0 & 0 & -12 & 6L & 24 & 0 & -12 & -6L & 0 \\
0 & 0 & 0 & 0 & 0 & 0 & 0 & 0 & 0 & 0 & 0 & 0 & 0 & 0 & -6L & 2L^2 & 0 & 8L^2 & 6L & 2L^2 & 0 \\
0 & 0 & 0 & 0 & 0 & 0 & 0 & 0 & 0 & 0 & 0 & 0 & 0 & 0 & 0 & 0 & -12 & 6L & 24 & 0 & -12 & -6L \\
0 & 0 & 0 & 0 & 0 & 0 & 0 & 0 & 0 & 0 & 0 & 0 & 0 & 0 & 0 & 0 & -6L & 2L^2 & 0 & 8L^2 & 6L & 2L^2 \\
0 & 0 & 0 & 0 & 0 & 0 & 0 & 0 & 0 & 0 & 0 & 0 & 0 & 0 & 0 & 0 & 0 & 0 & -12 & 6L & 12 & 6L \\
0 & 0 & 0 & 0 & 0 & 0 & 0 & 0 & 0 & 0 & 0 & 0 & 0 & 0 & 0 & 0 & 0 & 0 & -6L & 2L^2 & 6L & 4L^2
\end{bmatrix} \tag{C.3}$$

and

$$\mathbf{F}(t) = \begin{bmatrix} 0 \\ 0 \\ 0 \\ 0 \\ F_3 \\ 0 \\ 0 \\ 0 \\ F_5 \\ 0 \\ F(t) \\ 0 \\ F_7 \\ 0 \\ 0 \\ 0 \\ F_9 \\ 0 \\ 0 \\ 0 \\ 0 \\ 0 \end{bmatrix} \text{ and } \mathbf{x} = \begin{bmatrix} u_1 \\ \theta_1 \\ u_2 \\ \theta_2 \\ u_3 \\ \theta_3 \\ u_4 \\ \theta_4 \\ u_5 \\ \theta_5 \\ u_6 \\ \theta_6 \\ u_7 \\ \theta_7 \\ u_8 \\ \theta_8 \\ u_9 \\ \theta_9 \\ u_{10} \\ \theta_{10} \\ u_{11} \\ \theta_{11} \end{bmatrix} \tag{C.4}$$

Mass of one element is m and length of one element is L. Therefore the lumped masses and inertias are as follows: $m_1 = m_{11} = \frac{m}{2}$, $m_2 = m_3 = m_4 = m_5 = m_6 = m_7 = m_8 = m_9 = m_{10} = m$, $J_1 = J_{11} = \frac{mL^2}{24}$ and $J_2 = J_3 = J_4 = J_5 = J_6 = J_7 = J_8 = J_9 = J_{10} = \frac{mL^2}{12}$. Young's modulus E and second moment of area I are used in $\mathbf{K}$. The forces F_3, F_5, F_7 and F_9 represent the support forces. Displacements of nodes are denoted with u and rotations with θ, with the subscript indicating the node.

Friction supports

The example multiple degree-of-freedom friction support system of Section 3.4.2 is presented in Figures C.3 and C.4.

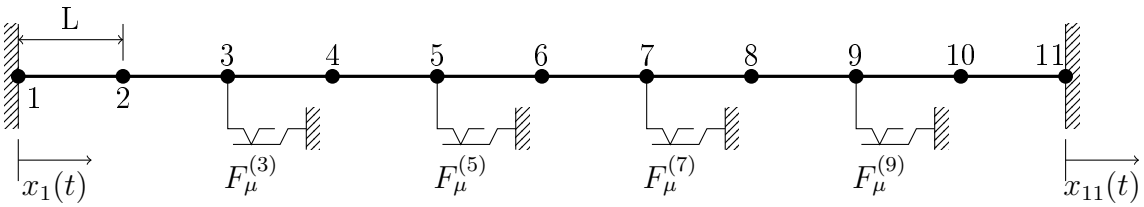

Figure C.3: Example multiple degree-of-freedom friction support system. Length of one bar element is L, $x_1(t)$ and $x_{11}(t)$ are the applied displacement loadings and $F_\mu^{(3)}$, $F_\mu^{(5)}$, $F_\mu^{(7)}$ and $F_\mu^{(9)}$ are the support friction forces. Node numbering is also shown.

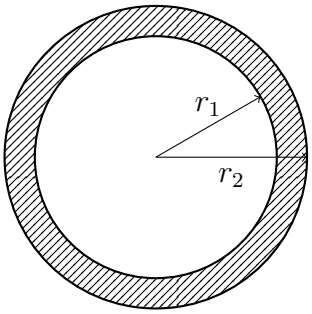

Figure C.4: Cross-section of the bar. r_1 is the inner radius and r_2 is the outer radius of the bar.

The system has 11 nodes and 11 degrees of freedom, of which two are controlled by assigning a forced displacement. No damping is present and the equation of motion becomes

$$\mathbf{M}\ddot{\mathbf{x}} + \mathbf{K}\mathbf{x} = \mathbf{F}(t) \tag{C.5}$$

where

$$\mathbf{M} = \begin{bmatrix} m_1 & 0 & 0 & 0 & 0 & 0 & 0 & 0 & 0 & 0 & 0 \\ 0 & m_2 & 0 & 0 & 0 & 0 & 0 & 0 & 0 & 0 & 0 \\ 0 & 0 & m_3 & 0 & 0 & 0 & 0 & 0 & 0 & 0 & 0 \\ 0 & 0 & 0 & m_4 & 0 & 0 & 0 & 0 & 0 & 0 & 0 \\ 0 & 0 & 0 & 0 & m_5 & 0 & 0 & 0 & 0 & 0 & 0 \\ 0 & 0 & 0 & 0 & 0 & m_6 & 0 & 0 & 0 & 0 & 0 \\ 0 & 0 & 0 & 0 & 0 & 0 & m_7 & 0 & 0 & 0 & 0 \\ 0 & 0 & 0 & 0 & 0 & 0 & 0 & m_8 & 0 & 0 & 0 \\ 0 & 0 & 0 & 0 & 0 & 0 & 0 & 0 & m_9 & 0 & 0 \\ 0 & 0 & 0 & 0 & 0 & 0 & 0 & 0 & 0 & m_{10} & 0 \\ 0 & 0 & 0 & 0 & 0 & 0 & 0 & 0 & 0 & 0 & m_{11} \end{bmatrix} \tag{C.6}$$

and

$$\mathbf{K} = \frac{EA}{L}\begin{bmatrix} 1 & -1 & 0 & 0 & 0 & 0 & 0 & 0 & 0 & 0 & 0 \\ -1 & 2 & -1 & 0 & 0 & 0 & 0 & 0 & 0 & 0 & 0 \\ 0 & -1 & 2 & -1 & 0 & 0 & 0 & 0 & 0 & 0 & 0 \\ 0 & 0 & -1 & 2 & -1 & 0 & 0 & 0 & 0 & 0 & 0 \\ 0 & 0 & 0 & -1 & 2 & -1 & 0 & 0 & 0 & 0 & 0 \\ 0 & 0 & 0 & 0 & -1 & 2 & -1 & 0 & 0 & 0 & 0 \\ 0 & 0 & 0 & 0 & 0 & -1 & 2 & -1 & 0 & 0 & 0 \\ 0 & 0 & 0 & 0 & 0 & 0 & -1 & 2 & -1 & 0 & 0 \\ 0 & 0 & 0 & 0 & 0 & 0 & 0 & -1 & 2 & -1 & 0 \\ 0 & 0 & 0 & 0 & 0 & 0 & 0 & 0 & -1 & 2 & -1 \\ 0 & 0 & 0 & 0 & 0 & 0 & 0 & 0 & 0 & -1 & 1 \end{bmatrix} \tag{C.7}$$

and

$$\mathbf{F}(t) = \begin{bmatrix} 0 \\ 0 \\ F_\mu^{(3)} \\ 0 \\ F_\mu^{(5)} \\ 0 \\ F_\mu^{(7)} \\ 0 \\ F_\mu^{(9)} \\ 0 \\ 0 \end{bmatrix} \text{ and } \mathbf{x} = \begin{bmatrix} x_1 \\ x_2 \\ x_3 \\ x_4 \\ x_5 \\ x_6 \\ x_7 \\ x_8 \\ x_9 \\ x_{10} \\ x_{11} \end{bmatrix} \tag{C.8}$$

Mass of one element is m and therefore the lumped masses are as follows: $m_1 = m_{11} = \frac{m}{2}$ and $m_2 = m_3 = m_4 = m_5 = m_6 = m_7 = m_8 = m_9 = m_{10} = m$. In the stiffness matrix E is the Young's modulus, A is the beam cross-sectional area and L is the length of one element. The forces $F_\mu^{(3)}$, $F_\mu^{(5)}$, $F_\mu^{(7)}$ and $F_\mu^{(9)}$ represent the support friction forces. Displacements are denoted with x with the subscript indicating the node. Two of the displacements are controlled, $x_1 = x_{11} = 0{,}1 \sin(80\pi t)$.

D Complete force-displacement relationships and bending moment magnitudes of the application of Section 4.5

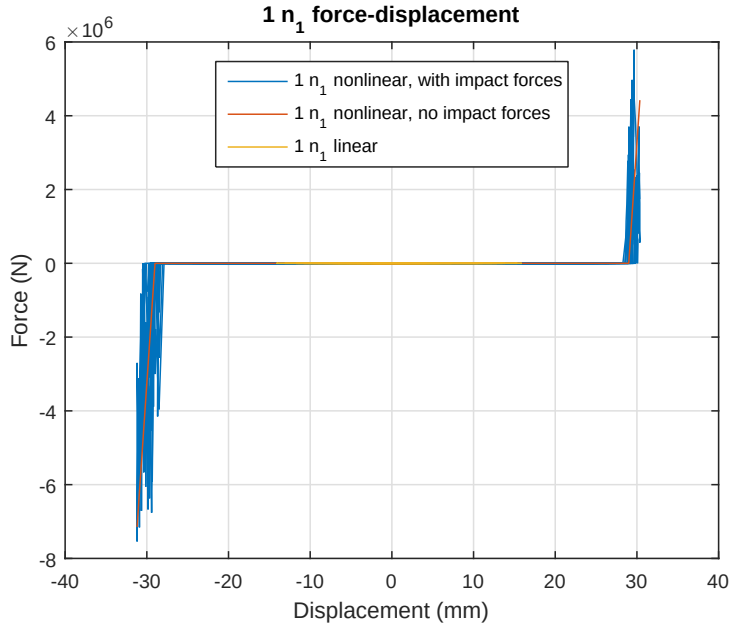

Figure D.1: Support 1 force-displacement relationship in the n_1-direction for the nonlinear support with and without impact forces and for the linear support.

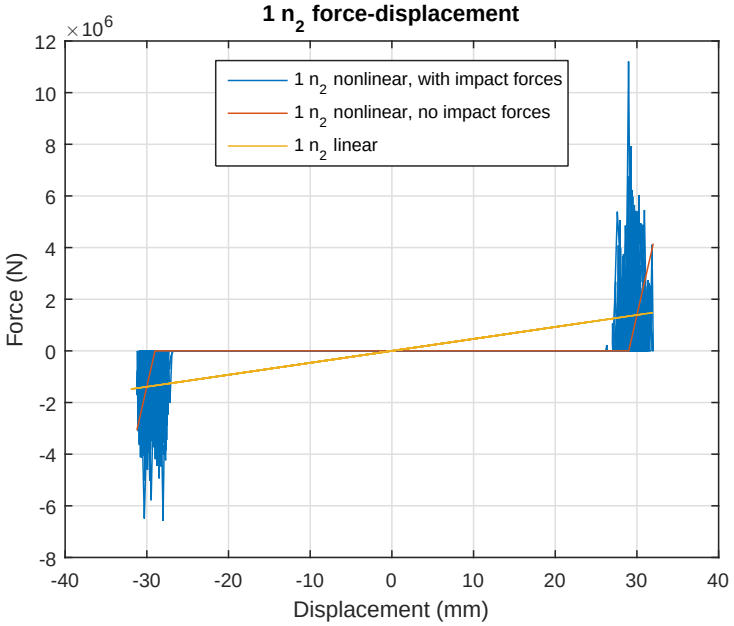

Figure D.2: Support 1 force-displacement relationship in the n_2-direction for the nonlinear support with and without impact forces and for the linear support.

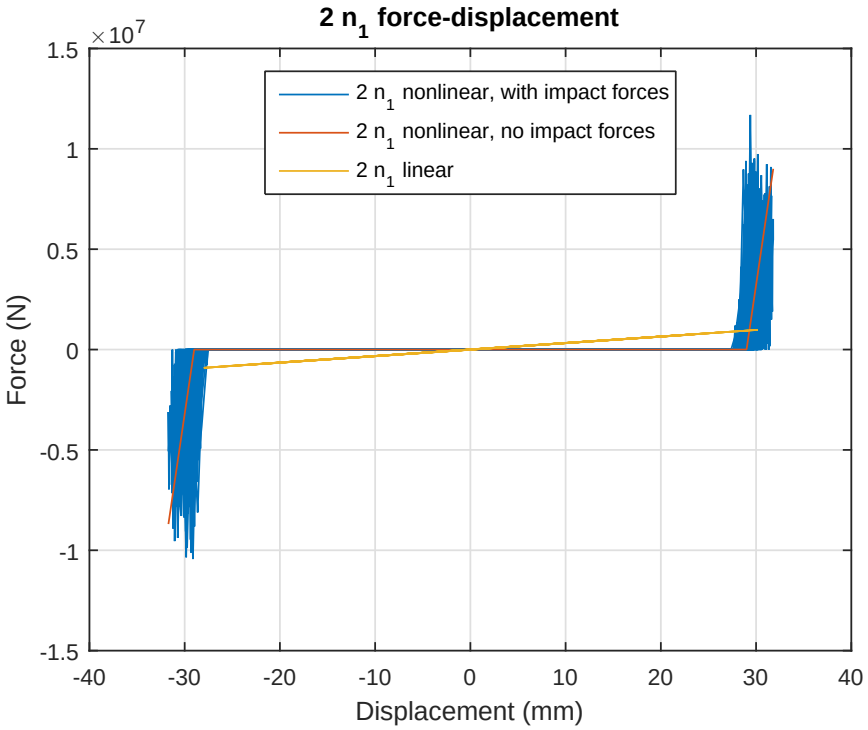

Figure D.3: Support 2 force-displacement relationship in the n_1-direction for the nonlinear support with and without impact forces and for the linear support.

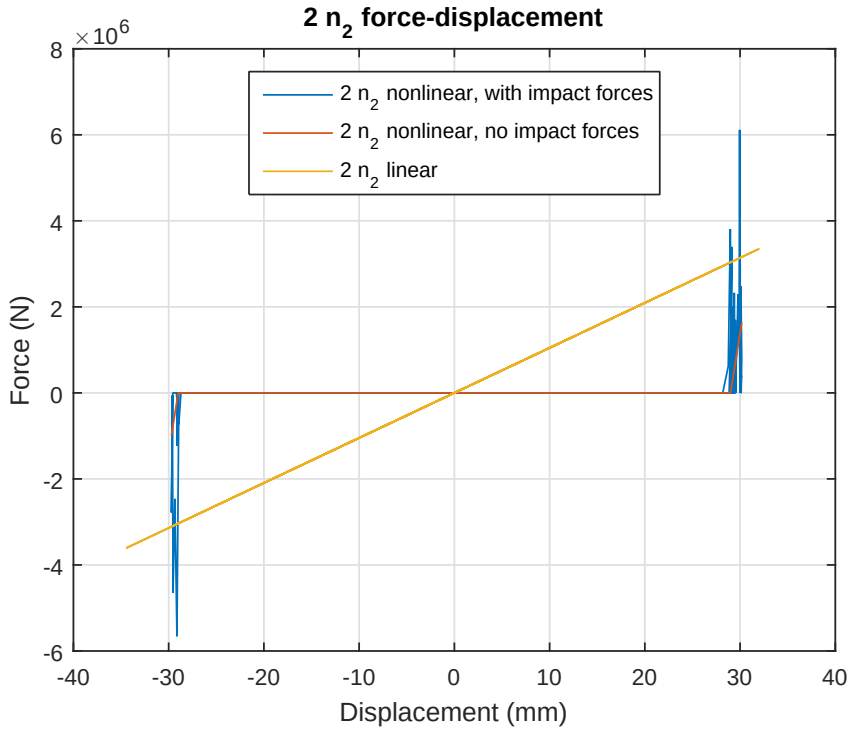

Figure D.4: Support 2 force-displacement relationship in the n_2-direction for the nonlinear support with and without impact forces and for the linear support.

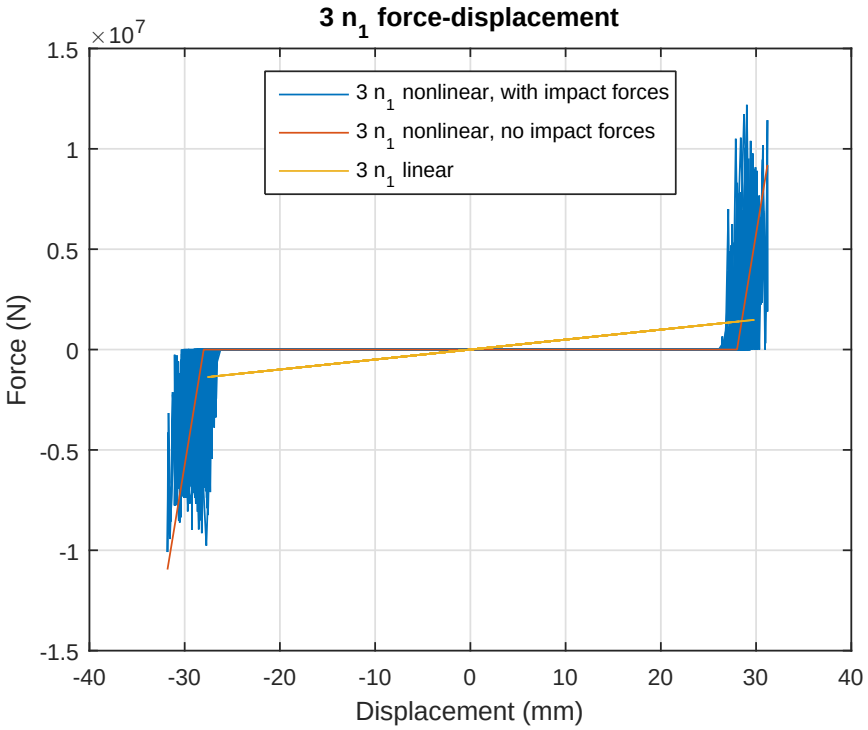

Figure D.5: Support 3 force-displacement relationship in the n_1-direction for the nonlinear support with and without impact forces and for the linear support.

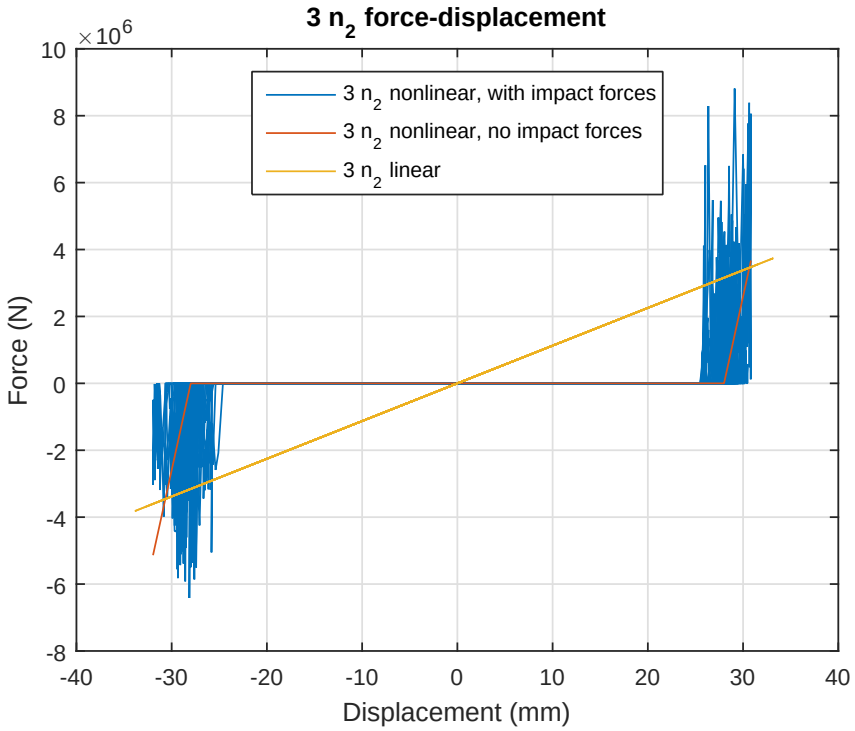

Figure D.6: Support 3 force-displacement relationship in the n_2-direction for the nonlinear support with and without impact forces and for the linear support.

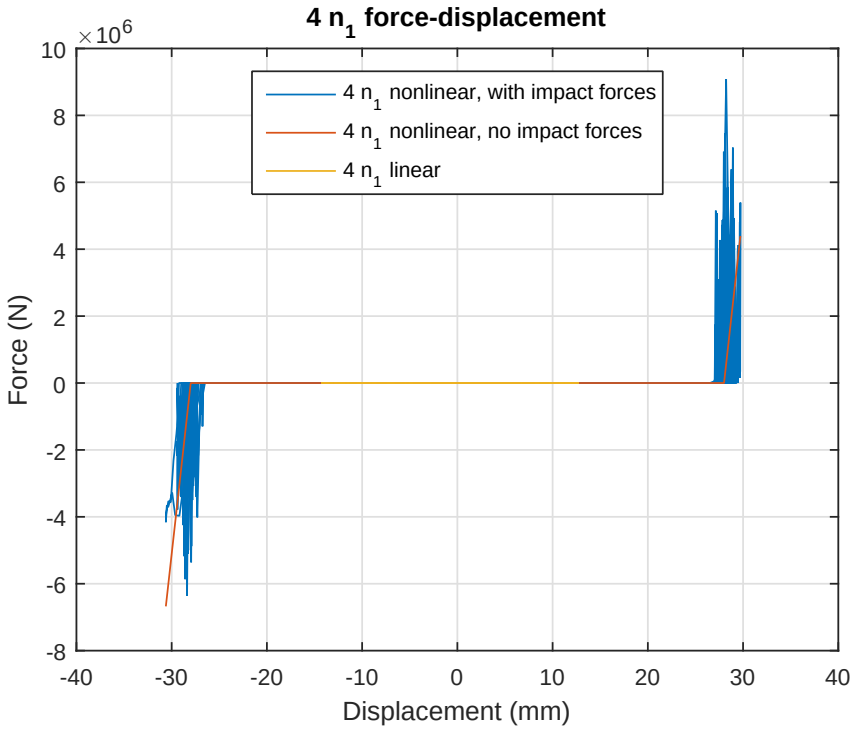

Figure D.7: Support 4 force-displacement relationship in the n_1-direction for the nonlinear support with and without impact forces and for the linear support.

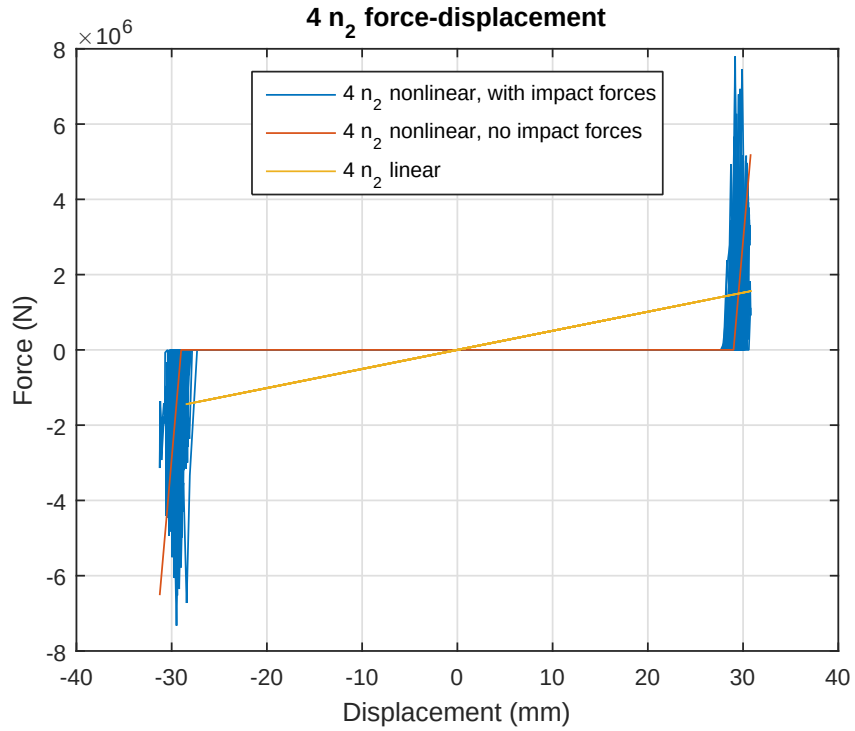

Figure D.8: Support 4 force-displacement relationship in the n_2-direction for the nonlinear support with and without impact forces and for the linear support.

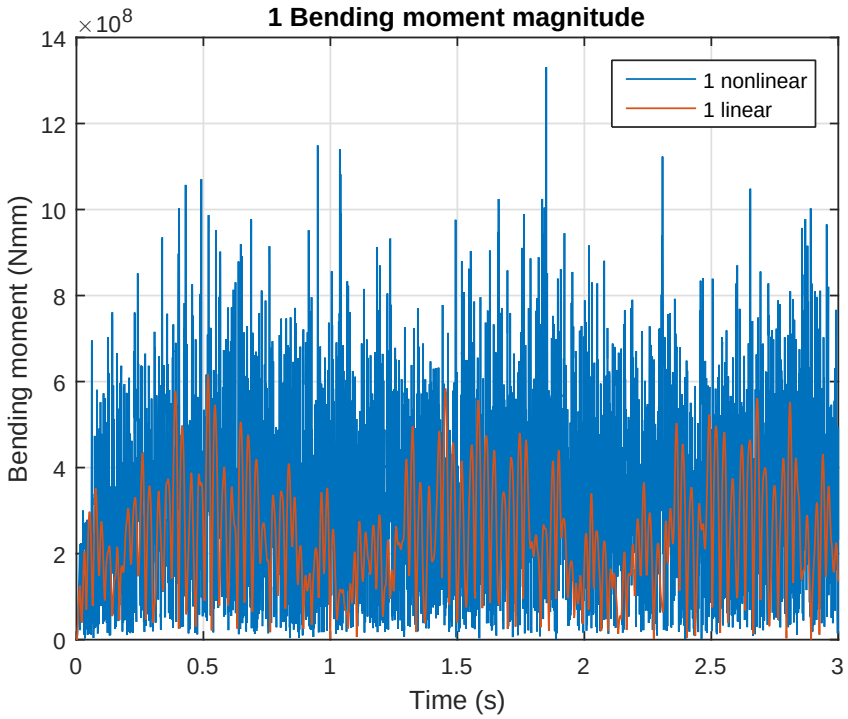

Figure D.9: Support 1 bending moment magnitude as function of time for the nonlinear and linear cases.

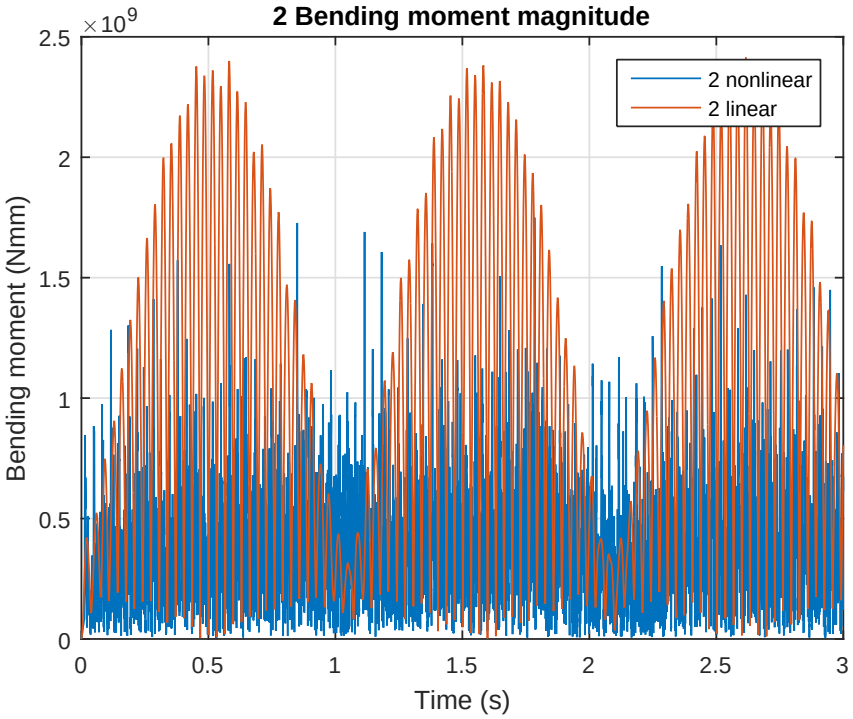

Figure D.10: Support 2 bending moment magnitude as function of time for the nonlinear and linear cases.

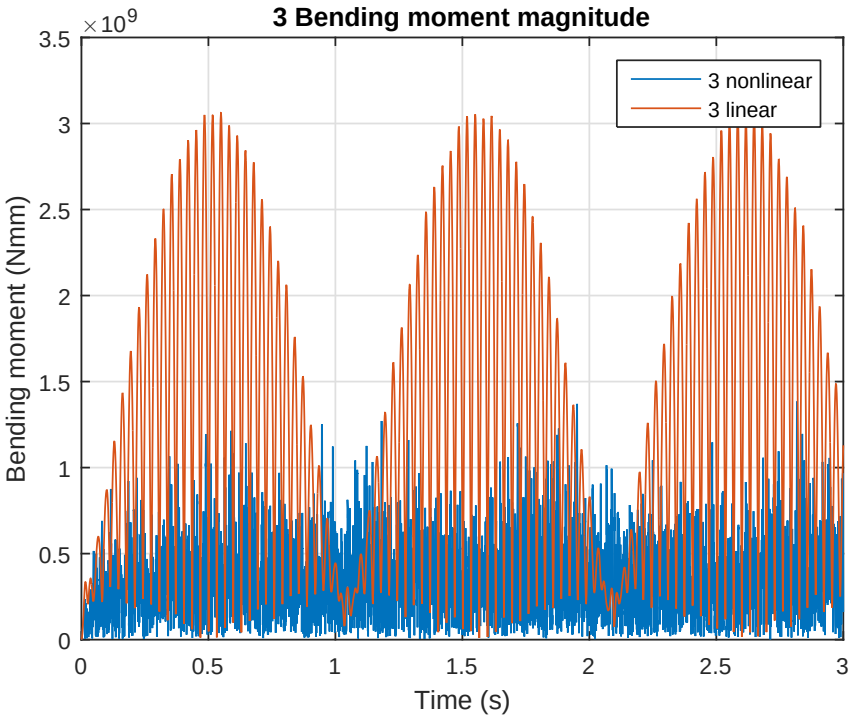

Figure D.11: Support 3 bending moment magnitude as function of time for the nonlinear and linear cases.

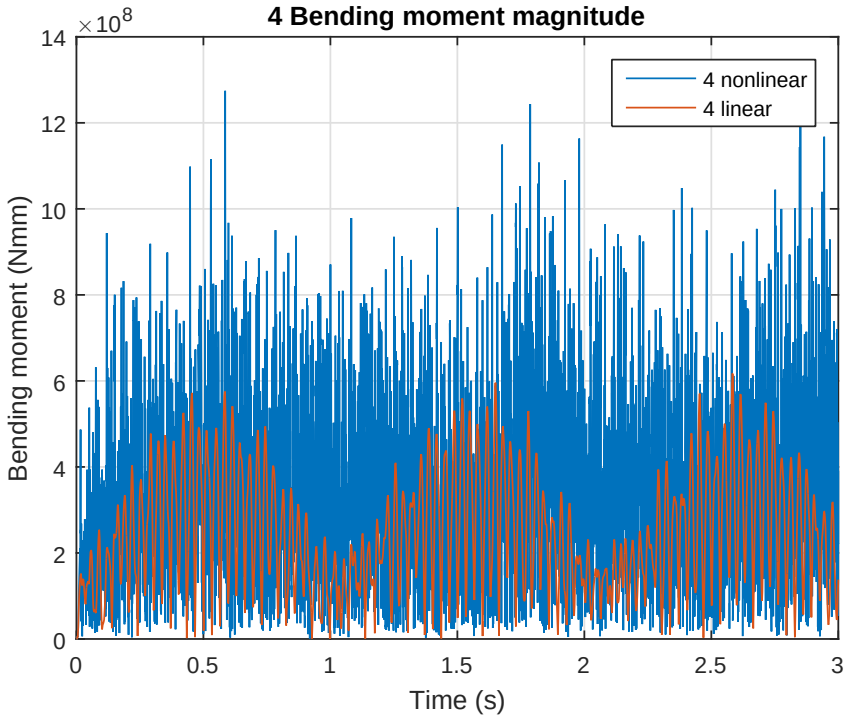

Figure D.12: Support 4 bending moment magnitude as function of time for the nonlinear and linear cases.